PALACKÝ UNIVERSITY IN OLOMOUC

FACULTY OF SCIENCE

DEPARTMENT OF BIOPHYSICS

The effect of singlet oxygen on unsaturated lipids and isoprenoid quinones in plants

Ph.D. thesis

Ursula Rácová

Ph.D. program Physics - Biophysics

Supervisor: Pavel Pospíšil

Olomouc 2023

Bibliographical identification

Author's first name and surname: Mgr. Ursula Rácová (maiden name: Ferretti)

Title: The effect of singlet oxygen on unsaturated lipids and isoprenoid quinones in plants

Type of thesis: Ph.D. thesis

Department: Department of Biophysics

Supervisor: Doc. RNDr. Pavel Pospíšil, Ph.D.

Consultant: Mgr. Marek Rác, Ph.D.

The year of presentation: 2023

Abstract:

Singlet oxygen is an excited form of molecular oxygen continuously generated in plants metabolic pathways. Singlet oxygen is very important component in signaling pathways of plant organisms, however its action may also be destructive. Singlet oxygen has also an impact on destructive processes. In our studies, we have examined the effect of singlet oxygen in *Arabidopsis thaliana* and *Chlamydomonas reinhardtii*. Due to a very effective antioxidant defense system, plants are able to keep the level of singlet oxygen in balance. When plants are exposed to various types of stress, such as high light intensity and heat investigated in this project, an overproduction of singlet oxygen may occur and become out of balance in the biological system. It is important to understand the role and mechanism of the antioxidant defense system in plants, such as the involvement of isoprenoid quinones, since it provides valuable information that may be used to prevent harmful effects. In the case of antioxidant failure, the resulting oxidative stress may damage biomolecules including proteins, nucleic acids, polysacharides and lipids. We have developed a model reaction to understand the mechanism of singlet oxygen chemical quenching by isoprenoid quinones and the formation of their oxidation products. In our studies, we have provided direct evidences that isoprenoid quinones and their oxidation products serve as effective chemical quenchers of singlet oxygen. We were able to detect singlet oxygen formation *in vivo* using microscopic techniques. Lipid peroxidation occurs in three phases: initiation, propagation and termination. The unsaturation of lipids significantly increases the probability of their interaction with neighbouring biomolecules. In *Chlamydomonas reinhardtii* we have observed that heat stress mainly causes an increase of primary and secondary products of lipid peroxidation due to lipoxygenases activity.

Key words: singlet oxygen, isoprenoid quinones, lipid peroxidation

Number of pages including references: 48

Number of appendices: 3

Language: English

Bibliografická identifikace

Jméno a příjmení autora: Mgr. Ursula Rácová (roz. Ferretti)

Název práce: Vliv singletního kyslíku na nenasycené lipidy a isoprenoidní chinony v rostlinách

Typ práce: doktorská

Oddělení: Katedra biofyziky

Vedoucí práce: Doc. RNDr. Pavel Pospíšil, Ph.D.

Konzultant: Mgr. Marek Rác, Ph.D.

Rok obhajoby práce: 2023

Abstrakt:

Singletní kyslík je excitovaná nepřetržitě generovaná forma molekulárního kyslíku v rostlinných metabolických drahách. Singletní kyslík je velmi důležitým prvkem v signálních cestách, nicméně má i zásadní vliv na destruktivní procesy v rostlinách. V našich studiích jsme zkoumali vliv singletního kyslíku u *Arabidopsis thaliana* a *Chlamydomonas reinhardtii*. Díky velmi účinnému antioxidačnímu obrannému systému jsou rostliny schopny udržovat hladinu singletního kyslíku v rovnováze. Při vystavení rostlin různým druhům stresu, v našem případě vysoké intenzitě světla a zvýšené teplotě, dochází k nadprodukci singletního kyslíku a k nerovnováze v biologickém systému. Důležitost pochopení role a mechanismu antioxidačního obranného systému rostlin, jako je zapojení isoprenoidních chinonů, poskytuje cenné informace, jak předcházet škodlivým faktorům. V případě selhání antioxidantů, dochází k oxidačnímu stresu a poškození biomolekul jako jsou proteiny, nukleové kyseliny, polysacharidy a lipidy. Vytvořili jsme modelovou reakci k pochopení mechanismu chemického zhášení singletního kyslíku isoprenoidními chinony a následné tvorby jejich oxidačních produktů. V našich studiích jsme poskytli přímé důkazy, že isoprenoidní chinony a jejich oxidační produkty slouží jako účinné chemické zhášeče singletního kyslíku. Pomocí mikroskopických technik jsme byli schopni detekovat tvorbu singletního kyslíku *in vivo*. K peroxidaci lipidů dochází ve třech fázích: iniciace, propagace a terminace. Nenasycenost lipidů výrazně zvyšuje pravděpodobnost jejich interakce se sousedními biomolekulami. U Chlamydomonas reinhardtii jsme pozorovali, že tepelný stres způsobuje především navýšení primárních a sekundárních produktů peroxidace lipidů v důsledku aktivity lipoxygenáz.

Klíčové slova: singletní kyslík, isoprenoidní chinoly, lipidová peroxidace

Počet stran včetně seznamu literatury: 48

Počet příloh: 3

Jazyk: Anglický

Declaration

I hereby declare that I have written this thesis independently as the orginal work. The complete list of used literature and other information sources is included in the section "References".

Olomouc, Czech Republic, 2023   Author

Content

List of Publications

This thesis is based on three papers, referred in the text by name of the first author. These research papers are enclosed at the end of the thesis.

I. **<u>Ferretti U.(35%)</u>, Ciura J., Ksas B., Rác M., Sedlářová M., Kruk J., Havaux M., Pospíšil P. (2018)** Chemical quenching of singlet oxygen by plastoquinols and their oxidized products in Arabidopsis. Plant Journal 95, 849-861 IF: 5.775
(Ferretti U. designed the experiments; performed sample preparation for all measurements; EPR; fluorescence spectroscopy measurements and participate to confocal laser scanning microscopy; attribute to writing the manuscript)

II. **Ksas B., Legeret B., <u>Ferretti U.(5%)</u>, Chevalier A., Pospíšil P., Alric J., Havaux M. (2018)** The plastoquinone pool outside the thylakoid membrane serves in plant photoprotection as a reservoir of singlet oxygen scavengers. Plant, Cell & Environment 41, 2277-2287 IF: 5.415
(Ferretti U. performed EPR measurements)

III. **Prasad A., <u>Ferretti U.(15%)</u>, Sedlářová M., Pospíšil P. (2016)** Singlet oxygen production in Chlamydomonas reinhardtii under heat stress. Scientific Reports 6, 20094 IF: 4.122
(Ferretti U. performed sample preparation, HPLC measurements, FOX assay measurements, EPR spectroscopy measurements, participate to confocal laser scanning microscopy measurements and participate to writing the manuscript)

Papers by U. Ferretti that are not included in the thesis:

IV. **Janečková H., Husičková A., Ferretti U.(5%), Prčina M., Pilařová E., Plačková L., Pospíšil P., Doležal K., Špundová M. (2018)** The interplay between cytokinins and light during senescence in detached Arabidopsis leaves. Plant, Cell & Environment 41, 1870-1885 IF: 5.415
(Ferretti U. performed HPLC measurements of MDA)

V. **Janečková H., Husičková A., Lazár D., Ferretti U.(5%), Pospíšil P., Špundová M. 2019.** Exogenous application of cytokinin during dark senescence eliminates the acceleration of photosystem II impairment caused by chlorophyll b deficiency in barley. Plant Physiology and Biochemistry 136: 43–51. IF (2017): 2.718
(Ferretti U. performed HPLC pigment analysis)

Abbreviations

Asc	-	ascorbic acid
$^1Chl^*$	-	singlet excited state of chlorophyll
$^3Chl^*$	-	triplet excited state of chlorophyll
Car	-	carotenoid
^3Car	-	triplet excited state of carotenoid
DNPH	-	2,4-dinitrophenylhydrazine
EPR	-	electron pramagnetic resonance
Fe^{2+}	-	ferrous ion
Fe^{3+}	-	ferric ion
GPX	-	glutathione peroxidase
HGA	-	homogentisic acid
$HO^{\bullet}$	-	hydroxyl radical
$HO_2^{\bullet}$	-	hydroperoxyl radical
H_2O_2	-	hydrogen peroxide
HPLC	-	high performance liquid chromatography
HPPD	-	4-hydroxyphenylpyruvate dioxygenase
HPPR	-	4-hydroxyphenylpyruvate reductase
HST	-	homogentisate solanesyl transferase
L	-	lipid molecule
$L^{\bullet}$	-	lipid alkyl radical
LOH	-	hydroxy fatty acid
LOOH	-	lipid hydroperoxide
$LO_2^{\bullet}$	-	lipid peroxyl radical
$LO^{\bullet}$	-	lipid alkoxyl radical
LOX	-	lipoxygenase
MDA	-	malondialdehyde
MEP/DOXP pathway	-	methylerythrito 4-phosphate/deoxy-d-xylulose-5-phosphate pathway
MSBQ	-	2,3-dimethyl-6-solanesyl-1,4-benzoquinol
$^3O_2$	-	molecular oxygen
$^1O_2$	-	singlet oxygen
O_3	-	ozone
$O_2^{\bullet -}$	-	superoxide anion radical
PC-8	-	plastochromanol-8
POBN	-	α-(4-pyridyl-1-oxide)-N-tert-butylnitrone
PQ-9	-	plastoquinone-9
PQ-n	-	PQ with n isoprenoid units in the side-chain
PQ pool	-	plastoquinone pool
PQH_2-9	-	plastoquinol-9
$PQH^{\bullet}$-9	-	semiplastoquinone-9
PQ(OH)-9	-	hydroxyplastoquinone-9
$PQ(OH)_3$-9	-	trihydroxyplastoquinone-9
$^3[P680^{\bullet +}Pheo^{\bullet -}]$	-	triplet radical pair
PSI	-	photosystem I
PSII	-	photosystem II
$R^{\bullet}$	-	organic alkyl radical
ROOH	-	hydroperoxide
ROS	-	reactive oxygen species

RO$_2$$^\bullet$	-	peroxyl radical
RO$^\bullet$	-	alkoxyl radical
SOSG	-	singlet oxygen sensor green
SOSG-EP	-	SOSG endoperoxide
SPY-LHP	-	probe 2-(4-diphenylphosphanyl-phenyl)-9-(1-hexyl-heptyl)-anthra[2,1,9-def,6,5,10-d'e'f'] diiso-quinoline-1,3,8,10-tetraone
SPY-LHPox	-	oxidized form of SPY-LHP
SPD	-	solanesyl diphosphate
SPS	-	solanesyl diphosphate synthase
SPS1oex	-	*Arabidopsis thaliana* lines overexpressing the *solanesyl diphosphate synthase 1* gene
TAP	-	tris-acetate-phosphate medium
TAT	-	tyrosine aminotransferase
TEP	-	1,1,3,3-tetrahydroxypropane
TEMP	-	2,2,6,6-tetramethylpiperidine
TEMPO	-	2,2,6,6-tetramethylpiperidine-1-oxyl
TEMPONE	-	2,2,6,6-tetramethyl-4-piperidone-1-oxyl
TEMPD	-	2,2,6,6-tetramethyl-4-piperidone
TMPD	-	2,2,6,6-tetramethyl-4-piperidone hydrochlorid
TM	-	thylakoid membranes
Toc	-	tocopherol
TrxPX	-	thioredoxin peroxidase
vte1	-	*Arabidopsis thaliana* lines deficient in tocopherol
vte1SPS1oex	-	*Arabidopsis thaliana* lines crossed between vte1 and SPS1oex
VTE1	-	tocopherol cyclase
VTE3	-	phytylbenzoquinone methyltransferase
WT	-	wild type

1 Introduction

The presented theses describes the effect of singlet oxygen ($^1O_2$), formed under different stress conditions, in *Arabidopsis thaliana* and *Chlamydomonas reinhardtii*. The thesis focuses on the mechanism itself (oxidative and antioxidative) and on the specific products which are formed during the reaction process.

Reactive oxygen species (ROS) are reduced and excited forms of molecular oxygen. Reactive oxygen species, especially $^1O_2$, are very important elements in signaling pathways, although ROS may also have destructive effects (Foyer, 2018; Triantaphylides and Havaux, 2009). Plants are equipped with an antioxidant defense system (antioxidants), the function of which is to keep the level of $^1O_2$ in balance. Exposure of plants to various types of stress, abiotic or biotic, causes an overproduction of $^1O_2$ and a change in balance in biological system (Liebthal and Dietz, 2017; Triantaphylides and Havaux, 2009). Understanding the mechanisms by which $^1O_2$ is produced and eliminated provides valuable information about the importance of the role of antioxidants, such as isoprenoid quinones, in the plant defense against their harmful effects. In case of antioxidant failure, the resulting oxidative stress can damage biomolecules such as proteins, nucleic acids, polysacharides and lipids (Sachdev et al., 2021). Lipid peroxidation is an oxidative chain reaction, which is divided into three phases: initiation, propagation and termination. The presence and frequency of double bonds between carbon atoms in lipids, i. e. unsaturation, significantly increases the probability of their interaction with neighbouring biomolecules. During lipid peroxidation so-called primary and secondary products are formed (Porter et al., 1995; Yin et al., 2011).

The first chapter of the thesis describes ROS formation in plants, especially $^1O_2$. The second chapter deals with the plant antioxidant system, in particular with isoprenoid quinones and their function as efficient quenchers. The last chapter is focused on lipid peroxidation, its causes, and consequences.

The thesis is written in the form of a mini-review, summarizing the current knowledge related to the topic. The results of my research published in **Prasad et al., 2016; Ferretti et al., 2018; Ksas et al., 2018** are discussed in the context these up-to-date findings and are referenced in the text by bold purple letters. The publications themselves are enclosed in the Appendix of the thesis.

1.1 Reactive oxygen species

Reactive oxygen species (ROS) are known to be produced continuously by oxidative metabolic processes in organisms in these cell compartments: chloroplasts, mitochondria, plasma membrane, microbodies, and endoplasmic reticulum (Halliwell and Gutteridge, 2007; Halliwell, 2011; Khorobrykh et al., 2020). However, exposure of organisms to various types of abiotic or biotic stress, can cause an overproduction of ROS that changes the oxidative balance in the biological system. In photosynthetic organisms, it is well established that ROS are formed either by excitation energy transfer from triplet excited states of chlorophylls ($^3Chl^*$) to molecular oxygen ($^3O_2$) or by electron transport from highly reducing species to $^3O_2$ (Halliwell and Gutteridge, 2007). Reactive oxygen species can be classified as non-radical and radical forms. The non-radical form includes ROS with no unpair electron per oxygen atom, as singlet oxygen ($^1O_2$, $^1\Delta g$), hydrogen peroxide (H_2O_2) or ozone (O_3), while the radical forms include ROS with one or two unpaired electrons on an oxygen atom, as in the superoxide anion radical ($O_2^{\bullet-}$), hydroperoxyl radical ($HO_2^{\bullet}$), hydroxyl radical ($HO^{\bullet}$). Other molecules containing an active oxygen are classified as ROS derivatives such as organic peroxyl radical ($RO_2^{\bullet}$) and organic alkoxyl radical ($RO^{\bullet}$). It is well known that both the non-radical and radical forms of ROS and their derivatives are highly efficient at oxidising various biomolecules such as lipids, proteins and nucleic acids in the cell (Khorobrykh et al., 2020).

1.1.1 Non-radical forms

The main ROS formed during photooxidative stress in plants by photosystem II (PSII) is the very reactive $^1O_2$ (half life 1-4 µs). The formation of $^1O_2$ occurs by triplet-singlet energy transfer from triplet chlorophyll ($^3Chl^*$) to $^3O_2$ (Triantaphylides and Havaux, 2009; Fischer et al., 2013; Telfer, 2014; Pospíšil, 2016), (Fig. 1). Triplet chlorophyl is formed either by the intersystem crossing in the PSII antenna complex from singlet chlorophyll ($^1Chl^*$) or via the charge recombination of triplet radical pair $^3[P680^{\bullet+}Pheo^{\bullet-}]$ in the PSII reaction centre (Krieger-Liszkay et al., 2008; Triantaphylides and Havaux, 2009; Vass, 2012; Pospíšil 2012; van Amerongen and Croce, 2013). Singlet oxygen can be generated by several chemical reactions involving H_2O_2, $O_2^{\bullet-}$ and reactive oxygen derivatives such as hydroperoxides (ROOH) via the Russel mechanism (Prasad et al., 2016) or $RO_2^{\bullet}$ (Khorobrykh et al., 2020). Another stress that causes formation of $^1O_2$ in photosynthetic organisms such as cyanobacteria, algae and plants is heat, which is known to be involved in lipid peroxidation (Liu and Huang, 2000; Larkindale and Knight, 2002). There is evidence from *in vitro* experiments that supports $^1O_2$ formation in

chloroplasts, thylakoid and PSII membranes after their exposure to heat stress (Hideg et al., 1994; Pospíšil et al., 2007; Yamashita et al., 2008). Singlet oxygen may then be formed via enzymatic lipid peroxidation initiated by lipoxygenase (**Prasad et al., 2016**). Various types of low molecular weight antioxidants were shown to control the levels of $^1O_2$ by physical or chemical quenching (Foyer and Noctor, 2009; Triantaphylides and Havaux, 2009; Fischer et al., 2013; Pospíšil and Prasad, 2014). During mild stress, the antioxidant system maintains low $^1O_2$ levels, since $^1O_2$ is essential for the retrograde signaling in the acclimation response and programmed cell death (Mullineaux and Baker, 2010; Zhang et al., 2014; Laloi and Havaux, 2015; Dietz et al., 2016). When the stress becomes severe, the formation of $^1O_2$ exceeds the capacity of the antioxidant systems, and $^1O_2$ causes irreversible damage to biomolecules (lipids and proteins) associated with accidental cell death (Aro et al., 2005; Ledford and Niyogi, 2005; Van Breusegem and Dat, 2006; Farmer and Mueller, 2013; Pospíšil and Yamamoto, 2017).
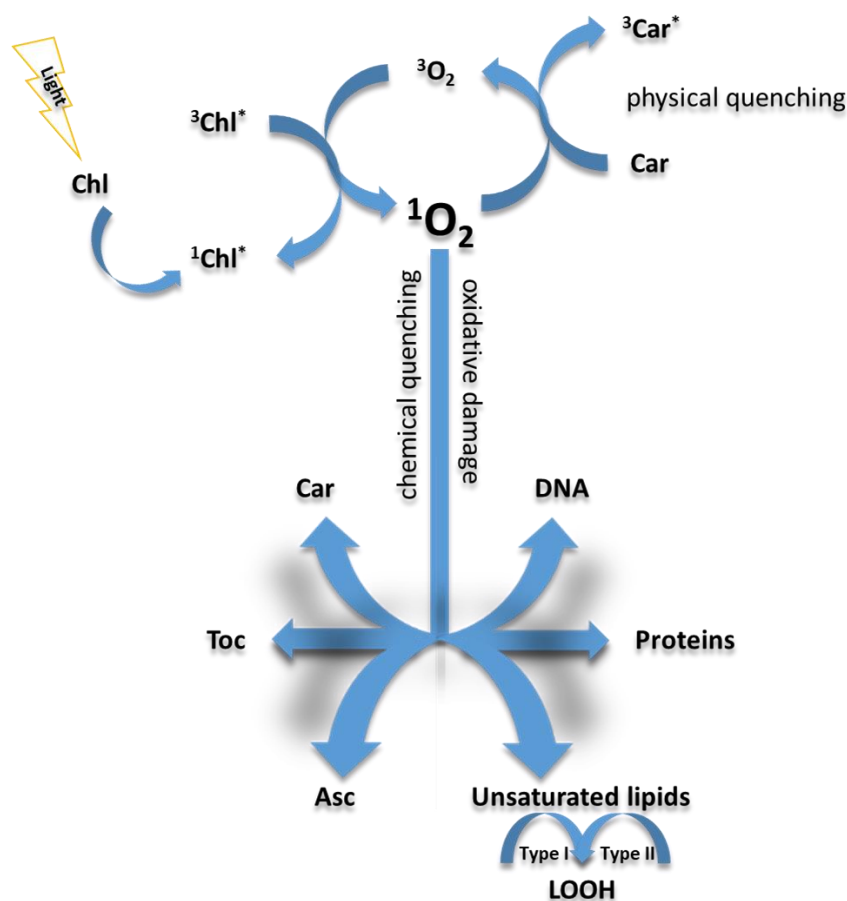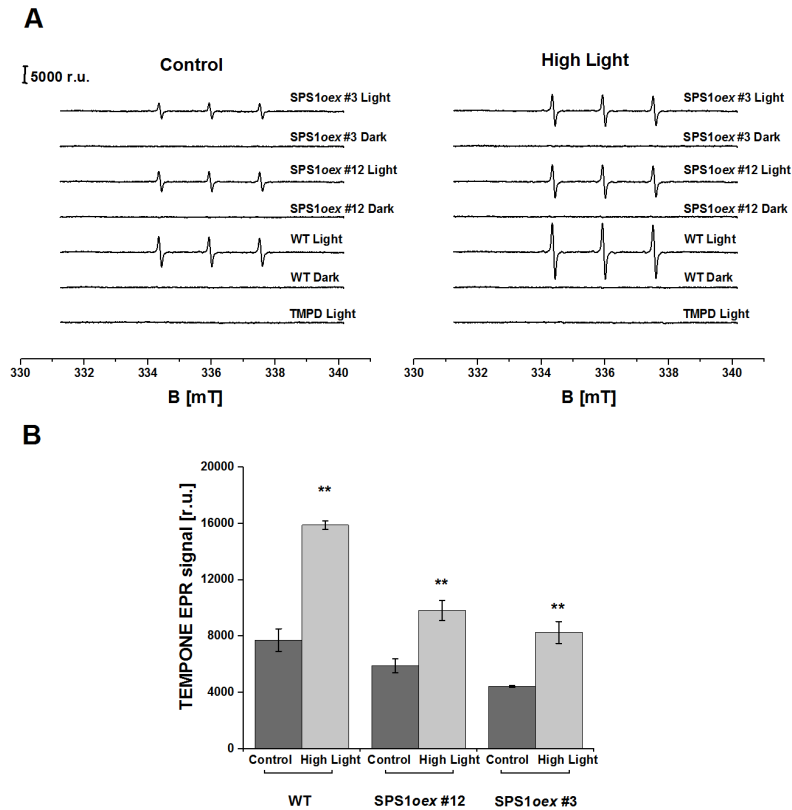

Figure 1. Singlet oxygen generation by excited chlorophyll and possible reaction pathways. $^3O_2$, molecular oxygen; $^1O_2$, singlet oxygen; Chl, chlorophyll; $^3Chl^*$, triplet excited state of chlorophyll; $^1Chl^*$, singlet excited state of chlorophyll; Car, carotenoid; ^3Car, triplet excited state of carotenoid; Toc, tocopherol; Asc, ascorbic acid; DNA, deoxyribonucleic acid; LOOH, lipid hydroperoxide. Scheme modified by Fischer et al., 2013

In our work (**Ferretti et al., 2018**), we have studied the role of plastoquinols as chemical quenchers of $^1O_2$ comparing *Arabidopsis thaliana* lines overexpressing the *solanesyl diphosphate synthase 1* gene (SPS1oex) with the wild-type Col 0 (WT). We detected the formation of $^1O_2$ in SPS1oex Arabidopsis leaves using confocal laser scanning microscopy using the fluorescent probe singlet oxygen sensor green (SOSG). SOSG reacts with $^1O_2$ forming a fluorescent SOSG endoperoxide (SOSG-EP) by the cycloaddition of $^1O_2$ (Flors et al., 2006). We provided evidence that plastoquinols and their oxidation products serve as effective chemical quenchers of $^1O_2$ *in vivo*. The localization of SOSG-EP fluorescence in leaf tissues of control and high light exposed WT and SPS1oex Arabidopsis is shown in Fig. 2. The SOSG-EP fluorescence in SPS1oex was apparently lower as compared to WT. Singlet oxygen imaging showed that $^1O_2$ was significantly chemically quenched in SPS1oex Arabidopsis leaves.
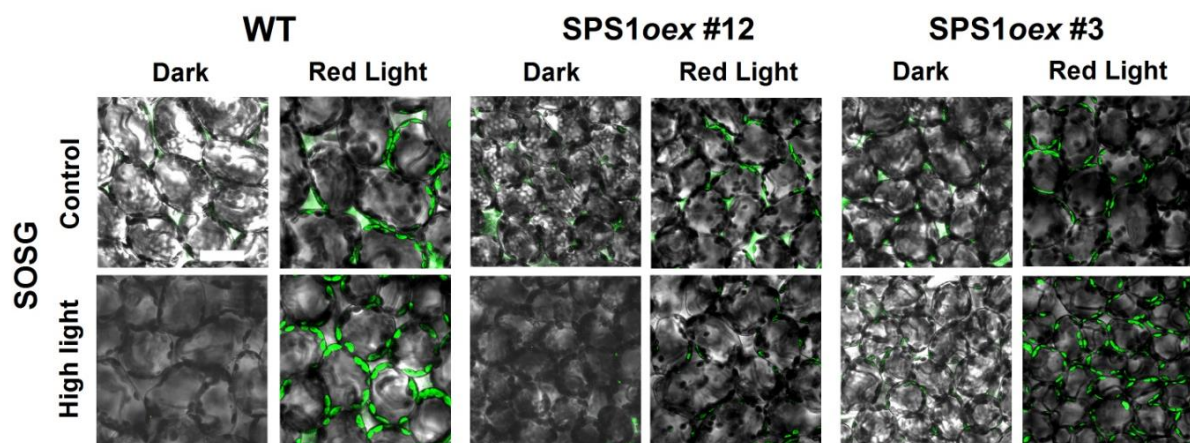

Figure 2. Singlet oxygen imaging in control and high light exposed WT and SPS1oex Arabidopsis plants monitored by confocal laser scanning microscopy. Arabidopsis plants were kept under low light (120 µmol photons $m^{-2}s^{-1}$, 8 hrs and 25 ˚C) (control) or exposed to high light (1000 µmol photons $m^{-2}s^{-1}$, 13 hrs and 8 ˚C) (high light). Prior to measurement, Arabidopsis leaves were kept in the dark or illuminated with red light (1000 µmol photons $m^{-2}s^{-1}$) for 30 min in the presence of 50 µM SOSG. The images represent the combination of the Nomarski DIC and fluorescence channels. Bar represents 40 µm.

We (**Ferretti et al., 2018**) have analysed the formation of $^1O_2$ in broken chloroplasts isolated from WT and SPS1oex Arabidopsis. This was performed by electron paramagnetic resonance (EPR) spectroscopy applying the hydrophilic diamagnetic spin probe 2,2,6,6-tetramethyl-4-piperidone hydrochloride (TMPD) (Fig. 3A). The oxidation of TMPD by $^1O_2$ yields paramagnetic 2,2,6,6-tetramethyl-4-piperidone-1-oxyl (TEMPONE) (Moan and Wold, 1979). Data obtained by EPR spin-trapping spectroscopy revealed that about one half of $^1O_2$ was quenched by plastoquinols and their oxidized products (Fig. 3B).

Figure 3. Singlet oxygen formation in broken chloroplasts of control and high light exposed WT and SPS1oex Arabidopsis plants detected by EPR spin-trapping spectroscopy. (A) TEMPONE EPR spectra detected after 30 min white light treatment (1000 μmol photons $m^{-2} s^{-1}$) of broken chloroplasts from Arabidopsis in the presence of 50 mM TMPD. TEMPONE EPR spectrum of pure probe (bottom spectrum) was obtained after illumination of 50 mM TMPD and 40 mM MES-NaOH buffer (pH 6.5) with white light (1000 μmol photons $m^{-2} s^{-1}$) for 30 min. (B) The intensity of TEMPONE EPR signal was determined by measuring the relative height of central peak of the EPR absorption spectrum. Presented data are mean values (n = 3), ± SD. The asterisk indicates significant difference between control and high light exposed WT and SPS1oex Arabidopsis (Student´s test). Significant differences were confirmed also between WT and SPS1oex Arabidopsis (ANOVA).

In our work (**Ksas et al., 2018**), we have examined the photoprotective role of the plastoquinone pool (PQ pool) by comparing Arabidopsis lines of WT, deficient in tocopherol (vte1), SPS1oex described above and a cross between them (vte1SPS1oex). The formation of $^1O_2$ in thylakoid membranes from these Arabidopsis lines was monitored by EPR spectroscopy after applying the spin probe 2,2,6,6-tetramethyl-4-piperidone (TEMPD) (Fig. 4A). The oxidation of TEMPD by $^1O_2$ produces TEMPONE as well. The thylakoid membranes of vte1 produced the highest $^1O_2$ signal, while in thylakoid membranes from SPS1oex and the double mutant vte1SPS1oex $^1O_2$ formation was less than in WT, affirming the role of plastoquinols as chemical quenchers of $^1O_2$ (Fig. 4B).
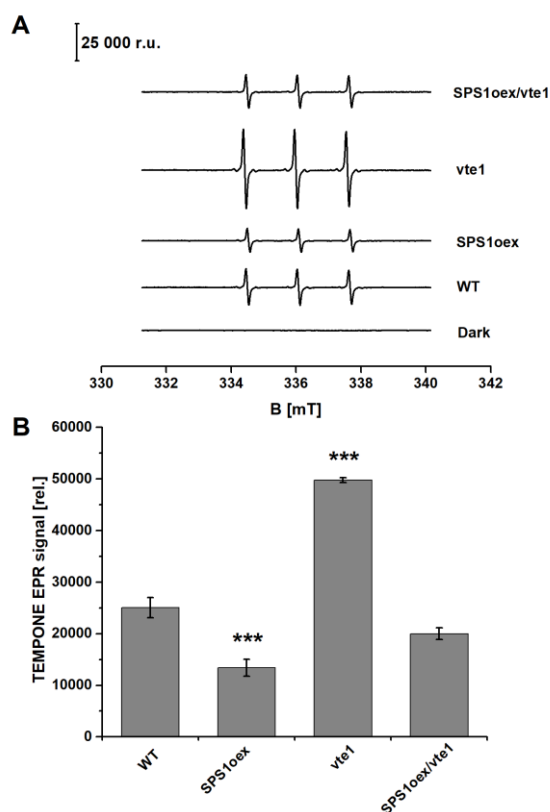
Figure 4. Singlet oxygen production by thylakoids: (A) TEMPONE EPR spectra detected after 30 min white light treatment (1500 μmol photons $m^{-2} s^{-1}$) of broken chloroplasts from Arabidopsis in the presence of 50 mM TMPD. TEMPONE EPR spectrum of pure probe (bottom spectrum) was obtained after illumination of 50 mM TMPD and 40 mM MES-NaOH buffer (pH 6.5) with white light (1500 μmol photons $m^{-2} s^{-1}$) for 30 min. (B) The intensity of TEMPONE EPR signal was determined by measuring the relative height of central peak of the EPR absorption spectrum. Presented data are mean values (n = 3), ± SD. The asterisk indicates significant difference of mutants from WT at $P < 0.01$, $P < 0.005$ and $P < 0.001$ (Student's t-test).

Singlet oxygen formation *in vivo* in the unicellular green alga *Chlamydomonas reinhardtii* was demonstrated in our work (Prasad et al., 2016). Chlamydomonas cells were exposed to heat stress (40 °C), after which $^1O_2$ formation was visualised by lase confocal scanning microscopy using the fluorescent probe SOSG. Figure 5 shows the Nomarski DIC images, the SOSG fluorescence, chlorophyll fluorescence and the integral distribution of SOSG fluorescence intensity measured in Chlamydomonas cells. The SOSG fluorescence representing the formation of $^1O_2$ had a very strong emission in cells exposed heat stress compared to those which where at room temperature. The SOSG intensity showed us that the integral distribution of fluorescence was enhanced by about 6 times. We observed that caffeic acid and catechol, which are inhibitors of lipoxygenase activity, significantly reduced the formation of $^1O_2$, consistent with lipoxygenase initiating lipid peroxidation leading to $^1O_2$ formation.
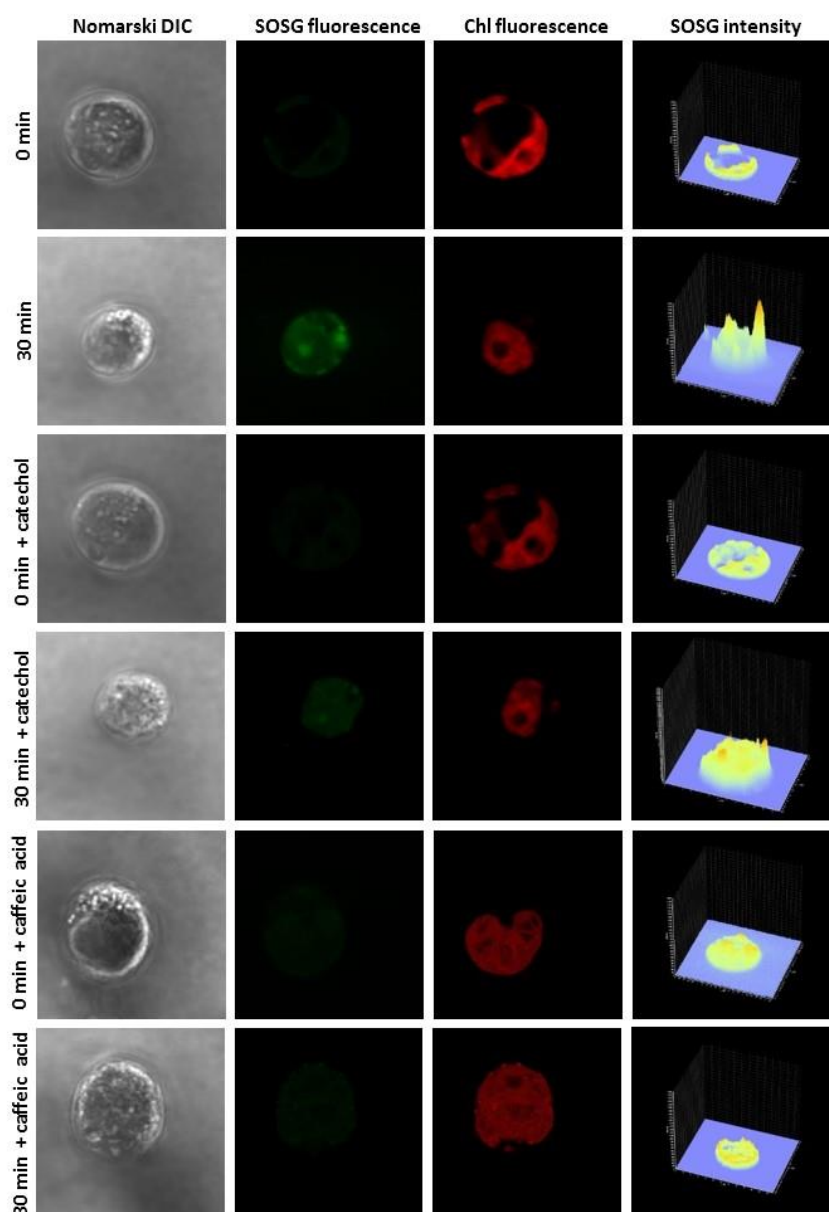
Figure 5. Detection of singlet oxygen in Chlamydomonas cells by laser confocal scanning microscopy. The formation of $^1O_2$ was measured in non-heated and heated Chlamydomonas cells in the presence and the absence of catechol and caffeic acid using fluorescent probe SOSG. Heated cells were treated for 30min in a water bath at 40 °C in the dark. The images represent from left to right: Nomarski DIC, SOSG fluorescence, chlorophyll fluorescence and integral distribution of SOSG signal intensity (0–4096) in the 12-bit microphotographs.

The $^1O_2$ formation in heated Chlamydomonas cells was quantified in our study (**Prasad et al., 2016**) using EPR spin-trapping spectroscopy. The detection of $^1O_2$ was achieved using the oxidation of $^1O_2$ with the lipophilic diamagnetic 2,2,6,6-tetramethylpiperidine (TEMP). This reaction yields paramagnetic 2,2,6,6-tetramethylpiperidine-1-oxyl (TEMPO) (Fig. 6). Due to the impurity of the spin trap a negligible TEMPO EPR signal was visible in non-heated Chlamydomonas cells. After the heat stress exposure of Chlamydomonas cells in the presence

of TEMP a clear increase in TEMPO EPR signal was produced (Fig. 6A). The result indicates that there is a linear increase of $^1O_2$ formation up to 30 min of heat exposure, which suggests that $^1O_2$ formation continuously increases heat exposure. The concentration of $^1O_2$ in treated cells was obtained using TEMPO as a standard (Fig. 6B, insert).
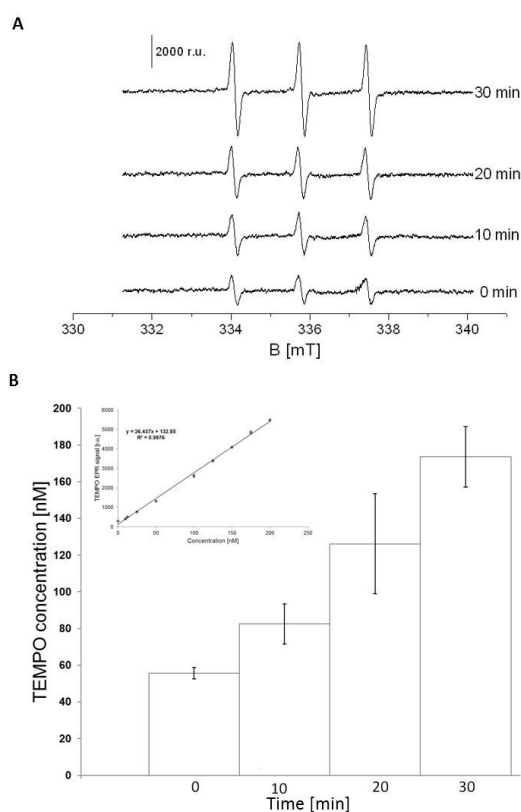
Figure 6. EPR spin-trapping detection of singlet oxygen formation from Chlamydomonas cells. Detection of $^1O_2$ by EPR spin-trapping spectroscopy in Chlamydomonas cells. EPR spectra were detected after heat treatment for 0, 10, 20 and 30min at 40 °C in the presence of 50mM TEMP. (A) shows the time profile of TEMPO EPR spectra. The intensity of the EPR signal was determined by measuring the relative height of central peak of the EPR absorption spectrum. Bar represents 2000 r.u. In (B) The presented data are expressed as the mean value and the standard deviation of at least three measurements (mean± SD, n= 3). (B) the concentrations of TEMPO established from the inserted calibration curve (equation y= 26.437x+ 132.85) were as follow: 55.64± 3.04 nM (0min), 82.49± 10.89 nM (10min), 126.09± 27.28 nM (20min) and 173.55± 16.39nM (30min). The coefficient of determination R^2 was determined as 0.9976.

Hydrogen peroxide is a stable non-radical form of ROS with hydrophobic character and long half life (1 ms). The formation of H_2O_2 in plants occurs in stroma in photosystem I (PSI) and PSII by enzymatic and non-enzymatic one-electron reduction of $O_2^{•-}$, respectively. It is also formed within the thylakoid membrane in the PQ-pool by the reaction of $^1O_2$ with plastoquinol-9 (PQH$_2$-9) or by the reaction of both the superoxide forms ($O_2^{•-}$, $HO_2^{•}$) with PQH$_2$-9 (Khorobrykh et al., 2015; Khorobrykh et al., 2020). Its ability to go through the plasma

membrane of the cell or organelle membranes makes H_2O_2 an excellent candidate for cellular signaling (Blokhina and Fagerstedt, 2010). It plays a key role as a regulator of physiological processes (photorespiration, photosynthesis, or growth and development of the cell) and as a secondary messenger for signals mediated by other ROS (Gill and Tuteja, 2010).

1.1.2 Radical forms

The superoxide anion radical is a moderately reactive radical with hydrophilic character and a very short half life (2-4 µs) (Halliwell, 2006). Therefore, it reacts only with molecules in its immediate vicinity. It is known that $O_2^{\bullet-}$ is formed by one-electron reduction of $^3O_2$ in PSII or by the Mehler reaction in PSI (Asada, 1999). Further, the reduction of $^3O_2$ to $O_2^{\bullet-}$ occurs either by plastosemiquinone in the PQ pool (Khorobrykh and Ivanov, 2002; Mubarakshina and Ivanov, 2010). The deleterious effect of $O_2^{\bullet-}$ is due to its capability to mediate the reduction of H_2O_2 to $HO^\bullet$ through the Fenton reaction. Further, the protonation of $O_2^{\bullet-}$ leads the formation of $HO_2^\bullet$, especially at the surface of the membrane, where the concentration of protons is high. Hydroperoxyl radical is more reactive than its anion form and can directly abstract a hydrogen atom from molecules even from greater distance due to its higher mobility (Khorobrykh et al., 2020).

One of the most powerful oxidizing agents with one unpaired electron is $HO^\bullet$. The hydrophobic character and very short half life <1ns allows $HO^\bullet$ to interact only with molecules in its immediate vicinity (Khorobrykh et al., 2020). The formation of $HO^\bullet$ occurs by metal-catalyzed reduction of either free or bound H_2O_2, in the well-known Fenton reaction. Generation of $HO^\bullet$ via free H_2O_2 occurs due to the classical reduction of free H_2O_2 with free ferrous ion (Fe^{2+}), liberated from damaged PSII. The reduction of bound H_2O_2 by the ferric-oxo species of PSII metal center produces $HO^\bullet$ as an intermediate product (Pospíšil 2012). Another well-known metal-catalyzed reaction, the Haber-Weiss reaction, forms $HO^\bullet$ by the decomposition of H_2O_2 by reaction with $O_2^{\bullet-}$. The $HO^\bullet$ is also produced via the photolysis of oxygen-containing species, such as nitrate anion or H_2O_2, which can absorb UV-B or UV-C radiation, respectively. Another source of $HO^\bullet$ is O_3, although O_3 has not been found in plants. The last reaction which might cause $HO^\bullet$ formation is a radical-radical reaction of $HO^\bullet$ with $RO_2^\bullet$ (Khorobrykh et al., 2020).

1.1.3 Reactive derivatives

The formation of $RO_2^\bullet$ occurs during peroxidation of biomolecules. In the non-radical reaction, the oxidation of a nearby biomolecule by $^1O_2$ produces ROOH or non-radical endoperoxide (D'Ambrosio et al., 2011; Griesbeck and de Kiff, 2013). It is known that ROOH are oxidized by ferric ion (Fe^{3+}) to produce $RO_2^\bullet$. As $RO_2^\bullet$ is able to abstract hydrogen atom from adjacent biomolecules, the oxidation propagates in the same way as lipid peroxidation. The radical reaction is initiated by hydrogen abstraction from biomolecule by $HO^\bullet$ or $HO_2^\bullet$. The product of this reaction, an organic alkyl radical ($R^\bullet$), is further oxygenated to produce $RO_2^\bullet$ which can cyclize to form a radical endoperoxide and subsequently bicyclic endoperoxide (Onyango and Baba, 2010). To prevent the propagation, an antioxidant donates its hydrogen atom to $RO_2^\bullet$ forming an antioxidant alkyl radical and ROOH. The radical chain is terminated by creating a low-reactivity derivative unable to abstract a hydrogen atom from another biomolecule. However, $RO_2^\bullet$ may continue to react further when transition metals are present in its vicinity to produce $RO^\bullet$. The formation of $RO^\bullet$ occurs by one-electron reduction of ROOH (Fedorova et al., 2007).

Although scavenging of $RO_2^\bullet$ by different quinol-based antioxidants such as PQH_2-9 (Nowicka et al., 2013) or ubiquinol-10 has been previously studied (Bentinger et al., 2007; Lokhmatikov et al., 2014), no evidences that plastoquinone-9 (PQ-9) or another quinone-based antioxidant might eliminate $RO_2^\bullet$ was provided in the chemical as well as in the biological systems.

In our work (Ferretti et al., 2018), we detected ROOH in Arabidopsis leaves using the fluorescent probe 2 - (4 - diphenylphosphanyl - phenyl) - 9 - (1 - hexyl - heptyl) - anthra [2, 1, 9 - def, 6, 5, 10 - d'e'f'] diiso - quinoline - 1, 3, 8, 10 – tetraone (SPY- LHP). The probe SPY-LHP reacts selectively with hydroperoxides forming a fluorescent complex SPY-LHPox (Soh et al., 2007). The localization of SPY-LHPox fluorescence in leaf tissues of WT and SPS1oex Arabidopsis exposed to control and high light conditions is shown in Fig. 7. The SPY-LHPox fluorescence increased in both high light exposed WT and SPS1oex after exposure to red light in compare with control plants.
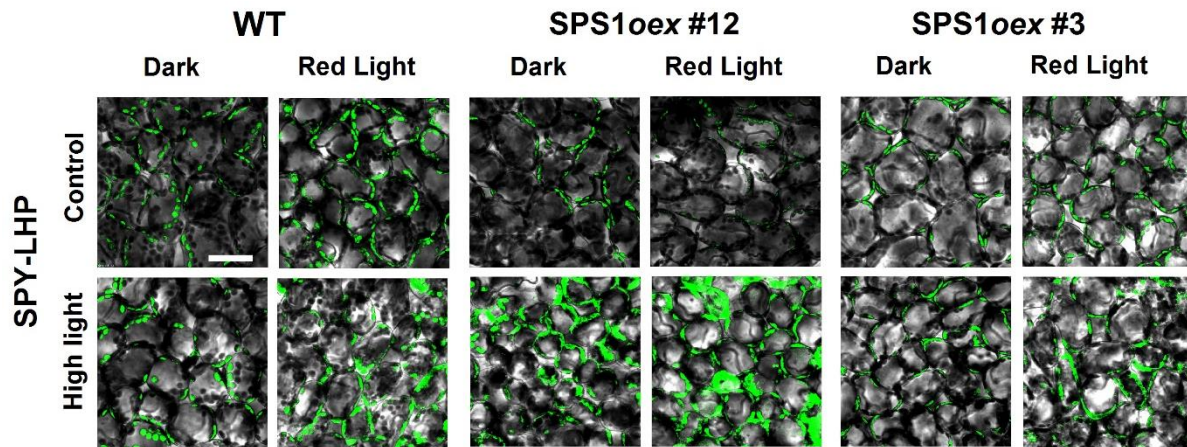
Figure 7. Organic hydroperoxides imaging in control and high light-exposed wild-type (WT) and SPS1oex Arabidopsis monitored by confocal laser scanning microscopy. Arabidopsis plants were kept under low light (120 μmol photons $m^{-2} s^{-1}$, 8 hrs and 25 °C) (control) or exposed to high light (1000 μmol photons $m^{-2} s^{-1}$, 13 hrs and 8 °C) (high light). Prior to measurement, Arabidopsis leaves were kept in the dark or illuminated with red light (1000 μmol photons $m^{-2} s^{-1}$) for 30 min in the presence of 50 μM SPY-LHP. The images represent the combination of the Nomarski DIC and fluorescence channels. Bar represents 40 μm.

The formation of R$^\bullet$ in Ferretti et al., 2018 was determined in broken chloroplasts isolated from WT and SPS1oex Arabidopsis by EPR spin-trapping spectroscopy applying the α-(4-pyridyl-1-oxide)-N-tert-butylnitrone (POBN) as spin-trap (Fig. 8). A paramagnetic form of POBN-R adduct is formed by the interaction of POBN with R$^\bullet$ (Buettner, 1987). Data obtained by EPR spin-trapping spectroscopy revealed a decline of R$^\bullet$ in SPS1oex Arabidopsis plants due to the scavenging activity of isoprenoid quinones.
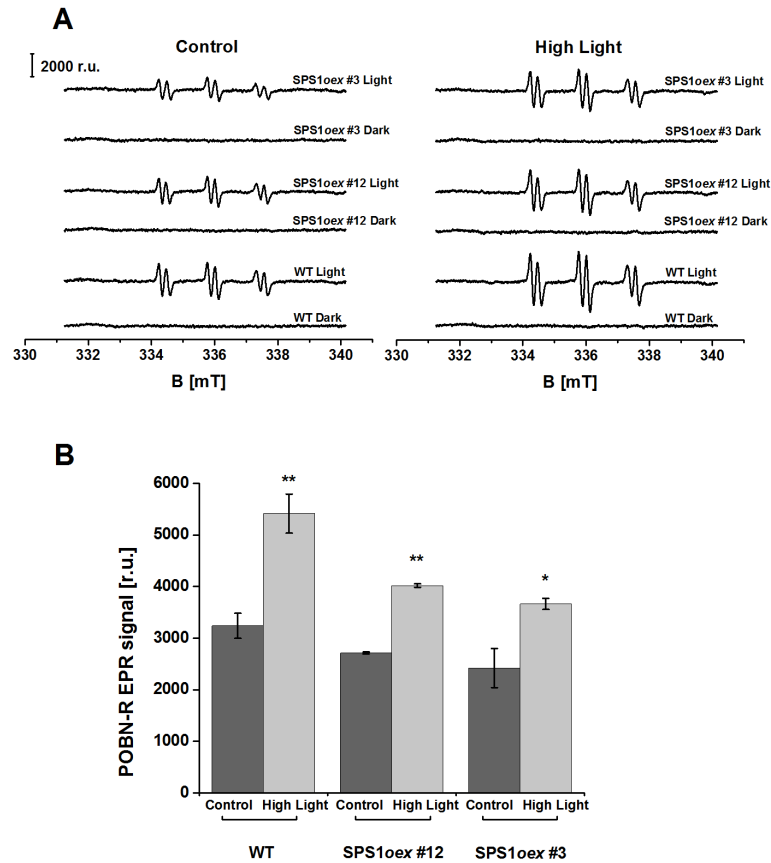
Figure 8. Organic radical formation in broken chloroplasts of control and high light exposed WT and SPS1oex Arabidopsis plants detected by EPR spin-trapping spectroscopy. (A) POBN-R adduct EPR spectra detected after 30 min white light treatment (1000 μmol photons m^{-2} s^{-1}) of broken chloroplasts from Arabidopsis in the presence of 50 mM POBN. (B) The intensity of POBN-R adduct EPR signal was determined by measuring the relative height of central peak of the EPR absorption spectrum. Presented data are mean values (n = 3), ± SD. The asterisk indicates significant difference between control and high light exposed WT and SPS1oex Arabidopsis (Student´s test). Significant differences were also confirmed between WT and SPS1oex Arabidopsis (ANOVA).

1.2 Antioxidant defense system – Isoprenoid quinones

The antioxidant defense system plays one of the most important roles in biological systems; it can be divided into non-enzymatic (low molecular weight) and enzymatic mechanisms.

Among the low molecular weight antioxidants, tocochromanols and isoprenoid quinones perform an important role in quenching excited oxygen species, such as $^1O_2$. Tocochromanols include tocopherols, tocotrienols and plastochromanols-8 (PC-8), all of which have in common a chromanol ring, but differ in chain length and saturation. Due to the chromanol ring, these substances are very effective in $^1O_2$ quenching (Trebst, 2003; Kruk et al., 2005; Krieger-Liszkay and Trebst, 2006; Dormann, 2007; Kruk et al., 2014). However, this limits their mobility and therefore reduces the possibility of interaction with $^1O_2$ (Kruk et al., 2014). Isoprenoid quinones, such as PQH_2-9 and PQ-9, are composed of a quinol or quinone ring and an unsaturated isoprenoid chain that contains nine double bonds (Eugeni Piller et al., 2012). Unlike the tocochromanols, the structure of isoprenoid quinones allows them to move easily (Jemiola-Rzeminska et al., 2003), which increases their likelihood of interaction with ROS. The PQH_2-9 and PQ-9 not only have an antioxidant function, but also serve as photosynthetic electron carriers in the thylakoid membranes of cyanobacteria, algae and higher plants. The different localization of these isoprenoid quinones (thylakoid membranes, plastoglobules and chloroplast envelopes) may indicate their diverse roles in chloroplasts (Figure 9). Whereas photoactive PQ-9 is located in the thylakoid membrane, non-photoactive PQ-9 involved in the antioxidant activity is stored in the plastoglobuli as well as in the inner chloroplast envelopes coupled to thylakoid membranes (Austin et al., 2006; Nowicka and Kruk, 2010; Havaux, 2020). Under high light stress, PQ-9 diffuses from the plastoglobules to the thylakoid to compensate the consumption of PQ-9 (Ksas et al., 2015; **Ksas et al., 2018**). Several lines of evidence indicate that PQ-9 and its reduced form perform chemical quenching of $^1O_2$ (Kruk and Trebst, 2008; Szymanska et al., 2014; Ksas et al., 2015; **Ksas et al., 2018**; **Ferretti et al., 2018**). Isoprenoid quinones comprise not only PQH_2-9 and PQ-9 but also their hydroxy forms formed by the reaction with $^1O_2$. These include hydroxyplastoquinone-9 (PQ(OH)-9 also known by the abbreviation PQ-C), which was identified in spinach (Kruk and Strzalka, 1998) and later in Arabidopsis (Szymanska et al., 2014)´, and trihydroxyplastoquinone-9 (PQ(OH)$_3$-9), which has been generated in a chemical system (Gruszka et al., 2008) and found in Arabidopsis (**Ferretti et al., 2018**).
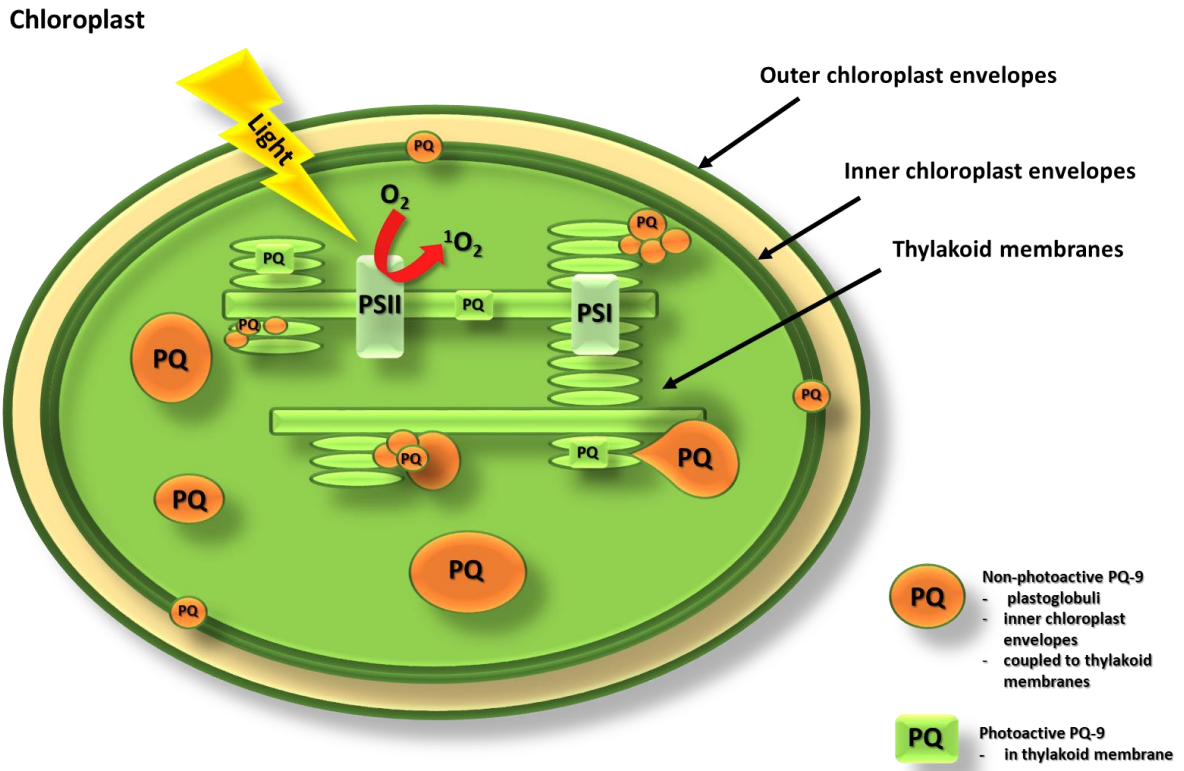
Figure 9. Localisation of non-photoactive and photoactive PQ-9 in chloroplast.

1.2.1 Biosynthesis

The isoprenoid quinones biosynthetic pathway in plants (Fig. 10) might be divided into two main parts. One part deals with the formation of the precursors of the quinone ring and the polyprenyl side chain. The second part comprise the condensation of the ring with side chain and the following modifications (Nowicka and Kruk, 2010; Liu and Lu, 2016; Havaux, 2020).

The head group precursor, homogentisic acid (HGA), is synthesized from tyrosine by tyrosine aminotransferase (TAT) and 4-hydroxyphenylpyruvate reductase (HPRP) to produce 4-hydroxyphenylpyruvate (HPP), from which HGA is formed by 4-hydroxyphenyl-pyruvate dioxygenase (HPPD). The polyprenyl side chain, also known as solanesyl diphosphate, is produced from glyceraldehyde 3-phosphate and pyruvate throught the methylerythritol 4-phosphate/deoxy-d-xylulose-5-phosphate (MEP/DOXP) pathway (Bouvier et al., 2005; Nowicka and Kruk, 2010; Liu et al., 2019; Havaux, 2020). Solanesyl diphosphate formation requires the activity of solanesyl diphosphate synthase (SPS) overexpression of the *SOLANESYL DIPHOSPHATE SYNTHASE* 1 gene in Arabidopsis (SPS1oex) results in accumulation of PQH_2-9, PQ-9 and PC-8; those overexpression lines were used in the **Ferretti et al., 2018** and **Ksas et al., 2018** studies. The condensation of HGA with solanesyl diphosphate is catalysed by homogentisate solanesyl transferase (HST) to form 2,3-dimethyl-6-solanesyl-1,4-benzoquinol (MSBQ). It is well known that the condensation reaction occurs in the inner chloroplast membrane and endoplasmic reticulum-golgi membranes (Soll et al., 1985; Swiezewska et al., 1993; Zbierzak et al., 2009). The MSBQ is then converted to PQH_2-9 by the catalytic activity of phytylbenzoquinone methyltransferase (VTE3) (Nowicka and Kruk, 2010). A fraction of the PQH_2-9 is converted by tocopherol cyclase (VTE1) to PC-8 (Szymanska and Kruk, 2010; Havaux, 2020). To investigate the role of PQ-9 in its localization and concentration, the vte1 Arabidopsis mutant, deficient in tocopherol and PC-8, was crossed with SPS1oex plants, described above, to generate vte1SPS1oex plants, which were used in **Ksas et al., 2018** studies.
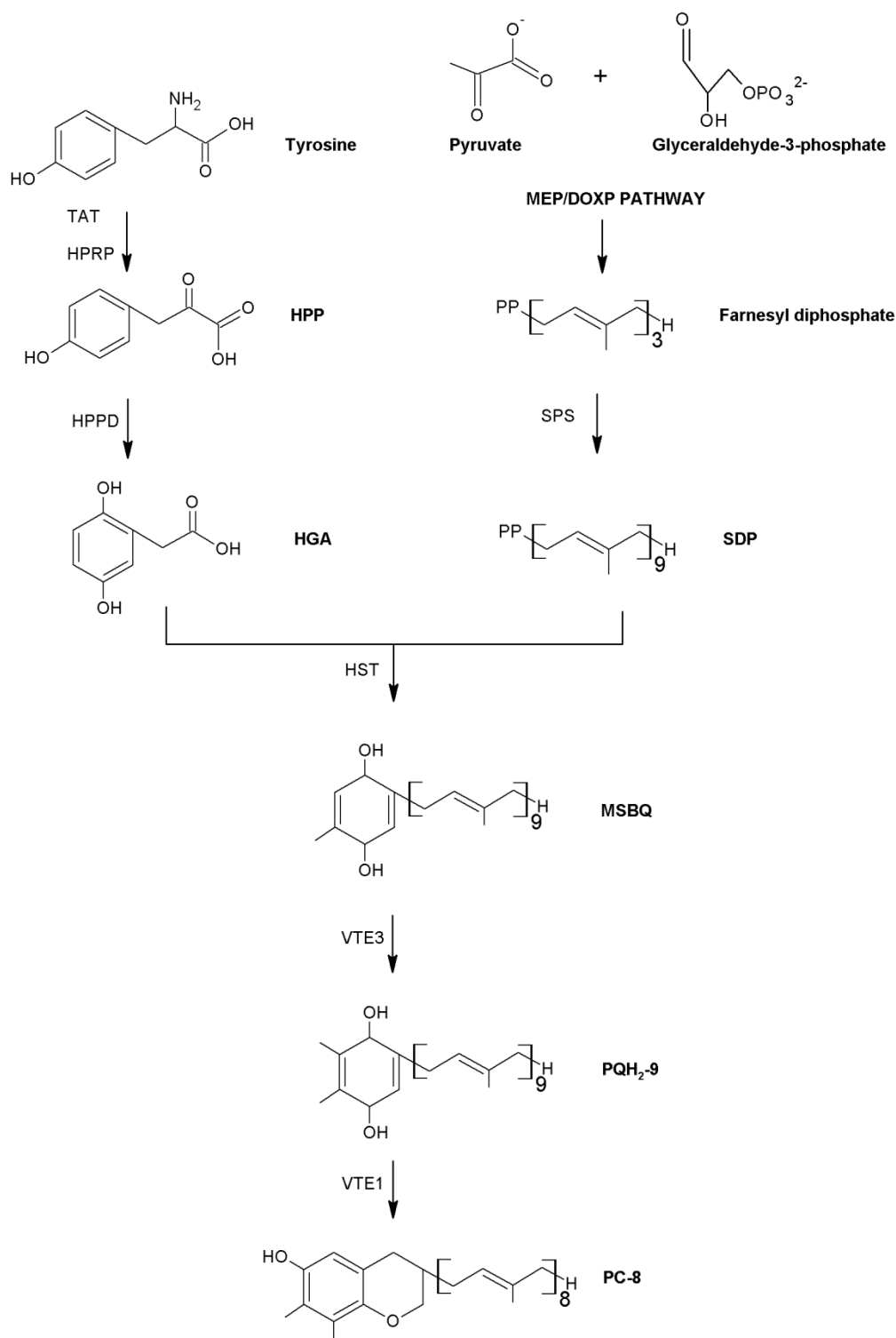
Figure 10. Plastoquinole-9 and plastochromanol-8 biosynthetic pathway. TAT, tyrosine aminotrasferase; HPRP, 4-hydroxyphenylpyruvate reductase; HPPD, 4-hydroxyphenylpyruvate dioxygenase; HGA, homogentisic acid; MEP/DOXP pathway, methylerythrito 4-phosphate/deoxy-d-xylulose-5-phosphate; SPS, solanesyl diphosphate synthase; SPD, solanesyl diphosphate; HST, homogentisate solanesyl transferase; MSBQ, 2,3-dimethyl-6-solanesyl-1,4-benzoquinol, VTE3, phytylbenzoquinone methyltransferase; VTE1, tocopherol cyclase. Scheme created by modifications from (Nowicka and Kruk, 2010; Havaux, 2020).

1.2.2 Antioxidant function

Isoprenoid quinones quench $^1O_2$ either by the excitation energy transfer (physical quenching) or by electron transport (chemical quenching) (Fig. 11) (Foote et al., 1970; Gorman et al., 1988; Mukai et al., 1993; Munné-Bosch, 2005). Physical quenching of $^1O_2$ by isoprenoid quinones occurs via singlet-triplet energy transfer, where the energy of $^1O_2$ is transferred to the quencher producing the triplet excited state, followed by heat dissipation (Gorman et al., 1988). During physical quenching one molecule of quencher can enable the deactivation of hundreds of molecules of $^1O_2$ might occur due to one molecule of quencher (Pospíšil 2012). Chemical quenching of $^1O_2$ by isoprenoid quinones results in oxidation of quinones forming a range of oxidation products (Mene-Saffrane and DellaPenna, 2010; Kruk et al., 2016). During chemical quenching the structure of the quencher is modified in such a way that only one molecule can quench just one molecule of $^1O_2$ (Pospíšil 2012). Chemical quenching of $^1O_2$ by isoprenoid quinones occurs by reaction with either the quinol ring or the unsaturated polyprenyl side-chain (**Ferretti et al., 2018**). It was previously demonstrated that the physical quenching of $^1O_2$ competes with the chemical quenching (Gorman et al., 1988).
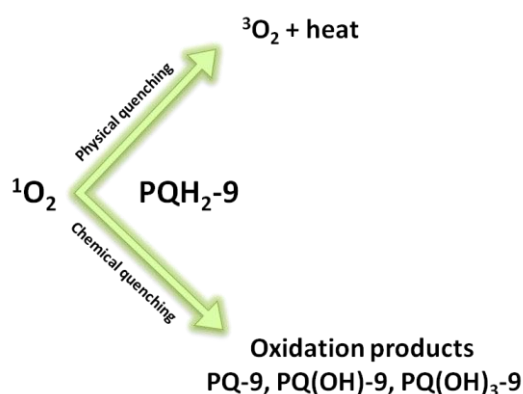
Figure 11. Scheme of physical and chemical quenching by PQH$_2$-9.

In our work (**Ferretti et al., 2018**), we have evaluated the amount of PQH$_2$-9, PQ-9 and total PQ-9 (PQH$_2$-9 + PQ-9) in leaves (Fig 12A) and broken chloroplasts (Fig 12B) from WT and SPS1oex Arabidopsis plants exposed to high light. For this purpose a high-performance liquid chromatography (HPLC) method was used. The content of PQH$_2$-9, PQ-9 and total PQ-9 was higher in SPS1oex than in WT. After exposure to high light, the content of PQH$_2$-9, PQ-9 and total PQ-9 noticeably decreased as compared to the control, presumably due to the chemical quenching activity in high light. From our work it appears that under normal conditions for quenching of $^1O_2$ by the available PQH$_2$-9, the physical quenching is more effective compared with chemical quenching. However, with the excessive $^1O_2$ formation due

to photooxidative stress, PQ-9 and other oxidation products act solely by chemical quenching. We have also determined the content of PC-8 in both leaves and broken chloroplasts (data not shown in thesis), and found that it was unchanged by high light stress. However, as the amount of the detected PC-8 was 40-times lower than that of isoprenoid quinones we considered its antioxidant function in this work to be negligible.
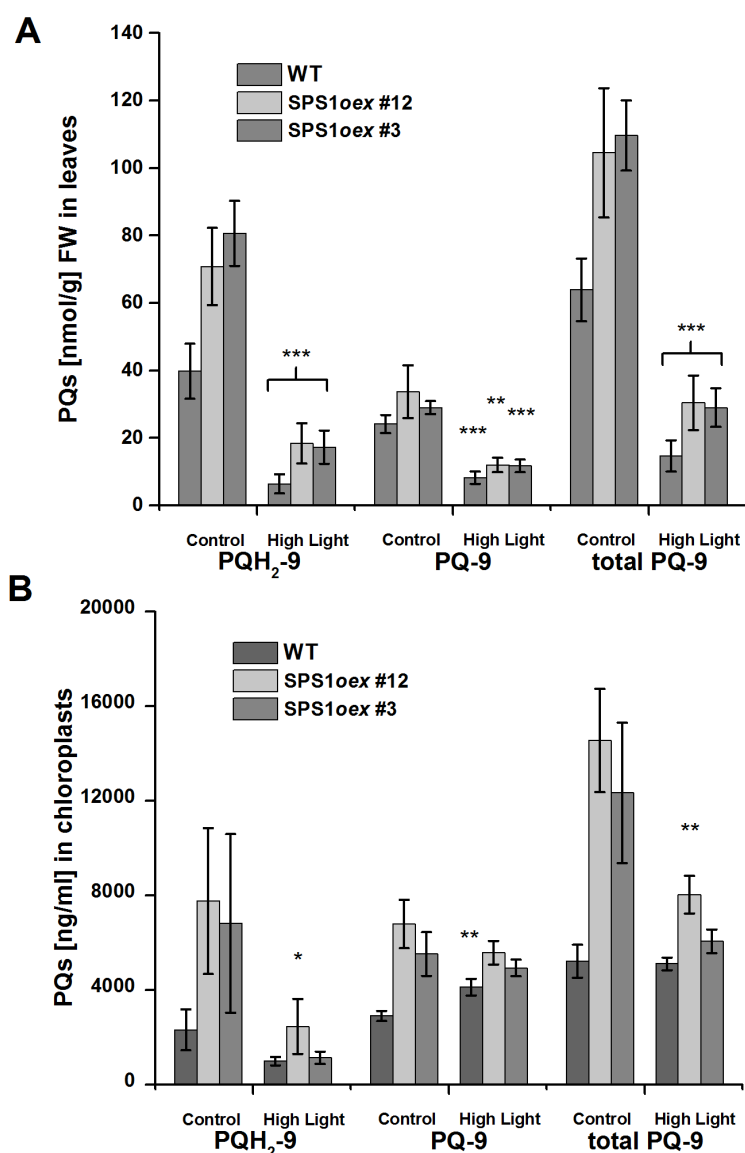
Figure 12. Plastoquinone content in leaves and broken chloroplasts of control and high light exposed WT and SPS1oex Arabidopsis plants determined by HPLC. A) Amount of PQH_2-9, PQ-9 and total PQ-9 in control and high light exposed WT, SPS1oex #12 and #3 Arabidopsis. Presented data are mean values (n = 4), ± SD. B) Amount of PQH_2-9, PQ-9 and total PQ-9 in broken chloroplasts of control and high light exposed WT, SPS1oex #12 and #3 Arabidopsis. Presented data are mean values (n = 3), ± SD. The asterisk indicates significant difference between control and high light exposed WT and SPS1oex Arabidopsis (Student's test): *, $P < 0.05$; **, $P < 0.01$; ***, $P < 0.001$. Significant differences were confirmed also between WT and SPS1oex Arabidopsis (ANOVA).

After measuring the isoprenoid quinone content, we monitored (**Ferretti et al., 2018**) the formation of PQH$_2$-9 oxidation products in WT and SPS1oex Arabidopsis plants using HPLC method. These include the very well-known PQ-9 and PQ(OH)-9 (Fig. 13, peaks at the retention time of 48 and about 15 min, respectively). Our work showed for the first time the appearance of another oxidation product of PQH$_2$-9 and that is PQ(OH)$_3$-9 (Fig. 13, peak at the retention time of about 7 min). This product was not previously identified *in vivo* and we confirmed it using a standard-containing a solution of illuminated PQ-9 with Rose Bengal (Fig. 13, bottom chromatogram). Another important finding from this study is that both PQ(OH)-9 and PQ(OH)$_3$-9 show the contribution of isomers.
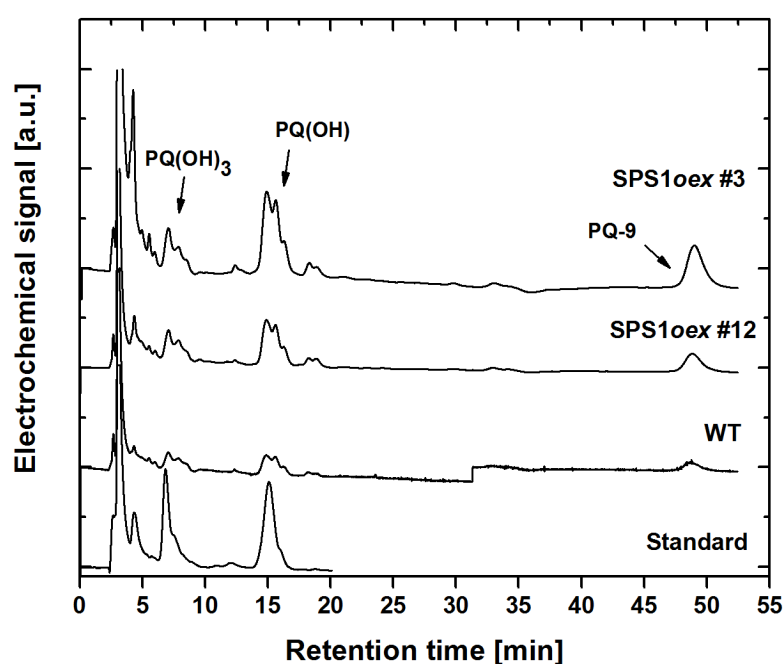
Figure 13. HPLC chromatograms of trihydroxyplastoquinone-9. Standard chromatogram of 10 µM PQ-9 in methanol with Rose Bengal as photosensitizer, after 10 min illumination (1500 µmol photons m^{-2} s^{-1}). Chromatograms of high light exposed WT and SPS1oex lines #12 and #3 Arabidopsis in methanol.

In (**Ferretti et al., 2018**), to clarify the role of light with PQ-9 in plants the content of total PQ-9 and its oxidized products was evaluated (Fig. 14). We showed that the amount of total PQ-9 produced in SPS1oex plants grown under control conditions was higher than in WT (Fig. 14A), while the amount of total PQ(OH)-9 and total PQ(OH)$_3$-9 produced in SPS1oex plants was approximately the same as in WT (Fig. 14B, C). However, in high light treated Arabidopsis plants the total PQ-9 content decreased noticeably as compared with control plants. At the same time the level of total PQ(OH)-9 and total PQ(OH)$_3$-9 increased, especially in SPS1oex plants (Fig. 14B, C).
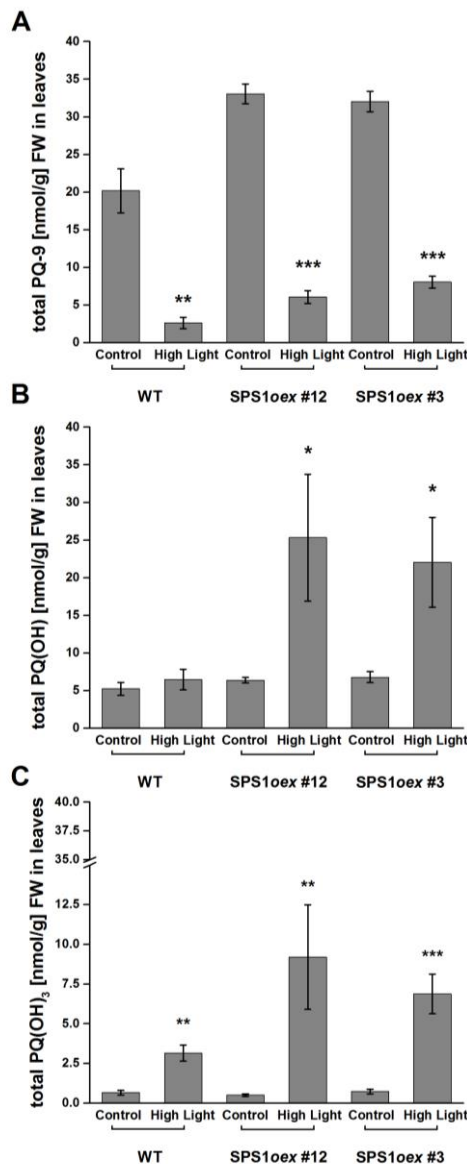
Figure 14. Content of oxidized products of plastoquinol-9 in control and high light exposed WT and SPS1oex Arabidopsis plants determined by HPLC. Total PQ-9 (A), total PQ(OH)-9 (B) and total PQ(OH)$_3$-9 (C) contents in control and high light exposed WT, SPS1oex #12 and #3 Arabidopsis. Presented data are mean values (n = 3), ± SE. Total = oxidized + reduced. The asterisk indicates significant difference between control and high light exposed WT and SPS1oex Arabidopsis (Student´s test). Significant differences were confirmed also between WT and SPS1oex Arabidopsis (ANOVA).

Based on the data, we proposed a model reaction in **Ferretti et al., 2018** to explain the mechanism of $^1O_2$ chemical quenching by isoprenoid quinones and the formation of PQH$_2$-9 oxidation products (Fig. 15). The difference in chemical structures between PQH$_2$-9 and PQ-9 indicates the way in which $^1O_2$ will interact with molecules. Reaction may occur with either the quinol ring or the unsaturated polyprenyl side-chain. However, alternative reaction pathways cannot be excluded.
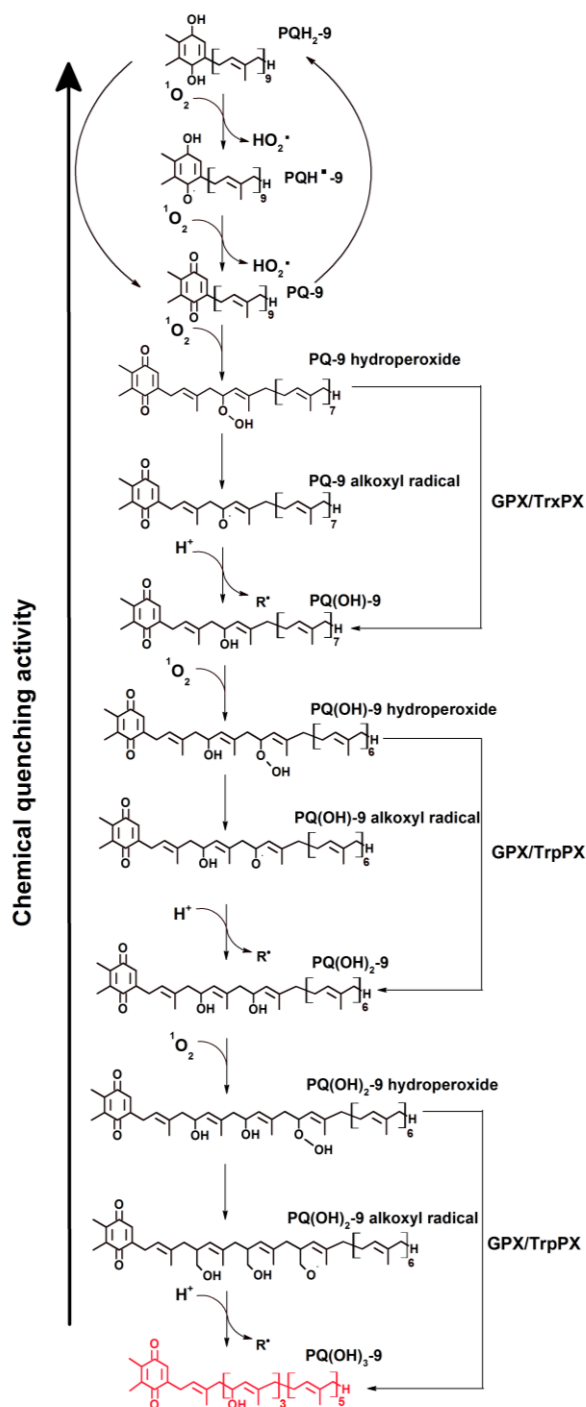
Figure 15. Formation of trihydroxyplastoquinone-9. Plastoquinol-9 function as an antioxidant of $^1O_2$ is illustrated. After PQH$_2$-9 oxidation with $^1O_2$ the well-known product PQ-9 is formed via PQH$^\bullet$-9, producing two molecules of HO$_2$$^\bullet$ which dismutate into H$_2$O$_2$. Subsequently reaction of PQ-9 with another $^1O_2$ molecule produces PQ(OH)-9 through decomposition of PQ-9 hydroperoxide by 1) radical reaction pathway comprising of PQ-9 alkoxyl radical as intermediate or 2) non-radical reaction pathway caused by enzymes of the gluthathione peroxidase (GPX) or thioredoxin peroxidase (TrxPX) families. Oxidation of PQ(OH)-9 probably proceeds similarly through PQ(OH)-9 hydroperoxide formation and decomposition by a radical or non-radical reaction to PQ(OH)$_2$-9, from which PQ(OH)$_3$-9 is produced via PQ(OH)$_2$-9 hydroperoxide in the same way.

As we observed from the collected data, the content of PQH$_2$-9 decreased after the exposure to high light, which can be caused by its reaction with $^1O_2$. Nontheless, different oxidation reactions may occur during chlororespiration (Kruk and Strzalka, 1999; Kruk and Karpinski, 2006; McDonald et al., 2011). We proposed that semiplastoquinone-9 (PQH$^\bullet$-9) might be produced with HO$_2^\bullet$ as a byproduct after the interaction of PQH$_2$-9 with $^1O_2$ (Fig. 15). Subsequently, PQH$^\bullet$-9 reacts with another $^1O_2$ molecule generating PQ-9 and another HO$_2^\bullet$ as a byproduct. The high accessibility of hydrogen atoms bounded in hydroxy groups on the quinol and semiquinone ring is necessary for the reaction with highly reactive $^1O_2$. The quinol and semiquinone ring functions as a conjugated system. Our proposal corresponds with the work presented by Wang and Eriksson, 2001, who showed that ubiquinones reacts with $^1O_2$ to produce a semiquinone radical and HO$_2^\bullet$. We proposed that by the dismutation of two molecules of HO$_2^\bullet$ an H$_2O_2$ molecule is formed. Our proposal was confirmed by the work of Khorobrykh et al., 2015, in which it was shown that H$_2O_2$ increases after the reaction of PQH$_2$-9 with $^1O_2$ generated by Rose Bengal. As described above, during physical quenching, one molecule of PQH$_2$-9 might quench hundreds of $^1O_2$ molecules, whereas during chemical quenching one molecule of PQH$_2$-9 can quench only one molecule of $^1O_2$ (Pospíšil 2012). In practice, in the initial period of high light stress PQ-9 undergoes re-reduction back to PQH$_2$-9 due to PSII (Rumeau et al., 2007; Lambreva et al., 2014), enabling one molecule of PQH$_2$-9 to quench several $^1O_2$ molecules. Once the amount of $^1O_2$ molecules produced during high light stress exceeds the amount of PQ-9, the re-reduction of PQ-9 becomes inefficient and the subsequent reaction of $^1O_2$ with the polyprenyl side chain of PQ-9 becomes predominant (Fig. 15).

The concomitant decrease in PQ-9 content and increase in PQ(OH)-9 content due to $^1O_2$ oxidation was monitored after the exposure of plants to high light (Fig. 14). We proposed that $^1O_2$ oxidizes PQ-9 to form PQ(OH)-9 through few reactions involving the inermediacy of PQ-9 hydroperoxide. PQ-9 hydroperoxide can be formed by the addition of $^1O_2$ by ene reaction to the carbon with the lowest electronegativity linked to two prenyl units of the PQ-9 side chain. This proposal was in agreement with our data (not shown in thesis), from oxidation of PQ-n by $^1O_2$ generated by Rose Bengal illumination to produce PQ-n hydroperoxides. After the formation of PQ-9 hydroperoxide, it was assumed that it decomposes to PQ(OH)-9 via either radical or non-radical reaction pathways (Fig. 15). The radical pathway of PQ-9 hydroperoxide decomposition might occur by the reduction caused by trace amounts of catalytic transition metal resulting in PQ-9 alkoxyl radical formation, which might subsequently abstract a hydrogen atom from a nearby biomolecule to form PQ(OH)-9 and an R$^\bullet$ as byproduct. The non-

radical pathway of PQ-9 hydroperoxide decomposition to PQ(OH)-9 probably occurs by two electron enzymatic reduction reactions requiring glutathione peroxidase (GPX) or thioredoxin peroxidase (TrxPX) (Fig. 15).

We confirmed an increased content of the newly identified PQ(OH)$_3$-9 after exposure to high light intensity also in plants (Fig. 14), mainly in SPS1oex mutants. We hypothesized in our study, that a plausible oxidation product, dihydroxyplastoquinone-9 (PQ(OH)$_2$-9), might be produced after the reaction of PQ(OH)-9 with $^1O_2$. Despite the fact that PQ(OH)$_2$-9 has not yet been identified anywhere, we proposed that it is a likely intermediate in the production of PQ(OH)$_3$-9. This probable reaction would occur in a similar manner to the oxidation of PQ-9 to PQ(OH)-9 (Fig. 15). We have also proposed that similar subsequent oxidation reactions generate the formation of other multiple PQ-9 hydroxides on the polyprenyl side-chain cannot be excluded. Further, more alternative pathways for PQ(OH)-9 consumption were mentioned (Henninger et al., 1966; Barr et al., 1967; Kruk and Strzalka, 1998; Eugeni Piller et al., 2011; Szymanska et al., 2014; Dluzewska et al., 2015).

Yadav et al., 2010 found that the chemical quenching of $^1O_2$ by exogenously added PQ-n to PSII membranes of spinach diminished with the length of the side-chain. In **Ferretti et al., 2018,** we determined also the chemical quenching of $^1O_2$, formed by the photosensitizing agent Rose Bengal, by PQ-n with different side-chain length (PQ with n isoprenoid units in the side-chain), using EPR spectroscopy in the presence of TMPD (Fig. 16). We observed also that chemical quenching of $^1O_2$ is dependent on the length of the PQ-n side-chain. Our proposal, that PQ-n with short side-chain should be better $^1O_2$ quenchers due to their better abbility to penetrate membranes given by their different polarity was than contradict by the fact that PQ-n with long side-chains are more effective $^1O_2$ quenchers due to their higher number of carbon prone to $^1O_2$ addition. Chemical quenching activity of isoprenoid quinones side-chain decreases with the number of oxidation reactions.
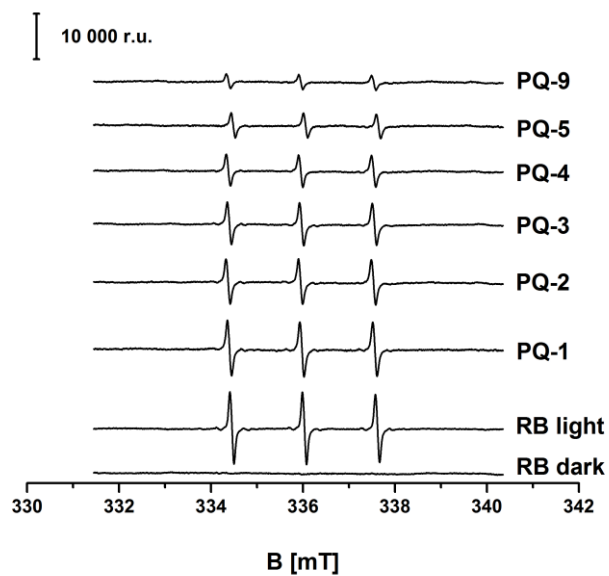
Figure 16. Effect of oxidized form of plastoquinone-n with different side-chain length on singlet oxygen produced by Rose Bengal photosensitization. TEMPONE EPR spectra measured after 5 min illumination (1000 µmol photons $m^{-2} s^{-1}$) of 100 µM plastoquinone-n with different side-chain length in the presence of 5 µM Rose Bengal, 40 Mm MES-NaOH (pH 6.5) and 50 mM TMPD.

1.3 Lipid peroxidation

Lipid peroxidation is an oxidative chain reaction. It is caused by various types of abiotic and biotic stresses, known to result in damage of unsaturated fatty acids (Porter et al., 1995). Oxidative damage of unsaturated lipids takes places in various cellular components including mitochondria, chloroplast, microbodies, peroxisomes and the plasma membrane. The level of lipid unsaturation, i.e. the position and frequency of double bonds between carbon atoms increases their reactivity with neighbouring biomolecules. Lipid peroxidation results in the formation of primary and secondary products (Porter et al., 1995; Yin et al., 2011), and as mentioned above, can be divided into three phases: initiation, propagation, and termination (Yin et al., 2011). It might be initiated by ROS (radical and non-radical) (Porter et al., 1995) or by metalloenzymes (lipoxygenases, LOX) (Smith and Murphy, 2002; Yin et al., 2011).

1.3.1 Initiation, propagation and termination

The first phase of lipid peroxidation is the initation process. This proceeds differently according to whether it occurs non-enzymatically (radical or non-radical type of ROS) or enzymatically (LOX). The radical ROS-mediated lipid peroxidation involves the abstraction of a weakly bonded hydrogen from a methylene group in a lipid molecule (L) to form lipid alkyl radical (L$^\bullet$). Reaction of L$^\bullet$ with $^3O_2$ results in formation of a lipid peroxyl radical (LO$_2{}^\bullet$) (Halliwell and Gutteridge, 2007), which subsequently abstracts hydrogen atom from another lipid molecule to form a lipid hydroperoxide (LOOH) (Girotti, 1998). The non-radical ROS-mediated lipid peroxidation is considered not to be a classical type of lipid peroxidation initiation, because the hydrogen atom is not abstracted. It occurs by the addition $^1O_2$ to an L via ene-reaction forming LOOH (Griesbeck and de Kiff, 2013). The enzymatic initiation of lipid peroxidation depends on the enzyme involved in the reaction. Lipoxygenases, studied in **Prasad et al. 2016**), as multifunctional non-heme iron enzymes have a dioxygenase activity. First, LOX catalyzes the abstraction of a hydrogen atom by the active site of enzyme to form L$^\bullet$, which reacts with $^3O_2$ to produce LO$_2{}^\bullet$. Finaly, LO$_2{}^\bullet$ is protonated forming LOOH (Fig. 17).
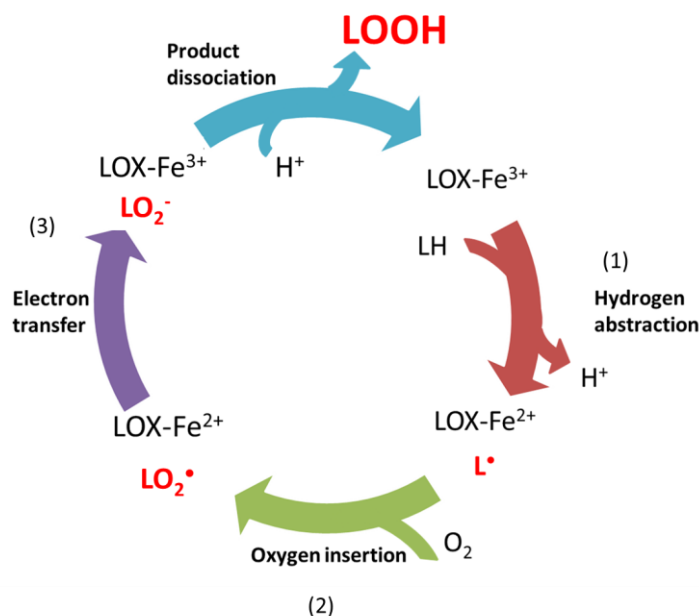
Figure 17. Lipoxygenase reaction mechanism. In reaction (1), the hydrogen is abstracted from unsaturated fatty acids (LH) by the active site of enzyme (LOX-Fe^{3+}) forming L$^•$, while the electron from carbon-hydrogen bond reduces ferric to ferrous non-heme iron, while proton is stored for following protonation (LOX-Fe^{2+}). In reaction (2), the addition of $^3O_2$ to L$^•$ leads to $LO_2^•$. In reaction (3), ferrous non-heme iron oxidizes to ferric non-heme iron, while protonates $LO_2^•$ to LOOH. Modified by Brash, 1999.

Propagation proceeds by the addition of $^3O_2$ to L$^•$ to form $LO_2^•$, followed by the abstraction of a hydrogen atom from an adjacent lipid by $LO_2^•$ producing another L$^•$ and LOOH. A single hydrogen abstraction may lead to hundreds of oxidations. Notwithstanding that LOOH can be considered a relatively stable molecule, when well stored (Kolakowska and Bartosz, 2011; Ayala et al., 2014). However, LOOH might decompose to LO$^•$ and $LO_2^•$, which might abstract another hydrogen from neighbouring molecule and thus further propagate the peroxidation. The LOOH might undergo numerous reactions to form secondary products such as hydroxy fatty acids or aldehydes. Propagation is a chain reaction lasting as long as there are molecules to oxidize or terminates. (Yin et al., 2011; Girotti, 1998).

Termination of lipid peroxidation takes place in different ways such as presence of antioxidant and recombination of radicals. Termination of lipid peroxidation by antioxidants involves the reduction of $LO_2^•$ by the antioxidant to form LOOH and an antioxidant radical (Repetto et al., 2012). Subsequently the antioxidant radical might react with another radical to produce a non-radical product. Termination of lipid peroxidation by the recombination of radicals involves combination of their unpaired electrons to form a non-radical product. The recombination of radicals depends on the concentration of oxygen (Caneba, 2010).

1.3.2 Primary and secondary products

Lipid hydroperoxides are known to be primary products of lipid peroxidation (Girotti, 1998). The hydroperoxy group can be attached to various types of lipid structures including free fatty acids, triacylglycerols or sterols. During the propagation phase of lipid peroxidation, LOOH might be oxidized and reduced to $LO^\bullet$ and $LO_2^\bullet$, respectively and contribute to the peroxidative damage by inducing the production of new LOOH molecules(Ayala et al., 2014). However, after several reactions LOOH produce secondary products of lipid peroxidation such as hydroxy fatty acids (LOH) or carbonyl species. As was mentioned above LOOH is relatively stable under specific conditions, but in the proximity of iron or another metal catalyst in becomes very unstable, undergoing Fenton reaction to produce reactive alkoxyl radicals (Kolakowska and Bartosz, 2011; Ayala et al., 2014).

The formation of LOOH in the unicellular green alga *Chlamydomonas reinhardtii* exposed to heat stress was demonstrated in our work (**Prasad et al., 2016**). The LOOH formation was detected by confocal laser scanning microscopy using the fluorescent probe SPY-LHP. It is well-known that SPY-LHP reacts with LOOH to produce its oxidized form SPY-LHPOx (Soh et al., 2007), which yields a strong fluorescence at 535 nm. Figure 18 shows Nomarski DIC, SPY-LHP fluorescence, chlorophyll fluorescence and integral distribution of SPY-LHP fluorescence intensity measured in Chlamydomonas cells. We observed a noticeable SPY-LHPOx fluorescence in the cells at 40 °C. After measuring the chlorophyll fluorescence we have found that the majority of LOOH was formed mainly in chloroplasts and in small-sized organelles such as vacuoles. The SPY-LHPOx intensity showed that the integral distribution of fluorescence was enhanced by about 4 times in comparison with non-heated Chlamydomonas cells. To understand the mechanism of lipid peroxidation inititation (non-enzymatic or enzymatic) we used catechol and caffeic acid as LOX inhibitors (Koshihara et al., 1984; Sudina et al., 1993). We observed that both catechol and caffeic acid significantly suppressed SPY-LHPox fluorescence in the heated Chlamydomonas cells, revealing that LOX initiates lipid peroxidation leading to the formation of LOOH.
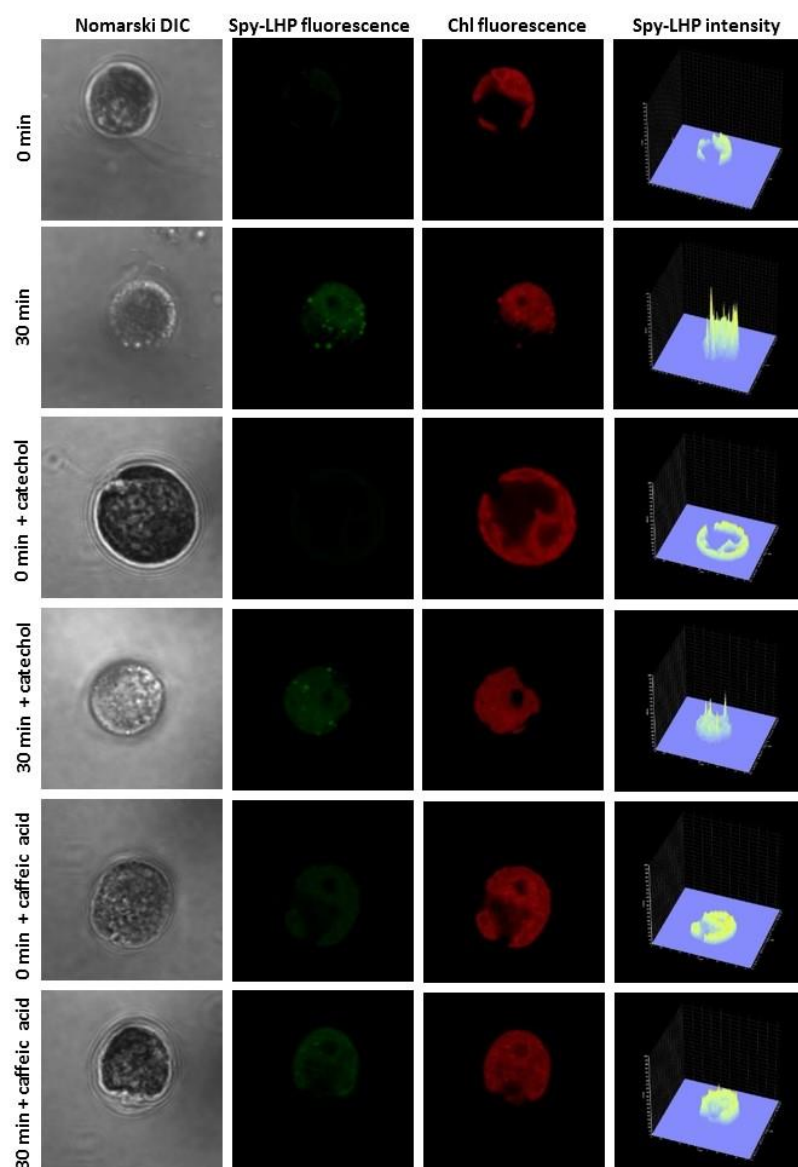
Figure 18. Detection of hydroperoxide in Chlamydomonas cells by laser confocal scanning microscopy. The formation of LOOH was measured in non-heated and heated Chlamydomonas cells in the presence and the absence of catechol and caffeic acid using fluorescent probe SPY-LHP. Heated cells were treated for 30 min in a water bath at 40 °C in the dark. The images represent from left to right: Nomarski DIC, SPY-LHP fluorescence, chlorophyll fluorescence and integral distribution of SPY-LHP signal intensity (0-4096) in the 12-bit microphotographs.

In our study (**Prasad et al., 2016**), LOOH formation was quantified in heated Chlamydomonas cells using the ferrous oxidation-xylenol orange (FOX) colorimetric assay (Fig. 19). The FOX assay is based on the oxidation of Fe^{2+} to Fe^{3+} ions by LOOH followed by the binding of ferric ions to the dye xylenol orange causing changes in colour of the solution from yellow to red. The observed difference in FOX absorption spectra from heated and non-heated Chlamydomonas cells indicated that the duration of the applied heat caused augmentation of LOOH formation (Fig. 19A). The concentration of LOOH formed in the cells

was determined from a calibration curve (insert) using H_2O_2 as substrate. We found that the concentration of LOOH reached about 7 µM after 30 minutes of heat stress (Fig. 19B).
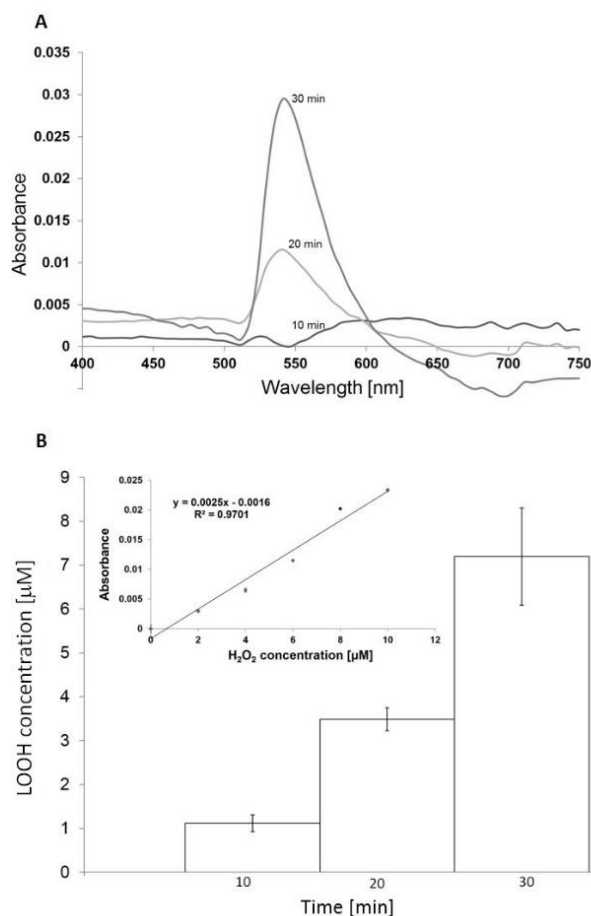
Figure 19. Quantification of hydroperoxide formation in Chlamydomonas cells ferrous oxidation-xylenol orange assay. In (A) absorption spectra of FOX reagent with Chlamydomonas cells heated for 10, 20 and 30 min measured in the spectral ranges of 400–750nm. In (B) the concentrations of LOOH was established from the calibration curve with H_2O_2 as substrate (equation $y = 0.0025x−0.0016$; shown in the insert) were as follow: 1.12±0.19 µM (10min), 3.49±0.26 µM (20min) and 7.19±1.11 µM (30min). The coefficient of determination R^2 was determined as 0.9701.

Secondary lipid peroxidation products are LOHs or reactive carbonyl species (aldehydes and ketones) (Ayala et al., 2014). Hydroxy fatty acids such as hydroxy octadecadienoic (HODEs) and hydroxy eicosatetraenoic acids (HETEs) are formed after reduction of the hydroperoxy group of LOOH. Aldehydes, including malondialdehyde (MDA) and 4-hydroxynonenal (4-HNE), are formed from unsaturated fatty acids during the lipid peroxidation by the cleavage of carbon-carbon bonds. MDA is generated by the decomposition of arachidonic acid and larger unsaturated fatty acids through enzymatic and nonenzymatic reactions (Ayala et al., 2014). Malondialdehyde is a three-carbon compound which exists in several different forms in aqueous solutions depending on pH (Del Rio et al., 2005). It is

commonly used as a marker of oxidative stress caused by high light (Havaux et al., 2005), UV radiation (Singh et al., 2013), high temperature (Mihailova et al., 2011; **Prasad et al., 2016**) and drought (Sekhar et al., 2017). Due to the capability of MDA to react with various biomolecules, it appears to be one of the most mutagenic products of lipid peroxidation (Mukai and Goldstein, 1976; Esterbauer et al., 1982; Grotto et al., 2009).

In our work (**Prasad et al., 2016**), we detected and quantified MDA as a secondary product of lipid peroxidation formed during heat stress applied to Chlamydomonas cells. It was analysed using isocratic reversed-phase HPLC separation of MDA-DNPH adduct (Fig. 20). For this purpose 2,4-dinitrophenylhydrazine (DNPH) as a derivatization compound was used (Pilz et al., 2000). We observed a peak for the MDA-DNPH adduct with a retention time of 2.75 min in the HPLC chromatogram (Fig. 20A). The MDA-DNPH adduct was confirmed (Fig. 20B) using 1,1,3,3-tetrahydroxypropane (TEP) as a standard and its concentration was determined using a calibration curve (insert). Our results showed an increasing production of MDA with duration of heat stress, accumulating to a concentration of several nM over 30 minutes.
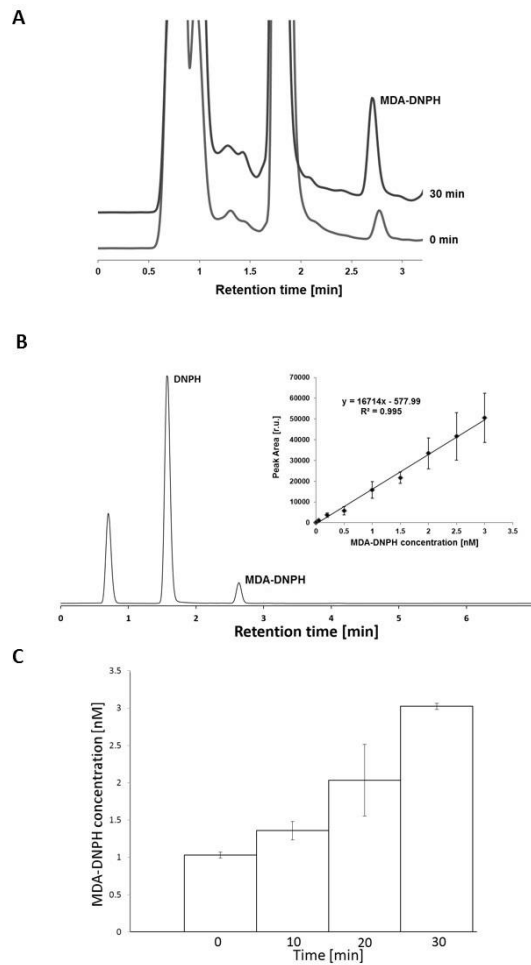
Figure 20. Detection of malondialdehyde by HPLC analysis in Chlamydomonas cells. The chromatogram of MDA-DNPH adduct in Chlamydomonas cells (A); MDA-DNPH adduct from standard TEP (B) and determination of MDA-DNPH adduct concentrations under heat stress (C). In A, chromatogram of MDADNPH adduct is shown in control (0min) and heated (30min) Chlamydomonas cells. Representative chromatograms were obtained as the average of 3 chromatograms. In (B) chromatogram of MDA-DNPH adduct from MDA standard with a retention time of 2.75min. The insert shows the dependence of average peak area (n=5, ±SD) on the concentration of MDA-DNPH adduct from MDA standard TEP. In (C) the concentrations of MDA-DNPH adduct established from calibration curve (y=16714x–577.99) were as following: 1.03±0.04nM (0min), 1.36±0.12nM (10min), 2.03±0.48nM (20min) and 3.02±0.04nM (30min), (n=3, ±SD). The coefficient of determination R^2 was determined as 0.995.

2   Aims of research

Singlet oxygen is a higly important component in metabolic and signal pathways of plants, however $^1O_2$ can also be considerably destructive. It is well-known that the defense mechanisms in response to over-production of $^1O_2$ includes the formation of unsaturated lipids as antioxidants, such as isoprenoid quinones. Isoprenoid quinones are composed of a quinol or quinone ring and an unsaturated isoprenoid chain that contains nine double bonds. Their structure allows them to move easily and thus increases their likelihood of interaction with $^1O_2$. However, there is only limited description of the probable mechanisms by which $^1O_2$ reacts with isoprenoid quinones. The aims of our investigations were as follows:

- To study the importance of the reaction of singlet oxygen with isoprenoid quinones during high light stress in *Arabidopsis thaliana,* comparing WT with a line overexpressing the solanesyl diphosphate synthase 1 gene (SPS1oex).
- To determine whether oxidation products are formed and their identity (if possible *in vivo*) and to describe the mechanism of their formation using a model during the reaction of singlet oxygen with isoprenoid quinols.
- To optimize microscopic techniques for detection of singlet oxygen detection *in vivo*
- To examine the photoprotective role of the plastoquinone pool against singlet oxygen comparing WT *Arabidopsis thaliana* with a line deficient in tocopherol (vte1), the solanesyl diphosphate synthase 1 overexpressing line (SPS1oex) and the cross between these lines (vte1SPS1oex).
- To reveal which type of lipid peroxidation is initiated during heat stress in *Chlamydomonas reinhardtii* and to identify the primary and secondary products of lipid peroxidation that are formed

3 Experimental approach

Plant material

For the study of **Ferretti et al., 2018**, *Arabidopsis thaliana*, WT (Columbia-0) and SPS1oex (lines #12 and #3) mutants (Ksas et al., 2015) were used. Plants were grown on a commercial substrate (Potgrond H, Klasmann-Deilmann Substrate, Germany) in a growing chamber (Photon Systems Instruments, Drásov, Czech Republic) under controlled conditions: photoperiod of 8 h light (120 µmol photons $m^{-2} s^{-1}$)/ 16 h dark, temperature of 22˚C and humidity 60%.

For the study of **Ksas et al., 2018**, *Arabidopsis thaliana*, WT (Columbia-0) were grown in a phytotron under controlled conditions of 8 h light (150 µmol photons $m^{-2} s^{-1}$)/ 16 h dark, temperature 20°C/18°C (day/night) and relative air humidity 60%. Several mutant/transformed plants were examined in this work: the tocopherol cyclase mutant vte1 deficient in tocopherols (Porfirova et al., 2002), SPS1-overexpressing lines (lines #12 and #14 in Ksas et al., 2015) and a crossing between them (vte1SPS1oex). Selection of homozygous vte1SPS1oex plants was achieved first by screening the progeny for resistance to the herbicide BASTA and then by screening for the total absence of tocopherol and PC-8 by HPLC analyses.

For the study of **Prasad et al., 2016**, algae strain, *Chlamydomonas reinhardtii* (wild type: CC-002) was obtained from the Chlamydomonas Genetic Center (Duke University, Durham, NC, USA). The cells were cultivated in Tris-Acetate-Phosphate (TAP) medium in a continuous white light (100 µmol µmol photons $m^{-2} s^{-1}$) in Algaetron AG 230 (Photon Systems Instruments, Drásov, Czech Republic). The growth was achieved under a permanently stirred condition using a shaker (Orbital Shaker PSU-10i, Biosan, Riga, Latvia) to obtain constant CO_2 concentration in the growing medium. The cells were studied at a density of approximately 7×10^7 cells ml^{-1} during the stationary growth phase. The cell density was determined by an automated cell counter (TC20 Automated Cell Counter, BioRad, Hercules, CA, U.S.A.).

Chloroplast preparation

For the study of **Ferretti et al., 2018**, broken chloroplasts from Arabidopsis were prepared according to (Casazza et al., 2001) with some modifications. Leaves were homogenized in 10-20 ml of grinding buffer consisting of 400 mM sorbitol, 5 mM Na-EDTA, 5 mM EGTA, 10 mM $NaHCO_3$, 5 mM $MgCl_2.6H_2O$, 20 mM Tricine/NaOH and 0.5% (w/v)

BSA. The homogenate was rapidly filtered through double layer of cheesecloth and centrifuged at 2 600 x g for 3 min at 4 ˚C. The supernatant was discarded and the pellet was resuspended in 1-2 ml of the grinding buffer. Isolated broken chloroplasts were immediately used for measurements. During the isolation procedure, all the steps were carried out in dim light at 4 ˚C.

Thylakoid membrane preparation

For the study of Ksas et al., 2018, the preparation of thylakoid membranes, 7 g of leaves (fresh weight) were grinded for 2 s in 50 ml of extraction buffer (330 mM sorbitol, 50 mM Tricine, 2 mM EDTA(Na$_2$), 1 mM MgCl$_2$, 2 mM Ascorbate, pH 7.7) with 5 mM dithiothreitol (DTT) in a Warring blendor at low speed. The liquid phase was removed and set aside, and 50 ml of extraction buffer was added for a second extraction. The extracts were filtered onto 4 Miracloth layers, and the filtrate was centrifuged for 4 min at 1500 g at 4°C. The pellet was washed twice with the extraction buffer and centrifuged for 4 min at 1500 g at 4°C. The washed pellet was resuspended in 21 ml of lysis buffer pH 7.8 (10 mM Tricine, 10 mM NaCl, 10 mM MgCl$_2$) with 1 mM PMSF (phenyl methylsulfonyl fluoride) with occasional stirring for 15 min. The sample was centrifuged at 48 400 g for 15 min. The pellet was resuspended in 1.75 ml of storage buffer (100 mM Tricine, 10 mM NaCl, 10 mM MgCl$_2$, 400 mM sucrose, pH 7.8) and stored at -80°C before analyses.

High light exposure and heat treatment

For the study of Ferretti et al., 2018, four to six week-old plants were harvested at the light period for experiments (control) or exposed to white light (1000 μmol photons m^{-2} s^{-1}) in Algaetron AG 230 (Photon Systems Instruments, Drásov, Czech Republic) for 13 h at temperature of 8 ˚C (high light). Formation of $^1O_2$ by illumination with red light (1000 μmol photons m^{-2} s^{-1}) in plants or broken chloroplasts was performed using a light emitting diode (LED) panel source with a light guide (ZETT Optics 177 GmbH 38116, Braunschweig, Germany). To avoid the auto photosensitization of fluorescent probes a long-pass edge interference filter (> 600 nm) (Andover corporation, Salem, NH, USA) was used to eliminate blue-green region of the spectrum. Formation of $^1O_2$ by illumination with white light (1000 μmol photons m^{-2} s^{-1}) in plants, broken chloroplasts or chemical system was performed using a LED panel (LED Light Source SL 3500, PSI, Drásov, Czech Republic). In chemical system, $^1O_2$ formation was induced by illumination of 5 μM Rose Bengal in 40 mM MES-NaOH buffer (pH 6.5) with white light as described previously (Yadav et al., 2010).

For the study of **Ksas et al., 2018**, photooxidative stress was induced by transferring plants to a growth chambre for 8 h light (1500 µmol photons $m^{-2} s^{-1}$)/ 16 h dark and temperature 7°C/15°C (day/night). Depending of the experiment, the duration of the treatment was 48 h (photooxidative stress experiments) or 8 h (dynamics of the PQ-9 pools), as indicated in the legend of the figures.

For the study of **Prasad et al., 2016**, the lipid peroxidation in Chlamydomonas cells were induced using heat stress for 10, 20 and 30 min at temperature of 40 °C using a water bath (Julabo GmbH, Germany) in Eppendorf tubes. Any effect of light was prevented.

Isoprenoid quinones

For the study of **Ferretti et al., 2018**, plastoquinone-9 was isolated by extraction of pigment from old leaves and direct HPLC separation of the total pigment extract (Kruk and Strzalka, 1998). Short-chain plastoquinones (PQ-1 to PQ-4) were a gift from Professor H. Koike (Department of Life Sciences, Himeji Institute of Technology, Hyogo, Japan), while PQ-5 was prepared from dimethylhydroquinone and all-E-pentaprenol (kindly provided by Dr. Thomas Netscher, Research and Development, DSMNutritional Products, Basel, Switzerland).

Isoprenoid quinones were measured using the method described in Ksas et al., 2015. Leaf discs were ground for 1 min in 2 ml of ethyl acetate with an Ultra-Turrax at 24 000 rpm. After centrifugation at 16 900 x g for 3 min, 600 µl of extract was filtered with 0.2 µm PTFE filter. The extract was evaporated under a stream of nitrogen, resuspended in 1 ml of solution methanol and hexane in ratio of 17/1 (v/v) prior analysis by HPLC-UV/fluorescence. The samples were subjected to reverse phase HPLC using a Phenomenex Kinetex 2.6 µm C18 column (100 x 4.6 mm) operating in the isocratic mode with mobile phase containing methanol and hexane (17/1, v/v) at a flow rate of 0.8 ml/min. For determination of PQH_2-9 and PC-8, except PQ-9, fluorescence detection was used (λ_{ex} = 290 nm, λ_{em} = 330 nm). Plastoquinone-9 was measured using absorbance at 255 nm. Plastoquinones and plastochromanol standards were obtained as described previously (Gruszka et al., 2008).

Arabidopsis leaves were ground with 2 ml of ethyl acetate, the extract evaporated in a stream of nitrogen, dissolved in 400 µl of absolute ethanol and 50 µl of 5 mM ferricyanide was added to oxidize the prenylquinols. After 10 min of incubation, the solution was evaporated to dryness and dissolved in the HPLC solvent. Total (oxidized and reduced) PQ-9 and PQ(OH)-9 were determined using C18 reverse-phase column (Nucleosil 100, 5 µm, 25 x 0.4 cm, Teknokroma, Barcelona, Spain), using a mobile phase containing methanol and hexane in ratio

17/1 (v/v) at the flow rate of 1 ml/min, absorption detection at 255 nm and Pt post column reduction and fluorescence detection (λ_{ex} = 290 nm, λ_{em} = 330 nm). Total PQ(OH)$_3$-9 was determined using C18 reverse-phase column (Nucleosil 100, 5 μm, 25 x 0.4 cm, Teknokroma, Barcelona, Spain), N$_2$-flushed methanol containing 25 mM NaClO$_4$ as an eluent, flow rate of 1 ml/min, decade electrochemical amperometric detector and VT-03 flowcell (ANTEC Leyden, The Netherlands), -0.3 to -0.4 V reducing potential and temperature of 25 ˚C. Standard of PQ(OH)$_3$-9 was prepared as described in Gruszka et al., 2008.

Confocal laser scanning microscopy

For the study of **Ferretti et al., 2018**, imaging of $^1O_2$ and ROOH in leaves was performed using fluorescent probes SOSG (Molecular Probes Inc., Eugene, OR, USA) and SPY-LHP (Dojindo Molecular Technologies Inc. Rockville, MD, USA), respectively. SOSG and SPY-LHP probes are commonly used for their high selectivity to $^1O_2$ and ROOH, respectively, without any side-reactions with other reactive oxygen species ($O^{2\bullet-}$, H_2O_2, HO$^\bullet$). As SOSG-EP fluorescence is in the visible range of the spectrum, the detection is convenient compared to another fluorescent probe (indocyanine green) known to absorb in the near-infrared range. As excitation of SPY-LHPox is in the visible range of the spectrum, live cells are minimally damaged compared to another fluorescent probes (diphenyl-1-pyrenylphosphine) known to absorb in the ultraviolet range. Arabidopsis leaf blade cuts (2x2 mm) were incubated in the presence of either 50 μM SOSG or 50 μM SPY-LHP and 40 mM HEPES buffer (pH 7.6) in the dark or under red light for 30 min. Afterwards, the samples were visualized by confocal microscope (FV1000, Olympus Czech Group, Prague, Czech Republic). The excitation of both fluorochromes was performed using a 488 nm line of argon laser and signal was detected by 505-525 nm emission filter set for $^1O_2$ or by 505-550 nm emission filter set for ROOH. The proper intensity of the laser was set according to unstained samples at the beginning of each experiment (Sedlářová et al., 2011). Post-processing of original images for more clear presentation of results included a three-fold increase of contrast in fluorescence channels and setting of signal intensities from initial 0-4095 grades of brightness to 400-1200 for SOSG and 120-800 for SPY-LHP, respectively.

For the study of **Prasad et al., 2016**, *in vivo* imaging of LOOH and $^1O_2$ was based on their reaction with a SPY-LHP (Dojindo Molecular Technologies Inc. Rockville, MD, USA) and SOSG (Molecular Probes Inc., Eugene, OR, USA), respectively. Chlamydomonas cells were incubated either in the presence of 20 μM SPYy-LHP or 50 μM SOSG in darkness for 30

min. To study an influence of temperature stress, samples were kept at room temperature or subjected to 40 °C. Immediately after staining, the cells were transferred to a fresh TAP medium and visualized by confocal laser scanning microscopy (Fluorview 1000 unit attached to IX80 microscope; Olympus Czech Group, Prague, Czech Republic). The excitation of both fluorochromes were achieved by a 488 nm line of an argon laser and signal was detected either by a 505-550 nm emission filter for LOOH or by a 505-525 nm emission filter for $^1O_2$. Chlorophyll fluorescence from chloroplasts of Chlamydomonas cells was achieved by excitation with 543 nm helium-neon laser, and emission recorded with a 655-755 nm band filter. Cell morphology was visualized by a transmitted light detection module with 405 nm excitation using a near-ultraviolet (405 nm) diode laser and Nomarski DIC filters. The proper intensity of all lasers was set according to unstained samples at the beginning of each experiment (Sedlářová et al., 2011). The integral distribution of signal intensity (0-4096) in 12-bit microphotographs were evaluated by image analysis software FV10-ASW Viewer (Olympus).

Electron paramagnetic resonance spectroscopy

For the study of Ferretti et al., 2018, singlet oxygen formation was determined by EPR spectroscopy employing TMPD probe. Broken chloroplasts at a concentration of 200 µg Chl ml-1 were kept in dark or illuminated with white light for 30 min in the presence of 50 mM TMPD and 40 mM MES-NaOH buffer (pH 6.5). The chemical system containing PQ-n with different side-chain length and Rose Bengal were kept in the dark or illuminated with white light for 5 min in the presence of 50 mM TMPD and 40 mM MES-NaOH buffer (pH 6.5). The oxidation of TEMPD by $^1O_2$ forms TEMPONE detectable by EPR spectroscopy. After illumination, samples were centrifuged at 1 000 x g for 2 min to separate broken chloroplasts or PQ-n samples from TEMPONE and measured by EPR spectrometer.

The formation of R$^•$ was measured by EPR spin-trapping spectroscopy using POBN spin-trap. Broken chloroplasts at a concentration of 200 µg Chl ml^{-1} were kept in dark or illuminated with white light (1000 µmol photons m^{-2} s^{-1}) for 30 min in the presence of 50 mM POBN and 40 mM MES-NaOH buffer (pH 6.5). After illumination, POBN-R adduct EPR spectra were obtained. EPR spectra were recorded using an EPR spectrometer MiniScope MS400 (Magnettech GmbH, Berlin, Germany). EPR measurement conditions were as follows: microwave power, 10 mW; modulation amplitude, 1 G; modulation frequency, 100 kHz; sweep width, 89 G, scan rate, 1.62 G s^{-1}, gain, 500.

For the study of **Ksas et al., 2018**, singlet oxygen formation was monitored by EPR spectroscopy using the spin probe TEMPD purified by vacuum distillation. Thylakoid membranes (25 µg Chl ml^{-1}) were illuminated in the presence of 50 mM TEMPD and 40 mM MES-NaOH buffer (pH = 6.5) for 30 min under 1000 µmol photons m^{-2} s^{-1}. After illumination, thylakoid membranes were centrifuged at 1 000 x g for 2 min to separate the sample from the spin probe. The EPR spectra were recorded using an EPR spectrometer Mini Scope MS400 (Magnettech GmbH, Berlin, Germany). EPR measurement conditions were as follows: microwave power, 10 mW; modulation amplitude, 1 G; modulation frequency, 100 G; scan rate, 1.62 G s^{-1}.

For the study of **Prasad et al., 2016**, EPR spin-trapping spectroscopy was used to measure the $^1O_2$ production. Chlamydomonas cells suspended in TAP media with 50mM TEMP spin trap were heated at 40 °C and EPR spectra were recorded using an EPR spectrometer MiniScope MS400 (Magnettech GmbH, Berlin, Germany). To eliminate impurity TEMPO EPR signal, TEMP was purified twice by vacuum distillation. EPR conditions are as follows: microwave power, 10 mW; modulation amplitude, 1 G; modulation frequency, 100 kHz; sweep width, 100 G; scan rate, 1.62 G s^{-1}.

MDA determination

For the study of **Prasad et al., 2016**, malondialdehyde was measured using HPLC. The isolation and derivatization of MDA using DNPH was performed as described in Pilz et al., 2000 with some modifications. After heat treatment, cells were centrifuged at 2 000 x g for 10 min and the supernatant was removed. The pellet was resuspended in 200 µl of phosphate buffer saline (PBS, pH = 7.5) and 100 µl 0.06% butylhydroxytoluene (BHT) dissolved in methanol. Using a sonicator for 90 s (Sonicator, Ultrasonic homogenizer Model 3000, Biologics Inc., Manassas, VA, U.S.A.), the Chlamydomonas cells were disrupted. This step was followed by centrifugation at 2000 x g for 10 min and 125 µl of supernatant was taken for following step. To achieve alkaline hydrolysis of protein bound MDA, 25 µl of 6 M aqueous sodium hydroxide was added to the samples and sample were treated in a 60 °C dry bath for 30 min (Thermo-Shaker TS100, Biosan, Riga, Latvia). To reach the precipitation of proteins in samples, 62.5 µl of 35% (v/v) perchloric acid was added to the sample, vortexed and centrifuged at 16 000 x g for 10 min. 125 µl of supernatant was taken into a vial and resuspended in 1 µl of 50 mM DNPH dissolved in 50% sulphuric acid and treated in dark at room temperature for 30 min. DNPH bound to MDA to create a MDA-DNPH derivative. An amount of 25 µl was injected into the

HPLC system (Alliance e 2695 HPLC System, Waters, Milford, MA, U.S.A.) and detected at 310 nm using UV/VIS detector. A Symmetry C18 (3.5 µm; 4.6 x 75 mm) Column (Waters, Milford, MA, U.S.A.) was used. The analysis was performed isocratically (1 ml/min at 35 °C) using mobile phase comprised of a mixture of 25 mM trimethylamine (pH 3.5) and acetonitrile in the ratio 50:50 (v:v). To remove impurities from the column after every measurement, the column was rinsed by 100% methanol.

Ferrous ion oxidation xylenol orange assay

For the study of **Prasad et al., 2016**, the quantification of LOOH in Chlamydomonas cells was performed using FOX assay (DeLong et al., 2002) with some modifications. Fox reagent was prepared by mixing 50 mM xylenol orange and 5 mM iron(II) sulfate heptahydrate in proportion 1:1. For the measurement 100 µl of sample/reference and 2000 µl Fox reagent was used. Fox reagent was added to Chlamydomonas cells prior to heat treatment and absorption changes were measured 30 min after start of heat treatment to keep the total period of constant. Hydroperoxide formation was monitored by following the absorbance changes at 560 nm using Olis RSM 1000 spectrometer (Olis Inc., Bogart, Georgia, USA).

STATISTICAL ANALYSIS

Origin software (version 8.5.1) was used for statistical analysis. Figures and data represent average and standard deviation values based on the number of total samples (n) taken from at least three independent sample replicates. To calculate significant differences Student´s test and ANOVA were used (P-value < 0.05).

4 Conclusion and future perspective

Based on the results described in this thesis we conclude that:

- In Arabidopsis plants, chemical quenching of $^1O_2$ by isoprenoid quinones and their oxidized products occurs during high light stress.

- Using *in vivo* microscopic and *in vitro* spectroscopic techniques we provide direct evidence for chemical quenching of $^1O_2$ by isoprenoid quinones and their oxidized products.

- We identified a natural product $PQ(OH)_3$-9 formed by interaction of isoprenoid quinones and their oxidized products with $^1O_2$ in Arabidopsis plants.

- We proposed a reaction mechanism for the interaction of isoprenoid quinones with $^1O_2$

- Use of the Arabidopsis mutant SPS1oex and double mutant vte1SPS1oex confirmed the photoprotective role of isoprenoid quinones as a chemical quenchers of $^1O_2$.

- The formation of $^1O_2$ was shown to occur *in vivo* in the unicellular green alga *Chlamydomonas reinhardtii.*

- Caffeic acid and catechol as inhibitors of lipoxygenase activity were shown to prevent the formation of $^1O_2$ and LOOH, revealing that lipoxygenase initiates lipid peroxidation leading to $^1O_2$ formation.

- During a longer period of heat stress primary and secondary products of lipid peroxidation, identified as LOOH and MDA, were shown to be produced in *Chlamydomonas reinhardtii.*

5 Acknowledgements

I would like to express my gratitude to my supervisor Dr. Pavel Pospíšil for his guidance, all the valuable advice and the time dedicated to helping me during my doctoral studies.

I extend my gratitude to Prof. Petr Ilík for allowing me to pursue my doctoral studies at the Department of Biophysics.

I am deeply grateful to Prof. Jerzy Kruk for the opportunity to be a part of his research group during my research stay at the Department of Plant Physiology and Biochemistry at Jagellonian University, Poland. I am particularly grateful for the assistance given by Dr. Beatrycze Nowicka, who guided me and helped me during this stay.

I would also like to express my gratitude to Dr. Michel Havaux for his collaboration and support for my research work.

I would like to sincerely thank Prof. Peter Hedden, Dr. Pavel Jaworek, Dr. Marek Szecówka and Tereza Miksteinová for their support and encouragement during writing this work.

I also take this opportunity to special thanks my friends and colleagues for their friendship, encouragement, helpfulness and support througout my doctoral study.

Finally, I would like to thank my husband and family from the bottom of my heart for their love and persistent support and encouragement.

6 References

Aro, E.M., Suorsa, M., Rokka, A., Allahverdiyeva, Y., Paakkarinen, V., Saleem, A., Battchikova, N., and Rintamäki, E. (2005). Dynamics of photosystem II: a proteomic approach to thylakoid protein complexes. Journal of Experimental Botany **56,** 347-356.

Asada, K. (1999). The water-water cycle in chloroplasts: Scavenging of active oxygens and dissipation of excess photons. Annu Rev Plant Physiol Plant Mol Biol **50,** 601-639.

Austin, J.R., 2nd, Frost, E., Vidi, P.A., Kessler, F., and Staehelin, L.A. (2006). Plastoglobules are lipoprotein subcompartments of the chloroplast that are permanently coupled to thylakoid membranes and contain biosynthetic enzymes. Plant Cell **18,** 1693-1703.

Ayala, A., Munoz, M.F., and Arguelles, S. (2014). Lipid peroxidation: production, metabolism, and signaling mechanisms of malondialdehyde and 4-hydroxy-2-nonenal. Oxid Med Cell Longev **2014,** 360438.

Barr, R., Henninger, M.D., and Crane, F.L. (1967). Comparative Studies on Plastoquinone II. Analysis for Plastoquinones A, B, C, and D. Plant Physiol **42,** 1246-1254.

Bentinger, M., Brismar, K., and Dallner, G. (2007). The antioxidant role of coenzyme Q. Mitochondrion **7 Suppl,** S41-50.

Blokhina, O., and Fagerstedt, K.V. (2010). Oxidative metabolism, ROS and NO under oxygen deprivation. Plant Physiology and Biochemistry **48,** 359-373.

Bouvier, F., Rahier, A., and Camara, B. (2005). Biogenesis, molecular regulation and function of plant isoprenoids. Progress in Lipid Research **44,** 357-429.

Brash, A.R. (1999) Lipoxygenases: Occurrence, functions, catalysis, and acquisition of substrate, Journal of Biological Chemistry, vol.274, no.34, pp. 23679-23682.

Buettner, G.R. (1987). Spin Trapping - Electron-Spin-Resonance Parameters of Spin Adducts. Free Radical Biology and Medicine **3,** 259-303.

Caneba, G. (2010). Free-Radical Retrograde-Precipitation Polymerization (FRRPP): Novel Concept, Processes, Materials, and Energy Aspects. Free-Radical Retrograde-Precipitation Polymerization (Frrpp): Novel Concept, Processes, Materials, and Energy Aspects**,** 1-310.

Casazza, A.P., Tarantino, D., and Soave, C. (2001). Preparation and functional characterization of thylakoids from *Arabidopsis thaliana*. Photosynth Res **68,** 175-180.

D'Ambrosio, P., Tonucci, L., d'Alessandro, N., Morvillo, A., Sortino, S., and Bressan, M. (2011). Water-Soluble Transition-Metal-Phthalocyanines as Singlet Oxygen Photosensitizers in Ene Reactions. European Journal of Inorganic Chemistry**,** 503-509.

Del Rio, D., Stewart, A.J., and Pellegrini, N. (2005). A review of recent studies on malondialdehyde as toxic molecule and biological marker of oxidative stress. Nutrition Metabolism and Cardiovascular Diseases **15,** 316-328.

DeLong, J.M., Prange, R.K., Hodges, D.M., Forney, C.F., Bishop, M.C., and Quilliam, M. (2002). Using a modified ferrous oxidation-xylenol orange (FOX) assay for detection of lipid hydroperoxides in plant tissue. Journal of Agricultural and Food Chemistry **50,** 248-254.

Dietz, K.J., Turkan, I., and Krieger-Liszkay, A. (2016). Redox- and Reactive Oxygen Species-Dependent Signaling into and out of the Photosynthesizing Chloroplast. Plant Physiol **171,** 1541-1550.

Dluzewska, J., Zielinski, K., Nowicka, B., Szymanska, R., and Kruk, J. (2015). New prenyllipid metabolites identified in Arabidopsis during photo-oxidative stress. Plant Cell Environ **38,** 2698-2706.

Dormann, P. (2007). Functional diversity of tocochromanols in plants. Planta **225,** 269-276.

Esterbauer, H., Cheeseman, K.H., Dianzani, M.U., Poli, G., and Slater, T.F. (1982). Separation and characterization of the aldehydic products of lipid-peroxidation stimulated by ADP-Fe^{2+} in rat-liver microsomes. Biochemical Journal **208,** 129-140.

Eugeni Piller, L., Abraham, M., Dormann, P., Kessler, F., and Besagni, C. (2012). Plastid lipid droplets at the crossroads of prenylquinone metabolism. Journal of Experimental Botany **63,** 1609-1618.

Eugeni Piller, L., Besagni, C., Ksas, B., Rumeau, D., Brehelin, C., Glauser, G., Kessler, F., and Havaux, M. (2011). Chloroplast lipid droplet type II NAD(P)H quinone oxidoreductase is essential for prenylquinone metabolism and vitamin K1 accumulation. Proc Natl Acad Sci U S A **108,** 14354-14359.

Farmer, E.E., and Mueller, M.J. (2013). ROS-mediated lipid peroxidation and RES-activated signaling. Annu Rev Plant Biol **64,** 429-450.

Fedorova, G.F., Trofimov, A.V., Vasil'ev, R.F., and Veprintsev, T.L. (2007). Peroxy-radical-mediated chemiluminescence: mechanistic diversity and fundamentals for antioxidant assay. Arkivoc, 163-215.

Ferretti, U., Ciura, J., Ksas, B., Rac, M., Sedlářová, M., Kruk, J., Havaux, M., and Pospíšil, P. (2018). Chemical quenching of singlet oxygen by plastoquinols and their oxidation products in Arabidopsis. Plant Journal **95,** 848-861.

Fischer, B.B., Hideg, E., and Krieger-Liszkay, A. (2013). Production, Detection, and Signaling of Singlet Oxygen in Photosynthetic Organisms. Antioxidants & Redox Signaling **18,** 2145-2162.

Flors, C., Fryer, M.J., Waring, J., Reeder, B., Bechtold, U., Mullineaux, P.M., Nonell, S., Wilson, M.T., and Baker, N.R. (2006). Imaging the production of singlet oxygen in vivo using a new fluorescent sensor, Singlet Oxygen Sensor Green. J Exp Bot **57,** 1725-1734.

Foote, C.S., Chang, Y.C., and Denny, R.W. (1970). Chemistry of singlet oxygen. X. Carotenoid quenching parallels biological protection. J Am Chem Soc **92,** 5216-5218.

Foyer, C.H. (2018). Reactive oxygen species, oxidative signaling and the regulation of photosynthesis. Environ Exp Bot **154,** 134-142.

Foyer, C.H., and Noctor, G. (2009). Redox Regulation in Photosynthetic Organisms: Signaling, Acclimation, and Practical Implications. Antioxidants & Redox Signaling **11,** 861-905.

Gill, S.S., and Tuteja, N. (2010). Reactive oxygen species and antioxidant machinery in abiotic stress tolerance in crop plants. Plant Physiol Biochem **48,** 909-930.

Girotti, A.W. (1998). Lipid hydroperoxide generation, turnover, and effector action in biological systems. Journal of Lipid Research **39,** 1529-1542.

Gorman, A.A., Hamblett, I., Lambert, C., Spencer, B., and Standen, M.C. (1988). IDENTIFICATION OF BOTH PREEQUILIBRIUM AND DIFFUSION LIMITS FOR REACTION OF SINGLET OXYGEN, O-2(1-DELTA-G), WITH BOTH PHYSICAL AND CHEMICAL QUENCHERS - VARIABLE-TEMPERATURE, TIME-RESOLVED INFRARED LUMINESCENCE STUDIES. Journal of the American Chemical Society **110,** 8053-8059.

Griesbeck, A.G., and de Kiff, A. (2013). A New Directing Mode for Singlet Oxygen Ene Reactions: The Vinylogous Gem Effect Enables a O-1(2) Domino Ene/ 4+2 Process. Organic Letters **15,** 2073-2075.

Grotto, D., Maria, L.S., Valentini, J., Paniz, C., Schmitt, G., Garcia, S.C., Pomblum, V.J., Rocha, J.B.T., and Farina, M. (2009). Importance of the Lipid Peroxidation Biomarkers and Methodological Aspects for Malondialdehyde Quantification. Quimica Nova **32,** 169-174.

Gruszka, J., Pawlak, A., and Kruk, J. (2008). Tocochromanols, plastoquinol, and other biological prenyllipids as singlet oxygen quenchers-determination of singlet oxygen quenching rate constants and oxidation products. Free Radic Biol Med **45,** 920-928.

Halliwell, B. (2006). Reactive species and antioxidants. Redox biology is a fundamental theme of aerobic life. Plant Physiol **141,** 312-322.

Halliwell, B. (2011). Free radicals and antioxidants - quo vadis? Trends Pharmacol Sci **32,** 125-130.

Halliwell, B., and Gutteridge, J.M.C. (2007). Free radicals in biology and medicine. (Oxford ; New York: Oxford University Press).

Havaux, M. (2020). Plastoquinone In and Beyond Photosynthesis. Trends in Plant Science **25,** 1252-1265.

Havaux, M., Eymery, F., Porfirova, S., Rey, P., and Dormann, P. (2005). Vitamin E protects against photoinhibition and photooxidative stress in Arabidopsis thaliana. Plant Cell **17,** 3451-3469.

Henninger, M.D., Barr, R., and Crane, F.L. (1966). Plastoquinone B. Plant Physiol **41,** 696-700.

Hideg, E., Spetea, C., and Vass, I. (1994). Singlet oxygen production in thylakoid membranes during photoinhibition as detected by EPR spectroscopy. Photosynth Res **39,** 191-199.

Jemiola-Rzeminska, M., Kruk, J., and Strzalka, K. (2003). Fluorescence anisotropy of plant membrane prenyllipids as a tool in studies of their localization and mobility in model membranes. Advanced Research on Plant Lipids**,** 369-372.

Khorobrykh, S., Havurinne, V., Mattila, H., and Tyystjarvi, E. (2020). Oxygen and ROS in photosynthesis. Plants-Basel **9**.

Khorobrykh, S.A., and Ivanov, B.N. (2002). Oxygen reduction in a plastoquinone pool of isolated pea thylakoids. Photosynthesis Research **71,** 209-219.

Khorobrykh, S.A., Karonen, M., and Tyystjarvi, E. (2015). Experimental evidence suggesting that H2O2 is produced within the thylakoid membrane in a reaction between plastoquinol and singlet oxygen. FEBS Lett **589,** 779-786.

Khorobrykh, S.A., Khorobrykh, A.A., Yanykin, D.V., Ivanov, B.N., Klimov, V.V., and Mano, J. (2011). Photoproduction of catalase-insensitive peroxides on the donor side of manganese-depleted photosystem II: evidence with a specific fluorescent probe. Biochemistry **50,** 10658-10665.

Kolakowska, A., and Bartosz, G. (2011). Antioxidants. Chemical, Biological, and Functional Aspects of Food Lipids, 2nd Edition**,** 185-209.

Koshihara, Y., Neichi, T., Murota, S.I., Lao, A.N., Fujimoto, Y., and Tatsuno, T. (1984). CAFFEIC ACID IS A SELECTIVE INHIBITOR FOR LEUKOTRIENE BIOSYNTHESIS. Biochimica Et Biophysica Acta **792,** 92-97.

Krieger-Liszkay, A., and Trebst, A. (2006). Tocopherol is the scavenger of singlet oxygen produced by the triplet states of chlorophyll in the PSII reaction centre. Journal of Experimental Botany **57,** 1677-1684.

Krieger-Liszkay, A., Fufezan, C., and Trebst, A. (2008). Singlet oxygen production in photosystem II and related protection mechanism. Photosynth Res **98,** 551-564.

Kruk, J., and Strzalka, H. (1998). Identification of plastoquinone-C in spinach and maple leaves by reverse-phase high-performance liquid chromatography. Phytochemistry **49,** 2267-2271.

Kruk, J., and Strzalka, K. (1999). Dark reoxidation of the plastoquinone-pool is mediated by the low-potential form of cytochrome b-559 in spinach thylakoids. Photosynthesis Research **62,** 273-279.

Kruk, J., and Karpinski, S. (2006). An HPLC-based method of estimation of the total redox state of plastoquinone in chloroplasts, the size of the photochemically active

plastoquinone-pool and its redox state in thylakoids of Arabidopsis. Biochim Biophys Acta **1757,** 1669-1675.

Kruk, J., and Trebst, A. (2008). Plastoquinol as a singlet oxygen scavenger in photosystem II. Biochim Biophys Acta **1777,** 154-162.

Kruk, J., Hollander-Czytko, H., Oettmeier, W., and Trebst, A. (2005). Tocopherol as singlet oxygen scavenger in photosystem II. Journal of Plant Physiology **162,** 749-757.

Kruk, J., Szymanska, R., Cela, J., and Munne-Bosch, S. (2014). Plastochromanol-8: Fifty years of research. Phytochemistry **108,** 9-16.

Kruk, J., Szymanska, R., Nowicka, B., and Dluzewska, J. (2016). Function of isoprenoid quinones and chromanols during oxidative stress in plants. New Biotechnology **33,** 636-643.

Ksas, B., Becuwe, N., Chevalier, A., and Havaux, M. (2015). Plant tolerance to excess light energy and photooxidative damage relies on plastoquinone biosynthesis. Sci Rep **5,** 10919.

Ksas, B., Legeret, B., Ferretti, U., Chevalier, A., Pospíšil, P., Alric, J., and Havaux, M. (2018). The plastoquinone pool outside the thylakoid membrane serves in plant photoprotection as a reservoir of singlet oxygen scavengers. Plant Cell Environ **41,** 2277-2287.

Laloi, C., and Havaux, M. (2015). Key players of singlet oxygen-induced cell death in plants. Frontiers in Plant Science **6**.

Lambreva, M.D., Russo, D., Polticelli, F., Scognamiglio, V., Antonacci, A., Zobnina, V., Campi, G., and Rea, G. (2014). Structure/function/dynamics of photosystem II plastoquinone binding sites. Curr Protein Pept Sci **15,** 285-295.

Larkindale, J., and Knight, M.R. (2002). Protection against heat stress-induced oxidative damage in arabidopsis involves calcium, abscisic acid, ethylene, and salicylic acid. Plant Physiology **128,** 682-695.

Ledford, H.K., and Niyogi, K.K. (2005). Singlet oxygen and photo-oxidative stress management in plants and algae. Plant Cell and Environment **28,** 1037-1045.

Liebthal, M., and Dietz, K.J. (2017). The fundamental role of reactive oxygen species in plant stress response. Methods Mol Biol **1631,** 23-39.

Liu, M., and Lu, S. (2016). Plastoquinone and Ubiquinone in Plants: Biosynthesis, Physiological Function and Metabolic Engineering. Front Plant Sci **7,** 1898.

Liu, M.M., Ma, Y.M., Du, Q., Hou, X.M., Wang, M.Z., and Lu, S.F. (2019). Functional Analysis of Polyprenyl Diphosphate Synthase Genes Involved in Plastoquinone and Ubiquinone Biosynthesis in Salvia miltiorrhiza. Frontiers in Plant Science **10**.

Liu, X.Z., and Huang, B.R. (2000). Heat stress injury in relation to membrane lipid peroxidation in creeping bentgrass. Crop Science **40,** 503-510.

Lokhmatikov, A.V., Voskoboynikova, N.E., Cherepanov, D.A., Sumbatyan, N.V., Korshunova, G.A., Skulachev, M.V., Steinhoff, H.J., Skulachev, V.P., and Mulkidjanian, A.Y. (2014). Prevention of peroxidation of cardiolipin liposomes by quinol-based antioxidants. Biochemistry (Mosc) **79,** 1081-1100.

McDonald, A.E., Ivanov, A.G., Bode, R., Maxwell, D.P., Rodermel, S.R., and Huner, N.P. (2011). Flexibility in photosynthetic electron transport: the physiological role of plastoquinol terminal oxidase (PTOX). Biochim Biophys Acta **1807,** 954-967.

Mene-Saffrane, L., and DellaPenna, D. (2010). Biosynthesis, regulation and functions of tocochromanols in plants. Plant Physiology and Biochemistry **48,** 301-309.

Mihailova, G., Petkova, S., Buchel, C., and Georgieva, K. (2011). Desiccation of the resurrection plant Haberlea rhodopensis at high temperature. Photosynthesis Research **108,** 5-13.

Moan, J., and Wold, E. (1979). Detection of singlet oxygen production by ESR. Nature **279,** 450-451.

Mubarakshina, M.M., and Ivanov, B.N. (2010). The production and scavenging of reactive oxygen species in the plastoquinone pool of chloroplast thylakoid membranes. Physiol Plant **140,** 103-110.

Mukai, F.H., and Goldstein, B.D. (1976). Mutagenicity of malonaldehyde, a decomposition product of peroxidized polyunsaturated fatty-acids. Science **191,** 868-869.

Mukai, K., Itoh, S., Daifuku, K., Morimoto, H., and Inoue, K. (1993). Kinetic-Study of the Quenching Reaction of Singlet Oxygen by Biological Hydroquinones and Related-Compounds. Biochimica Et Biophysica Acta **1183,** 323-326.

Mullineaux, P.M., and Baker, N.R. (2010). Oxidative Stress: Antagonistic Signaling for Acclimation or Cell Death? Plant Physiology **154,** 521-525.

Munné-Bosch, S. (2005). The role of alpha-tocopherol in plant stress tolerance. Journal of Plant Physiology **162,** 743-748.

Nowicka, B., and Kruk, J. (2010). Occurrence, biosynthesis and function of isoprenoid quinones. Biochim Biophys Acta **1797,** 1587-1605.

Nowicka, B., Gruszka, J., and Kruk, J. (2013). Function of plastochromanol and other biological prenyllipids in the inhibition of lipid peroxidation-A comparative study in model systems. Biochim Biophys Acta **1828,** 233-240.

Onyango, A.N., and Baba, N. (2010). New hypotheses on the pathways of formation of malondialdehyde and isofurans. Free Radic Biol Med **49,** 1594-1600.

Pilz, J., Meineke, I., and Gleiter, C.H. (2000). Measurement of free and bound malondialdehyde in plasma by high-performance liquid chromatography as the 2,4-dinitrophenylhydrazine derivative. Journal of Chromatography B **742,** 315-325.

Porfirova, S., Bergmuller, E., Tropf, S., Lemke, R., and Dormann, P. (2002). Isolation of an Arabidopsis mutant lacking vitamin E and identification of a cyclase essential for all tocopherol biosynthesis. Proc Natl Acad Sci U S A **99,** 12495-12500.

Porter, N.A., Caldwell, S.E., and Mills, K.A. (1995). Mechanisms of free radical oxidation of unsaturated lipids. Lipids **30,** 277-290.

Pospíšil, P., and Prasad, A. (2014). Formation of singlet oxygen and protection against its oxidative damage in Photosystem II under abiotic stress. J Photochem Photobiol B **137,** 39-48.

Pospíšil, P., Snyrychova, I., and Naus, J. (2007). Dark production of reactive oxygen species in photosystem II membrane particles at elevated temperature: EPR spin-trapping study. Biochim Biophys Acta **1767,** 854-859.

Pospíšil , P. (2012). Molecular mechanisms of production and scavenging of reactive oxygen species by photosystem II. Biochim Biophys Acta **1817,** 218-231.

Pospíšil, P. (2016). Production of Reactive Oxygen Species by Photosystem II as a Response to Light and Temperature Stress. Frontiers in Plant Science **7**.

Pospíšil, P., and Yamamoto, Y. (2017). Damage to photosystem II by lipid peroxidation products. Biochimica Et Biophysica Acta-General Subjects **1861,** 457-466.

Prasad, A., Ferretti, U., Sedlařová, M., and Pospíšil, P. (2016). Singlet oxygen production in Chlamydomonas reinhardtii under heat stress. Scientific Reports **6,** 13.

Repetto, M., Semprine, J., and Boveris, A. (2012). Lipid Peroxidation: Chemical Mechanism, Biological Implications and Analytical Determination. In Lipid Peroxidation, A. Catala, ed (Rijeka: Intech Europe), pp. 3-30.

Rumeau, D., Peltier, G., and Cournac, L. (2007). Chlororespiration and cyclic electron flow around PSI during photosynthesis and plant stress response. Plant Cell Environ **30,** 1041-1051.

Sachdev, S., Ansari, S.A., Ansari, M.I., Fujita, M., and Hasanuzzaman, M. (2021). Abiotic Stress and Reactive Oxygen Species: Generation, Signaling, and Defense Mechanisms. Antioxidants **10**.

Sedlařová, M., Petřivalský, M., Piterková, J., Luhová, L., Kočířová, J., and Lebeda, A. (2011). Influence of nitric oxide and reactive oxygen species on development of lettuce downy mildew in Lactuca spp. European Journal of Plant Pathology **129**, 267-280.

Sekhar, K.M., Reddy, K.S., and Reddy, A.R. (2017). Amelioration of drought-induced negative responses by elevated CO2 in field grown short rotation coppice mulberry (Morus spp.), a potential bio-energy tree crop. Photosynthesis Research **132**, 151-164.

Singh, S., Agrawal, M., and Agrawal, S.B. (2013). Differential sensitivity of spinach and amaranthus to enhanced UV-B at varying soil nutrient levels: association with gas exchange, UV-B-absorbing compounds and membrane damage. Photosynthesis Research **115**, 123-138.

Smith, W.L., and Murphy, R.C. (2002). Biochemistry of Lipids, Lipoproteins and Membranes. (Elsevier Science).

Soh, N., Ariyoshi, T., Fukaminato, T., Nakajima, H., Nakano, K., and Imato, T. (2007). Swallow-tailed perylene derivative: a new tool for fluorescent imaging of lipid hydroperoxides. Org Biomol Chem **5**, 3762-3768.

Soll, J., Schultz, G., Joyard, J., Douce, R., and Block, M.A. (1985). Localization and synthesis of prenylquinones in isolated outer and inner envelope membranes from spinach chloroplasts. Arch Biochem Biophys **238**, 290-299.

Sudina, G.F., Mirzoeva, O.K., Pushkareva, M.A., Korshunova, G.A., Sumbatyan, N.V., and Varfolomeev, S.D. (1993). CAFFEIC ACID PHENETHYL ESTER AS A LIPOXYGENASE INHIBITOR WITH ANTIOXIDANT PROPERTIES. Febs Letters **329**, 21-24.

Swiezewska, E., Dallner, G., Andersson, B., and Ernster, L. (1993). BIOSYNTHESIS OF UBIQUINONE AND PLASTOQUINONE IN THE ENDOPLASMIC RETICULUM-GOLGI MEMBRANES OF SPINACH LEAVES. Journal of Biological Chemistry **268**, 1494-1499.

Szymanska, R., and Kruk, J. (2010). Plastoquinol is the main prenyllipid synthesized during acclimation to high light conditions in Arabidopsis and is converted to plastochromanol by tocopherol cyclase. Plant Cell Physiol **51**, 537-545.

Szymanska, R., Nowicka, B., and Kruk, J. (2014). Hydroxy-plastochromanol and plastoquinone-C as singlet oxygen products during photo-oxidative stress in Arabidopsis. Plant Cell Environ **37**, 1464-1473.

Telfer, A. (2014). Singlet Oxygen Production by PSII Under Light Stress: Mechanism, Detection and the Protective role of beta-Carotene. Plant and Cell Physiology **55**, 1216-1223.

Trebst, A. (2003). Function of beta-carotene and tocopherol in photosystem II. Zeitschrift Fur Naturforschung Section C-a Journal of Biosciences **58**, 609-620.

Triantaphylides, C., and Havaux, M. (2009). Singlet oxygen in plants: production, detoxification and signaling. Trends Plant Sci **14**, 219-228.

van Amerongen, H., and Croce, R. (2013). Light harvesting in photosystem II. Photosynthesis Research **116**, 251-263.

Van Breusegem, F., and Dat, J.F. (2006). Reactive oxygen species in plant cell death. Plant Physiology **141**, 384-390.

Vass, I. (2012). Molecular mechanisms of photodamage in the Photosystem II complex. Biochim Biophys Acta **1817**, 209-217.

Wang, Y.N., and Eriksson, L.A. (2001). Theoretical studies of electron and hydrogen transfer reactions between semiquinone radicals and oxygen. Theoretical Chemistry Accounts **106,** 158-162.

Yadav, D.K., Kruk, J., Sinha, R.K., and Pospíšil, P. (2010). Singlet oxygen scavenging activity of plastoquinol in photosystem II of higher plants: electron paramagnetic resonance spin-trapping study. Biochim Biophys Acta **1797,** 1807-1811.

Yamashita, A., Nijo, N., Pospíšil, P., Morita, N., Takenaka, D., Aminaka, R., Yamamoto, Y., and Yamamoto, Y. (2008). Quality control of photosystem II: reactive oxygen species are responsible for the damage to photosystem II under moderate heat stress. J Biol Chem **283,** 28380-28391.

Yin, H.Y., Xu, L.B., and Porter, N.A. (2011). Free Radical Lipid Peroxidation: Mechanisms and Analysis. Chemical Reviews **111,** 5944-5972.

Zbierzak, A.M., Kanwischer, M., Wille, C., Vidi, P.A., Giavalisco, P., Lohmann, A., Briesen, I., Porfirova, S., Brehelin, C., Kessler, F., and Dormann, P. (2009). Intersection of the tocopherol and plastoquinol metabolic pathways at the plastoglobule. Biochem J **425,** 389-399.

Zhang, S.R., Apel, K., and Kim, C.H. (2014). Singlet oxygen-mediated and EXECUTER-dependent signalling and acclimation of Arabidopsis thaliana exposed to light stress. Philosophical Transactions of the Royal Society B-Biological Sciences **369,** 7.

7 Appendix

I. **Ferretti U., Ciura J., Ksas B., Rác M., Sedlářová M., Kruk J., Havaux M., Pospíšil P. (2018)** Chemical quenching of singlet oxygen by plastoquinols and their oxidized products in Arabidopsis. Plant Journal 95, 849-861 IF: 5.775

II. **Ksas B., Legeret B., Ferretti U., Chevalier A., Pospíšil P., Alric J., Havaux M. (2018)** The plastoquinone pool outside the thylakoid membrane serves in plant photoprotection as a reservoir of singlet oxygen scavengers. Plant, Cell & Environment 41, 2277-2287 IF: 5.415

III. **Prasad A., Ferretti U., Sedlářová M., Pospíšil P. (2016)** Singlet oxygen production in Chlamydomonas reinhardtii under heat stress. Scientific Reports 6, 20094 IF: 4.122

Chemical quenching of singlet oxygen by plastoquinols and their oxidation products in Arabidopsis

Ursula Ferretti[1] (iD), Joanna Ciura[2], Brigitte Ksas[3], Marek Rác[1] (iD), Michaela Sedlářová[4], Jerzy Kruk[2], Michel Havaux[3] and Pavel Pospíšil[1,*] (iD)

[1]*Department of Biophysics, Centre of the Region Haná for Biotechnological and Agricultural Research, Faculty of Science, Palacký University, Šlechtitelů 27, Olomouc 783 71, Czech Republic,*

[2]*Department of Plant Physiology and Biochemistry, Faculty of Biochemistry, Biophysics and Biotechnology, Jagiellonian University, Kraków 30-387, Poland,*

[3]*Laboratoire d'Écophysiologie Moléculaire des Plantes, CEA, CNRS UMR 7265 BVME, Aix-Marseille Université, CEA/Cadarache, Saint-Paul-lez-Durance, F-13108, France, and*

[4]*Department of Botany, Faculty of Science, Palacký University, Šlechtitelů 27, Olomouc 783 71, Czech Republic*

SUMMARY

Prenylquinols (tocochromanols and plastoquinols) serve as efficient physical and chemical quenchers of singlet oxygen ($^1O_2$) formed during high light stress in higher plants. Although quenching of $^1O_2$ by prenylquinols has been previously studied, direct evidence for chemical quenching of $^1O_2$ by plastoquinols and their oxidation products is limited *in vivo*. In the present study, the role of plastoquinol-9 (PQH_2-9) in chemical quenching of $^1O_2$ was studied in *Arabidopsis thaliana* lines overexpressing the *SOLANESYL DIPHOSPHATE SYNTHASE 1* gene (SPS1oex) involved in PQH_2-9 and plastochromanol-8 biosynthesis. In this work, direct evidence for chemical quenching of $^1O_2$ by plastoquinols and their oxidation products is presented, which is obtained by microscopic techniques *in vivo*. Chemical quenching of $^1O_2$ was associated with consumption of PQH_2-9 and formation of its various oxidized forms. Oxidation of PQH_2-9 by $^1O_2$ leads to plastoquinone-9 (PQ-9), which is subsequently oxidized to hydroxyplastoquinone-9 [PQ(OH)-9]. We provide here evidence that oxidation of PQ(OH)-9 by $^1O_2$ results in the formation of trihydroxyplastoquinone-9 [$PQ(OH)_3$-9]. It is concluded here that PQH_2-9 serves as an efficient $^1O_2$ chemical quencher in Arabidopsis, and $PQ(OH)_3$-9 can be considered as a natural product of $^1O_2$ reaction with PQ(OH)-9. The understanding of the mechanisms underlying $^1O_2$ chemical quenching provides information on the role of plastoquinols and their oxidation products in the response of plants to photooxidative stress.

Keywords: singlet oxygen, prenylquinols, trihydroxyplastoquinone-9, photooxidative stress, *Arabidopsis thaliana*.

INTRODUCTION

Under environmental conditions, plants are exposed to various types of abiotic (high light, heat, cold, drought, flooding, salinity, heavy metals) or biotic (pathogens, parasitic plants, pests) stress conditions. Response of plants to high light is associated with formation of singlet oxygen ($^1O_2$) in PSII. Singlet oxygen is formed by triplet-singlet energy transfer from triplet chlorophyll ($^3Chl^*$) to molecular oxygen (Triantaphylides and Havaux, 2009; Fischer *et al.*, 2013; Telfer, 2014; Pospíšil, 2016). The formation of $^3Chl^*$ occurs either by the intersystem crossing in the PSII antenna complex from singlet chlorophyll or via the charge recombination of triplet radical pair $^3[P680^{\bullet+}Pheo^{\bullet-}]$ in the

PSII reaction centre (Krieger-Liszkay *et al.*, 2008; Triantaphylides and Havaux, 2009; Pospíšil, 2012; Vass, 2012; Van Amerongen and Croce, 2013). To control the levels of $^1O_2$, various types of low molecular weight antioxidants were shown to quench $^1O_2$ (Foyer and Noctor, 2009; Triantaphylides and Havaux, 2009; Pospíšil and Prasad, 2014). Under mild stress, when the antioxidant system maintains low $^1O_2$ levels, $^1O_2$ plays a crucial role in the retrograde signalling during acclimation response and programmed cell death (Mullineaux and Baker, 2010; Zhang *et al.*, 2014; Laloi and Havaux, 2015; Dietz *et al.*, 2016). Under severe stress, when $^1O_2$ formation exceeds the capacity of the

antioxidant systems, deleterious $^1O_2$ causes irreversible damage of biomolecules (lipids and proteins) associated with accidental cell death (Aro *et al.*, 2005; Ledford and Niyogi, 2005; Van Breusegem and Dat, 2006; Farmer and Mueller, 2013; Pospíšil and Yamamoto, 2017).

Among many low molecular weight antioxidants, lipophilic prenylquinols (tocochromanols and isoprenoid quinols) play a crucial role in quenching of $^1O_2$. Tocochromanols involve tocopherols, tocotrienols and plastochromanol-8 (PC-8). Isoprenoid quinols comprise plastoquinols (PQH$_2$-9) and their oxidation products, which consist of plastoquinone-9 (PQ-9), hydroxyplastoquinone-9 [PQ(OH)-9] and trihydroxyplastoquinone-9 [PQ(OH)$_3$-9; Figure 1]. Prenylquinols quench $^1O_2$ either by the excitation energy transfer (physical quenching) or by electron transport (chemical quenching; Foote *et al.*, 1970; Gorman *et al.*, 1988; Mukai *et al.*, 1993; Munné-Bosch, 2005). Physical quenching of $^1O_2$ by prenylquinols occurs by electron transfer producing singlet exciplex known to undergo to triplet exciplex via intersystem crossing followed by the dissociation to prenylquinol and molecular oxygen (Gorman *et al.*, 1988). Chemical quenching of $^1O_2$ by prenylquinols proceeds through their oxidation, forming various types of oxidation products (Mene-Saffrane and Dellapenna, 2010; Kruk *et al.*, 2016). Tocochromanols contain a common chromanol ring and either a saturated (tocopherol) or unsaturated (tocotrienol and PC-8) polyprenyl side-chain (Trebst, 2003; Kruk *et al.*, 2005, 2014; Krieger-Liszkay and Trebst, 2006; Dormann, 2007). Due to their aromatic chromanol ring, tocochromanols are effective antioxidants of $^1O_2$; however, the chromanol ring limits the mobility of tocochromanols and thus decreases the probability of their interactions with $^1O_2$ (Kruk *et al.*, 2014). Plastoquinols and their oxidation products contain either a quinol or quinone ring, and an unsaturated polyprenyl side-chain (Eugeni Piller *et al.*, 2012). Due to the quinol ring, PQH$_2$-9 seems to be less effective in chemical quenching of $^1O_2$ than tocochromanols; however, as a result of its high mobility (Jemiola-Rzeminska *et al.*, 2003), PQH$_2$-9 has been shown to have an efficient $^1O_2$ chemical quenching activity within artificial lipid membranes (Gruszka *et al.*, 2008).

Several lines of evidence for chemical quenching of $^1O_2$ by PQH$_2$-9 were previously provided mainly based on the protective effect on lipids, the consumption of PQH$_2$-9 content and the formation of oxidation products of PQH$_2$-9. It has been recently demonstrated that *SOLANESYL DIPHOSPHATE SYNTHASE 1* overexpressing (SPS1oex) Arabidopsis plants, known to possess enhanced PQH$_2$-9 and PC-8 biosynthesis, exhibit a lower level of lipid peroxidation (Ksas *et al.*, 2015). A decrease in PQH$_2$-9 content was demonstrated after the addition of inhibitor of hydroxyphenylpyruvate dioxygenase involved in PQH$_2$-9 and tocopherol biosynthesis in Chlamydomonas cells (Kruk *et al.*, 2005; Kruk and Trebst, 2008). In agreement with this observation, it has been recently demonstrated that exposure of Arabidopsis leaves to high light resulted in pronounced consumption of PQH$_2$-9 (Ksas *et al.*, 2015). Several oxidation products formed by the interaction of $^1O_2$ with PQH$_2$-9 were recognized during the past two decades. Production of PQ-9 by the interaction of $^1O_2$ with PQH$_2$-9 was demonstrated in Chlamydomonas cells (Kruk and Trebst, 2008). PQ(OH)-9 (denoted as plastoquinone-C, PQ-C) formed by the interaction of $^1O_2$ with PQ-9 was identified in spinach (Kruk and Strzalka, 1998) and Arabidopsis (Szymanska *et al.*, 2014). In a chemical system with exogenous plastoquinols and $^1O_2$ generated by photosensitizers, PQ(OH)$_3$-9 was found to be formed by interaction of $^1O_2$ with PQ(OH)-9 (Gruszka *et al.*, 2008); however, PQ(OH)$_3$-9 has never been found *in vivo*. Chemical quenching of $^1O_2$ by PQH$_2$-9 was previously observed using electron paramagnetic resonance (EPR) spectroscopy (Yadav *et al.*, 2010). It was shown that the addition of exogenous PQH$_2$-9 to PQ-depleted spinach PSII membranes pronouncedly suppressed $^1O_2$ production. However, spectroscopic evidence for chemical quenching of $^1O_2$ by plastoquinols and their oxidation products has not been provided yet *in vivo*.
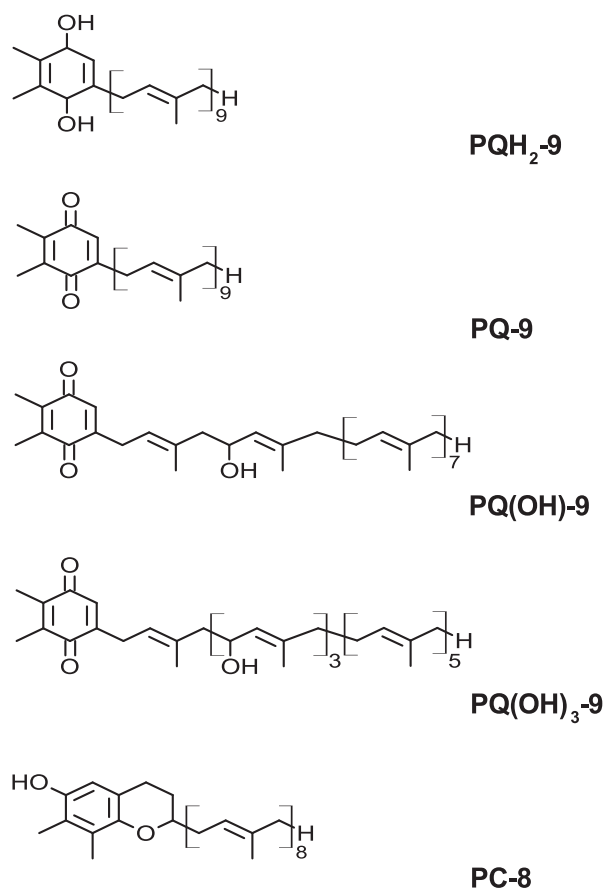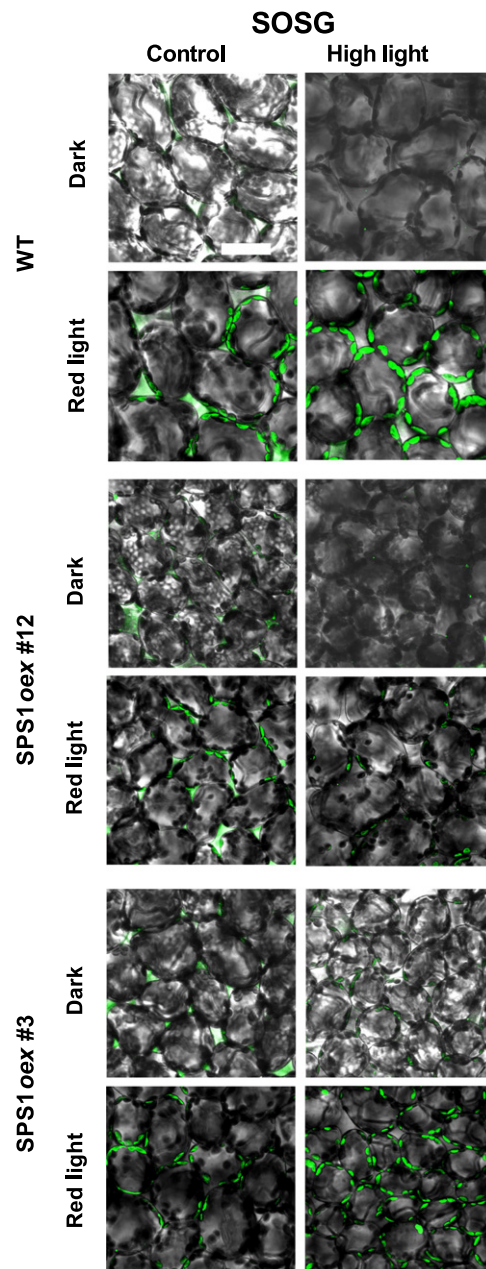

Figure 1. Molecular structure of prenylquinols.

In the present study, chemical quenching of $^1O_2$ by plastoquinols and their oxidation products and formation of a natural oxidation product PQ(OH)$_3$-9 was studied in wild-type (WT) and SPS1oex Arabidopsis during photooxidative stress. The obtained results clearly show that plastoquinols and their oxidation products serve as effective chemical quenchers of $^1O_2$ *in vivo*. By bringing together available knowledge, comprehensive description of mechanistic aspects on chemical quenching of $^1O_2$ by plastoquinols and their oxidation products is provided in terms of basic chemical reactions of $^1O_2$ with either the quinol ring or the unsaturated polyprenyl side-chain of the plastoquinols and their oxidation products. Complete understanding on the role of plastoquinols and their oxidation products in plant antioxidant responses might bring valuable information on the importance of plastoquinols and their oxidation products as chemical quenchers and potential signalling molecules in plant survival under abiotic stresses.

RESULTS

Singlet oxygen formation

Detection of $^1O_2$ formation in leaves was performed by confocal laser scanning microscopy using the fluorescent probe singlet oxygen sensor green (SOSG). SOSG reacts selectively with $^1O_2$ forming a fluorescent SOSG endoperoxide (SOSG-EP) by the cycloaddition of $^1O_2$ (Flors *et al.*, 2006). Figure 2 shows localization of SOSG-EP fluorescence in leaf tissues of control and high light-exposed WT and SPS1oex Arabidopsis. In the dark, no SOSG-EP fluorescence was observed in control and high light-exposed WT and SPS1oex. After illumination of samples with red light, the SOSG-EP fluorescence was observed in chloroplasts from the spongy mesophyll cells of all plants. In addition, SOSG-EP fluorescence in high light-exposed WT and SPS1oex was higher as compared with control plants. Interestingly, SOSG-EP fluorescence in SPS1oex was noticeably lower as compared with WT. These observations indicate that a decrease in $^1O_2$ formation in high light-exposed SPS1oex Arabidopsis occurs due to chemical quenching activity of plastoquinols and their oxidation products.
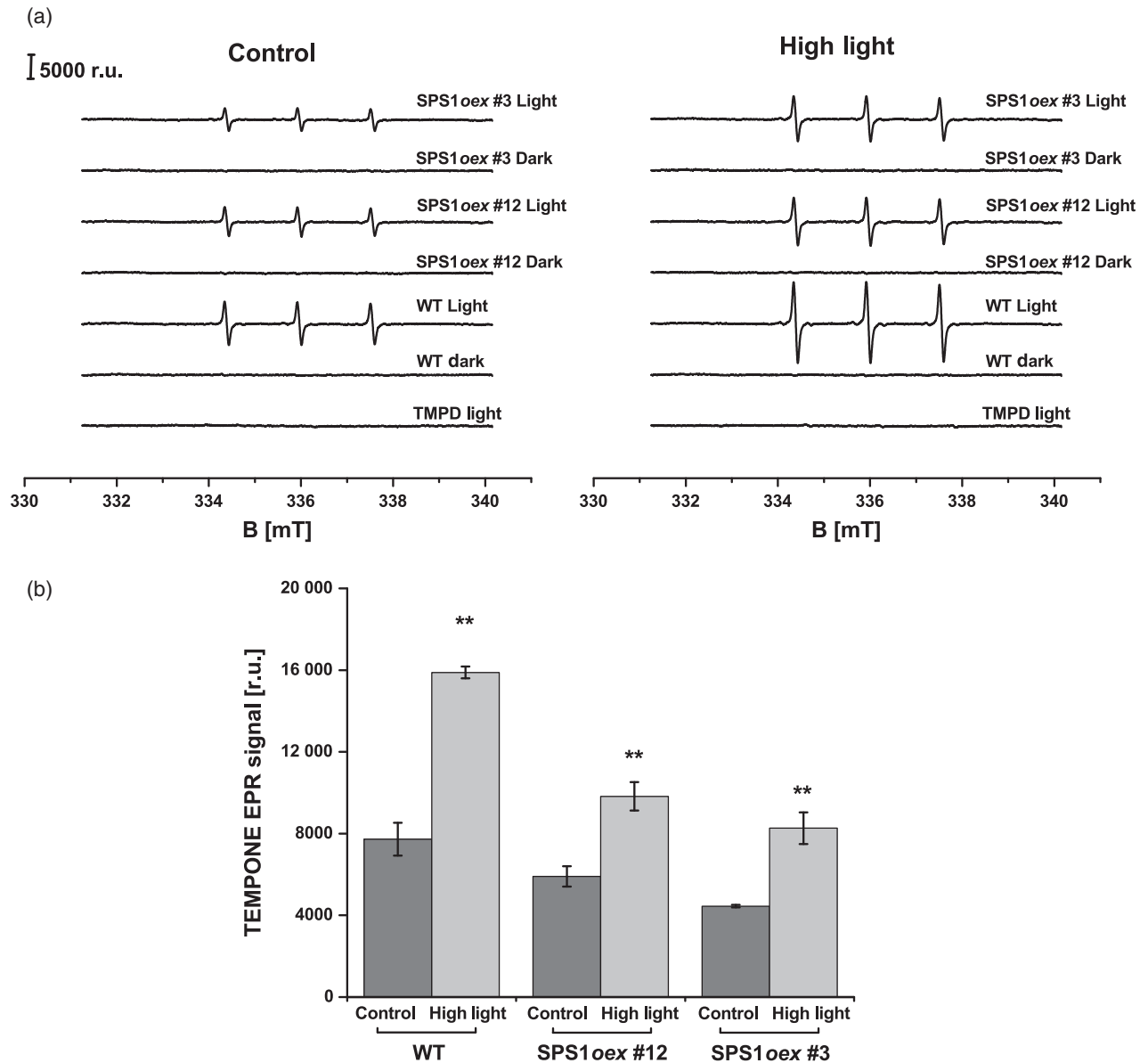
To determine $^1O_2$ formation in broken chloroplasts isolated from WT and SPS1oex Arabidopsis, EPR spectroscopy was performed using the hydrophilic diamagnetic spin probe 2,2,6,6-tetramethyl-4-piperidone (TMPD; Figure 3). The oxidation of TMPD by $^1O_2$ yields paramagnetic 2,2,6,6-tetramethyl-4-piperidone-1-oxyl (TEMPONE; Moan and Wold, 1979). When pure TMPD was illuminated with white light, no TEMPONE EPR signal was observed. In the dark, no TEMPONE EPR signal was observed in broken chloroplasts from control and high light-exposed WT and SPS1oex, whereas illumination of samples with white light in the presence of TMPD resulted in the appearance of the

Figure 2. Singlet oxygen imaging in control and high light-exposed wild-type (WT) and SPS1oex Arabidopsis monitored by confocal laser scanning microscopy.
Arabidopsis were kept under low light (120 μmol photons m^{-2} sec^{-1}, 8 h and 25°C) (control) or exposed to high light (1000 μmol photons m^{-2} sec^{-1}, 13 h and 8°C) (high light). Prior to measurement, leaves were kept in the dark or illuminated with red light (1000 μmol photons m^{-2} sec^{-1}) for 30 min in the presence of 50 μM singlet oxygen sensor green (SOSG). The images represent a combination of the Nomarski DIC and fluorescence channels. Scale bar: 40 μm.

TEMPONE EPR signal (Figure 3a). TEMPONE EPR signal from broken chloroplasts from SPS1oex decreased as compared with WT. TEMPONE EPR signal from broken

(a)

(b)

Figure 3. Singlet oxygen formation in broken chloroplasts from control and high light-exposed wild-type (WT) and SPS1oex Arabidopsis detected by electron paramagnetic resonance (EPR) spin-trapping spectroscopy.
(a) TEMPONE EPR spectra detected after 30 min white light treatment (1000 μmol photons m^{-2} sec^{-1}) of broken chloroplasts in the presence of 50 mM TMPD. TEMPONE EPR spectrum of pure probe (bottom spectrum) was obtained with illumination of 50 mM TMPD and 40 mM MES-NaOH buffer (pH 6.5) with white light (1000 μmol photons m^{-2} sec^{-1}) for 30 min.
(b) The intensity of the TEMPONE EPR signal was determined by measuring the relative height of the central peak of the EPR absorption spectrum. Presented data are mean values ($n = 3$), ±SD. The asterisk indicates a significant difference between control and high light-exposed WT and SPS1oex (Student's *t*-test). Significant differences were confirmed also between WT and SPS1oex (ANOVA).

chloroplasts from high light-exposed WT increased twice as compared with control WT (Figure 3b). Interestingly, TEMPONE EPR signal from broken chloroplasts from high light-exposed SPS1oex increased twice as compared with control SPS1oex. This evidence shows that plastoquinols and their oxidation products effectively decrease $^1O_2$ formation in control and high light-exposed SPS1oex Arabidopsis.

To determine chemical quenching of $^1O_2$, formed by the photosensitizer Rose Bengal, by PQ-*n* with different side-chain length (PQ with *n* isoprenoid units in the side-chain), EPR spectroscopy was performed using TMPD (Figure S1). In the dark, no TEMPONE EPR signal was observed, whereas exposure of Rose Bengal to white light in the presence of TMPD resulted in the appearance of the TEMPONE EPR signal (Figure S1). The TEMPONE EPR signal

from PQ-*n* decreased with the length of the side-chain in the following order: PQ-1 > PQ-2 > PQ-3 > PQ-4 > PQ-5 > PQ-9. These observations indicate that the chemical quenching of $^1O_2$ is dependent on the length of PQ-*n* side-chain.

Prenylquinols quantification

A high-performance liquid chromatography (HPLC) method was used to evaluate the amount of prenylquinols in leaves and broken chloroplasts from WT and SPS1oex Arabidopsis exposed to high light. Figure S2 shows the content of PQH_2-9, PQ-9 and total PQ-9 (PQH_2-9 + PQ-9) in leaves and broken chloroplasts. The content of PQH_2-9, PQ-9 and total PQ-9 levels was comparatively higher in SPS1oex compared with in WT. After exposure to high light, the content of PQH_2-9, PQ-9 and total PQ-9 noticeably decreased as compared with control, presumably due to chemical quenching activity in high light. Apart from plastoquinols and their oxidation products, the content of PC-8 in leaves and broken chloroplasts was determined (Figure S3a and b). No considerable changes in the content of PC-8 in control and high light-exposed leaves and broken chloroplasts were detected.

Formation of plastoquinol-9 oxidation products

Figure 4 shows representative chromatograms of PQH_2-9 oxidation products in high light-exposed Arabidopsis. The peaks at the retention time of 48 min and of about 15 min coincide with PQ-9 and PQ(OH)-9, respectively. The peak at the retention time of about 7 min that corresponds to PQ
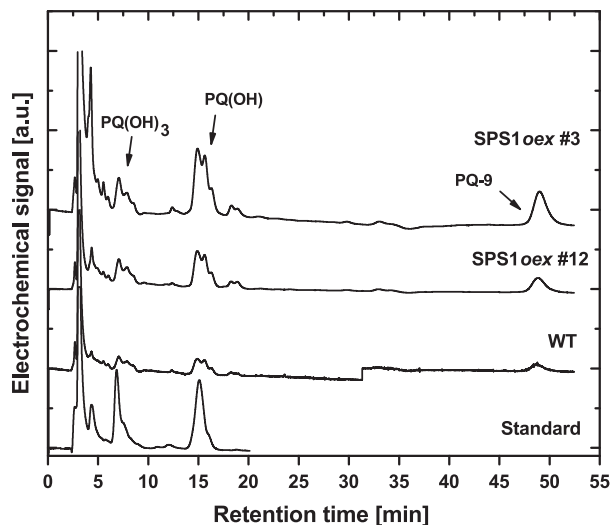
Figure 4. High-performance liquid chromatography (HPLC) of trihydroxyplastoquinone-9 [PQ(OH)$_3$-9].

Standard chromatogram of 10 μM plastoquinone-9 (PQ-9) in methanol with Rose Bengal as photosensitizer, after 10 min illumination (1500 μmol photons m^{-2} sec^{-1}). Chromatograms of high light-exposed wild-type (WT) and SPS1oex lines #12 and #3 in methanol.
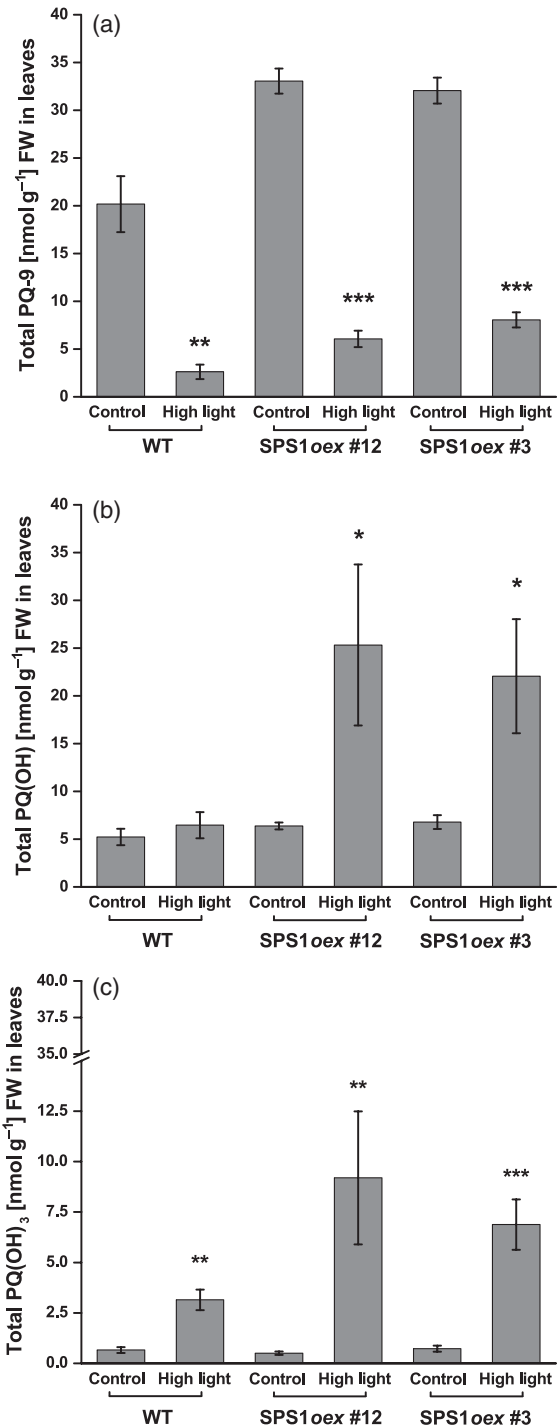
Figure 5. Content of oxidation products of plastoquinol-9 (PQH_2-9) in control and high light-exposed wild-type (WT) and SPS1oex Arabidopsis determined by high-performance liquid chromatography (HPLC).

Total plastoquinone-9 (PQ-9) (a), total hydroxyplastoquinone-9 [PQ(OH)-9] (b) and total trihydroxyplastoquinone-9 [PQ(OH)$_3$-9] (c) contents in control and high light-exposed WT, SPS1oex #12 and #3. The presented data are mean values ($n = 3$), ±SE. Total = oxidized + reduced. The asterisk indicates the significant difference between control and high light-exposed WT and SPS1oex (Student's *t*-test). Significant differences were confirmed also between WT and SPS1oex (ANOVA).

(OH)$_3$-9 was never identified before *in vivo*. To confirm plastoquinols and their oxidation products, a standard containing solution of illuminated PQ-9 with Rose Bengal was used (Figure 4, bottom chromatogram). The chromatogram shows that peaks of all detected PQH$_2$-9 oxidation products in SPS1oex considerably increased as compared with WT. It is obvious that PQ(OH)-9 and PQ(OH)$_3$-9 peaks show the contribution of various PQ(OH)-9 and PQ(OH)$_3$-9 isomers (Figure 4). These results show that the oxidation of PQ(OH)-9 by $^1O_2$ results in PQ(OH)$_3$-9 formation in Arabidopsis. To determine oxidation products of PQH$_2$-9 in WT and SPS1oex Arabidopsis exposed to high light, total PQ-9, PQ(OH)-9 and PQ(OH)$_3$-9 were measured by HPLC (Figure 5). The amount of total PQ-9 formed in SPS1oex was remarkably higher as compared with WT (Figure 5a). The total PQ-9 levels decreased noticeably in high light-exposed WT and SPS1oex as compared with control plants. The level of total PQ(OH)-9 produced in control SPS1oex increased as compared with WT (Figure 5b). The total PQ(OH)-9 formed in high light-exposed SPS1oex substantially increased as compared with control WT and SPS1oex. These data demonstrate that the oxidation of total PQ-9 by $^1O_2$ produces total PQ(OH)-9. The amount of PQ(OH)$_3$-9 was measured in control and high light-exposed SPS1oex leaves (Figure 5c). The total PQ(OH)$_3$-9 content produced in high light-exposed WT and SPS1oex plants increased as compared with control plants. The total PQ(OH)$_3$-9 generated in high light-exposed SPS1oex increased noticeably as compared with WT.

Organic hydroperoxides formation

Organic (lipid, protein and PQ-9) hydroperoxides (ROOH) was detected in leaves by confocal laser scanning microscopy using the fluorescent probe 2-(4-diphenylphosphanyl-phenyl)-9-(1-hexyl-heptyl)-anthra[2,1,9-def,6,5,10-d'e'f'] diiso-quinoline-1,3,8,10-tetraone (SPY-LHP). SPY-LHP is highly selective to ROOH forming a SPY-LHPox fluorescent complex (Soh *et al.*, 2007). Figure 6 presents the localization of SPY-LHPox fluorescence measured within cells of control and high light-exposed WT and SPS1oex Arabidopsis leaves. In the dark, a low SPY-LHPox fluorescence was observed in chloroplasts of spongy mesophyll cells of both control and high light-exposed WT and SPS1oex. After the illumination of samples with red light in the presence of SPY-LHP probe, the SPY-LHPox fluorescence increased, especially in high light-exposed WT and SPS1oex. SPY-LHPox fluorescence in both control and high light-exposed SPS1oex negligibly decreased as compared with WT.

To determine ROOH formation in broken chloroplasts isolated from WT and SPS1oex Arabidopsis, fluorescence spectroscopy was performed using fluorescent probe SPY-LHP. Figure S4 presents the SPY-LHPox fluorescence spectra (Figure S4a) and the SPY-LHPox fluorescence intensity (Figure S4b) measured in broken chloroplasts from control
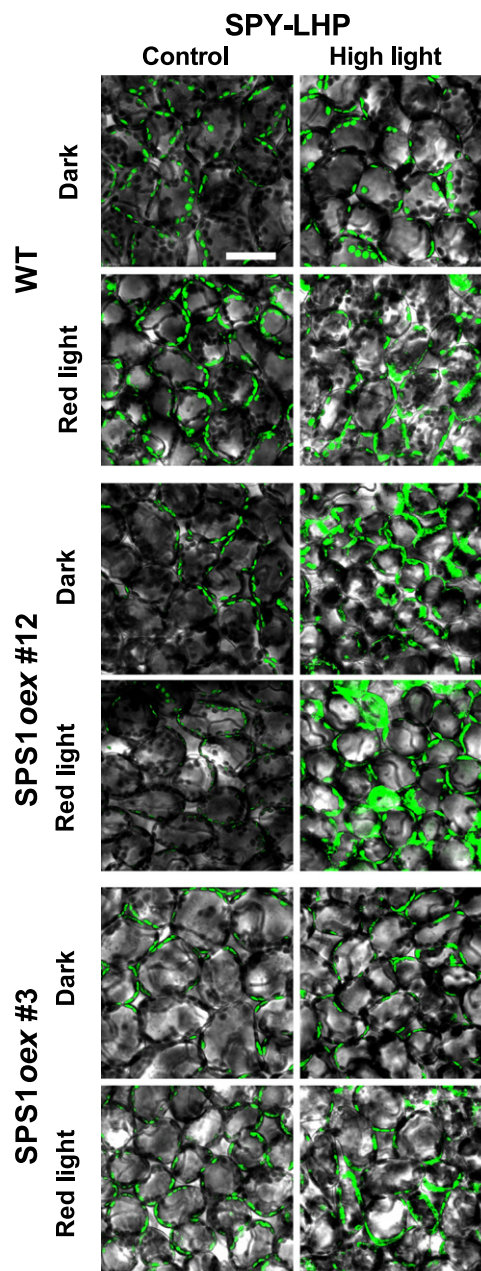

Figure 6. Organic hydroperoxides imaging in control and high light-exposed wild-type (WT) and SPS1oex Arabidopsis monitored by confocal laser scanning microscopy.
Arabidopsis were kept under low light (120 μmol photons m^{-2} sec^{-1}, 8 h and 25°C) (control) or exposed to high light (1000 μmol photons m^{-2} sec^{-1}, 13 h and 8°C) (high light). Prior to measurement, leaves were kept in the dark or illuminated with red light (1000 μmol photons m^{-2} sec^{-1}) for 30 min in the presence of 50 μM SPY-LHP. The images represent a combination of the Nomarski DIC and fluorescence channels. Scale bar: 40 μm.

and high light-exposed WT and SPS1oex. The SPY-LHPox fluorescence formed in high light WT and SPS1oex is 2.5 times higher as compared with control. The SPY-LHPox fluorescence in SPS1oex did not differ significantly from WT. In further, the measurement of plastoquinone-
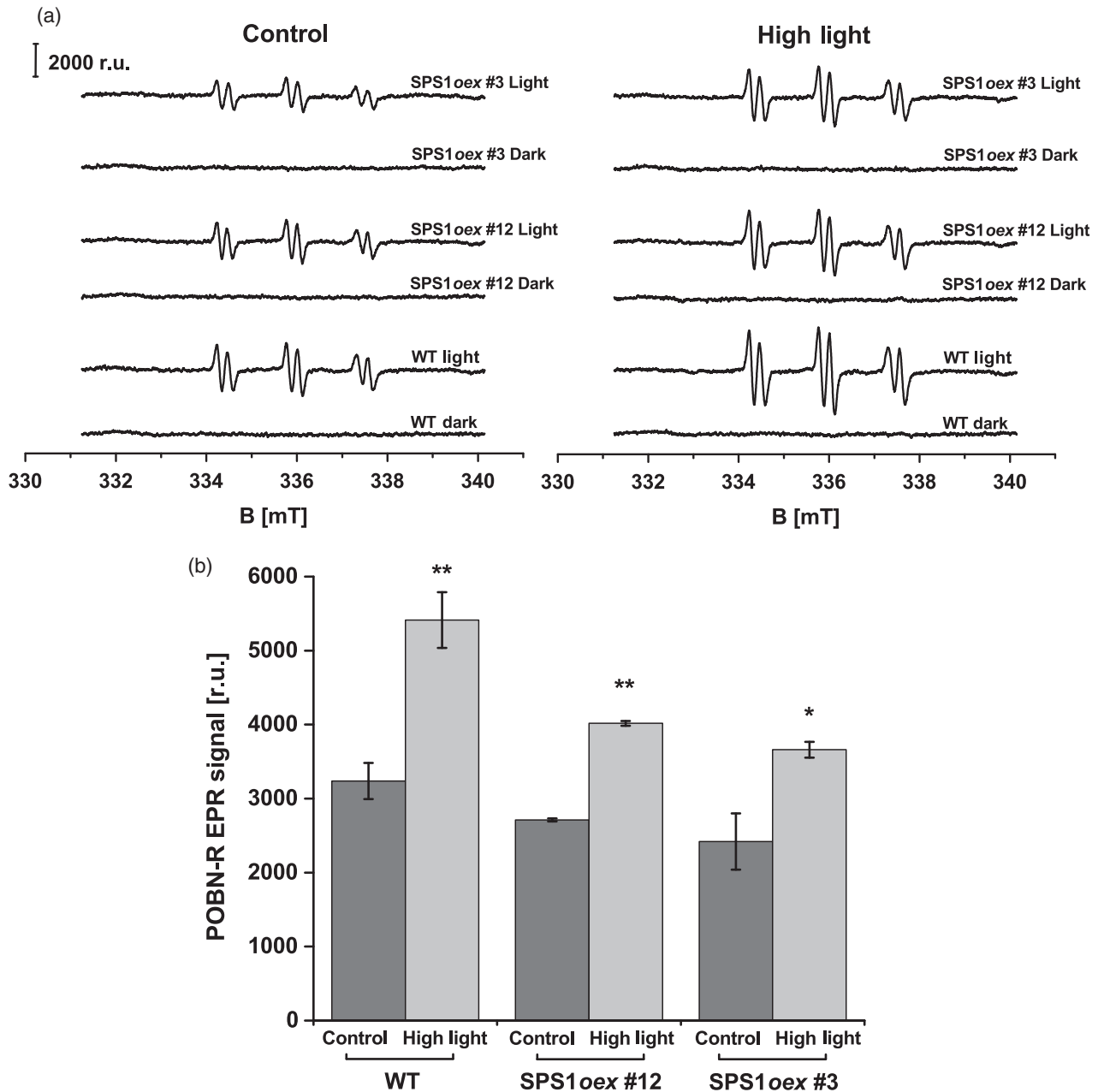
Figure 7. Organic radical formation in broken chloroplasts from control and high light-exposed wild-type (WT) and SPS1oex Arabidopsis detected by electron paramagnetic resonance (EPR) spin-trapping spectroscopy.
(a) POBN-R adduct EPR spectra detected after 30 min white light treatment (1000 μmol photons m^{-2} sec^{-1}) of broken chloroplasts in the presence of 50 mM POBN.
(b) The intensity of POBN-R adduct EPR signal was determined by measuring the relative height of the central peak of the EPR absorption spectrum. Presented data are mean values ($n = 3$), ±SD. The asterisk indicates the significant difference between control and high light-exposed WT and SPS1oex (Student's *t*-test). Significant differences were confirmed also between WT and SPS1oex (ANOVA).

hydroperoxides (PQ-*n* hydroperoxides) produced by $^1O_2$ reaction with PQ-*n* was performed using SPY-LHP fluorescence probe (Figure S5). The amount of PQ-*n* hydroperoxides increased with the length of the side-chain in the following order: PQ-1 < PQ-2 < PQ-4 < PQ-9. After the addition of ferrous iron, the amount of PQ-9 hydroperoxides noticeably decreased. These data show that PQ-*n*

hydroperoxide formation is dependent on the length of the PQ-*n* side-chain.

Formation of organic radical

For detection of organic radical (R˙), EPR spin-trapping spectroscopy was performed using α-(4-pyridyl-1-oxide)-N-tert-butylnitrone (POBN) as spin-trap (Figure 7). Interaction

of diamagnetic POBN with R• forms paramagnetic POBN-R adduct (Buettner, 1987). No POBN-R adduct EPR signal was observed in broken chloroplasts from control and high light-exposed WT and SPS1oex in the dark, while the illumination of samples with white light in the presence of POBN resulted in the detection of the POBN-R adduct EPR signal (Figure 7a). The intensity of POBN-R adduct EPR signal decreased in broken chloroplasts from SPS1oex as compared with WT. In broken chloroplasts from control SPS1oex, POBN-R adduct EPR signal slightly decreased as compared with WT. POBN-R adduct EPR signal from broken chloroplasts from high light-exposed WT increased by about half as compared with control WT (Figure 7b). Interestingly, POBN-R adduct EPR signal from broken chloroplasts from high light-exposed SPS1oex decreased by one-third as compared with high light-exposed WT. The decline of R• due to the scavenging activity of plastoquinols and their oxidation products was observed in control and high light-exposed SPS1oex Arabidopsis.

DISCUSSION

Chemical quenching of singlet oxygen by plastoquinols and their oxidation products

Absorption of excess light energy by chlorophylls promotes the formation of $^3Chl^*$, which subsequently reacts with molecular oxygen producing $^1O_2$ (Triantaphylides and Havaux, 2009; Pospíšil, 2012; Fischer et al., 2013; Telfer, 2014). Plastoquinols and their oxidation products were shown to effectively protect lipids by their $^1O_2$ chemical quenching (Ksas et al., 2015), their consumption followed by formation of oxidation products (Kruk and Trebst, 2008; Szymanska and Kruk, 2010; Nowicka and Kruk, 2012; Ksas et al., 2015), and direct chemical quenching of $^1O_2$ in vitro (Yadav et al., 2010). In this study, direct evidence for chemical quenching of $^1O_2$ by plastoquinols and their oxidation products obtained by microscopic technique in vivo is provided. Singlet oxygen imaging shows that $^1O_2$ was significantly chemically quenched in SPS1oex leaves (Figure 2). Quantitative analysis of $^1O_2$ quenching obtained by EPR spin-trapping spectroscopy in SPS1oex chloroplasts indicates that about half of $^1O_2$ is chemically quenched by plastoquinols and their oxidation products (Figure 3). These data reveal that the plastoquinols and their oxidation products serve as efficient quenchers of $^1O_2$. It was previously demonstrated that the physical quenching of $^1O_2$ competes with the chemical quenching (Gorman et al., 1988). It is proposed here that under low $^1O_2$ formation, when the amount of PQH$_2$-9 prevails, the physical quenching is more effective compared with the chemical quenching. On the other hand, during photooxidative stress, when $^1O_2$ formation is high, PQ-9 and other oxidation products accomplished solely chemical quenching (Figures S2 and 3). It is suggested that the effective chemical quenching is maintained at the Q$_B$ pocket (a domain of D1 protein that comprises the PQ-9 binding site), where PQ-9 is reduced to PQH$_2$-9. As the fatty acids in the vicinity of the Q$_B$ site are predominantly polyunsaturated, it was shown that fatty acids at the Q$_B$ pocket are easily oxidation by $^1O_2$ forming lipid hydroperoxides (Pospíšil and Yamamoto, 2017). It is assumed here that the chemical quenching of $^1O_2$ by PQH$_2$-9 prevents the lipid peroxidation at the Q$_B$ pocket. When PQH$_2$-9 escapes the oxidation by $^1O_2$, it moves fast from the Q$_B$ pocket via channels to the PQ pool in the thylakoid membrane. Limited diffusion of PQH$_2$-9 through lipids in the membrane with the quinol ring oriented toward the lumen side of the thylakoid membrane maintains the optimal conditions for interaction of $^1O_2$ with both the quinol ring and polyprenyl side-chain during its diffusion to the quinol binding site of cytochrome b$_6$f (Kirchhoff et al., 2000; Kargul and Barber, 2008). Diffusion of plastoquinols and their oxidation products across the thylakoid membranes maintains effective quenching of $^1O_2$ known to diffuse to distances about 10 nm (Sies and Menck, 1992; Skovsen et al., 2005).

In this study, plastoquinols and their oxidation products were shown to prevent formation of the primary products of lipid peroxidation, lipid hydroperoxides (Figure 6), which decompose to the secondary products of lipid peroxidation, hydroxy octadecatrienoic acid (Ksas et al., 2015). Lipid hydroperoxides can be oxidation and reduced to lipid peroxyl and alkoxyl radicals, respectively (Stratton and Liebler, 1997). These radicals participate in the propagation of lipid peroxidation resulting in the formation of lipid alkyl radical (Figure 7; Farmer and Mueller, 2013). It is proposed here that the interaction of $^1O_2$ with plastoquinols and their oxidation products both increases the formation of PQ-9 hydroperoxides and decreases the production of lipid hydroperoxides. Our current data on the detection of ROOH do not completely allow us to distinguish between lipid and PQ-9 hydroperoxides. The slight changes in the formation of ROOH in chloroplasts detected by microscopic techniques in vivo can be explained by a decrease in the production of lipid hydroperoxides and a simultaneous increase in PQ-9 hydroperoxides (Figure 6). The decrease in lipid hydroperoxides is almost compensated by the increase in PQ-9 hydroperoxides. This hypothesis is supported by the fact that the number of bound lipid molecules per PSII monomer was reported to be comparable to plastoquinols and their oxidation products (Ksas et al., 2015; Wei et al., 2016). It has to be mentioned that the observed chemical quenching of $^1O_2$ and the prevention of lipid peroxidation in SPS1oex plants might be partially caused by PC-8; however, as the amount of PC-8 in SPS1oex is 40 times less than plastoquinols and their oxidation products (Figure S2), its contribution is likely to be negligible.

Plastoquinols and their oxidation products

Chemical quenching of $^1O_2$ by plastoquinols and their oxidation products occurs by its reaction with either the quinol ring or the unsaturated polyprenyl side-chain. The plausible reaction pathway for the interaction of $^1O_2$ with plastoquinols and their oxidation products and the formation of their oxidation products is described below; however, alternative reaction pathways cannot be excluded.

Oxidation of PQH$_2$-9 by singlet oxygen forms PQ-9. From the obtained results, it is shown here that the content of PQH$_2$-9 decreased after exposure of Arabidopsis to high light (Figure S1). The decrease in PQH$_2$-9 content can be caused by its interaction with $^1O_2$; however, alternative reaction pathways comprising PQH$_2$-9 oxidation by plastoquinol oxidase involved in chlororespiration as plastoquinol terminal oxidase (Kruk and Karpinski, 2006; McDonald *et al.*, 2011) and cytochrome b_{559} (Kruk and Strzalka, 1999; Pospíšil *et al.*, 2006) cannot be excluded. It is proposed that the oxidation of PQH$_2$-9 by $^1O_2$ produces semiplastoquinone-9 radical (PQH$^•$-9) and hydroperoxyl radical (HO$_2^•$). Subsequently, PQH$^•$-9 may react with another $^1O_2$ forming PQ-9 and HO$_2^•$ (Figure 8). In these reactions, the quinol and semiquinone rings represent a conjugated system, which causes high accessibility of hydrogen atoms bounded in hydroxy groups for highly reactive $^1O_2$. Subsequent hydrogen abstraction from hydroxy groups by $^1O_2$ produces the quinone ring. Similarly, it was previously proposed that the reaction of ubiquinones (coenzyme Q10) with $^1O_2$ forms semiquinone radical and HO$_2^•$ (Wang and Eriksson, 2001). It is proposed here that the dismutation of HO$_2^•$ with another HO$_2^•$ forms hydrogen peroxide (H$_2O_2$). Accordingly, it has been recently shown that the amount of H$_2O_2$ increased after PQH$_2$-9 oxidation by $^1O_2$ generated by Rose Bengal (Khorobrykh *et al.*, 2015).

It is generally known that one molecule of PQH$_2$-9 can quench several hundreds of $^1O_2$ molecules during physical quenching, whereas one molecule of PQH$_2$-9 can quench only one $^1O_2$ molecule during chemical quenching (Pospíšil, 2012). Due to the re-reduction of PQ-9 to PQH$_2$-9 by PSII, it is assumed that one molecule of PQH$_2$-9 can quench several $^1O_2$ molecules. It is well established that re-reduction of PQ-9 to PQH$_2$-9 occurs by NADH dehydrogenase complex in the dark (Rumeau *et al.*, 2007), and by the primary quinone electron acceptor of PSII (Q$_A$) in the light (Lambreva *et al.*, 2014). It is proposed here that $^1O_2$ interacts with the PQH$_2$-9 in the initial period of high light stress when PSII sufficiently re-reduces PQ-9 to PQH$_2$-9 (Figure 8). Once the re-reduction of PQ-9 becomes inefficient, the reaction of $^1O_2$ with the polyprenyl side-chain of PQ-9 becomes predominant (Figure 8).
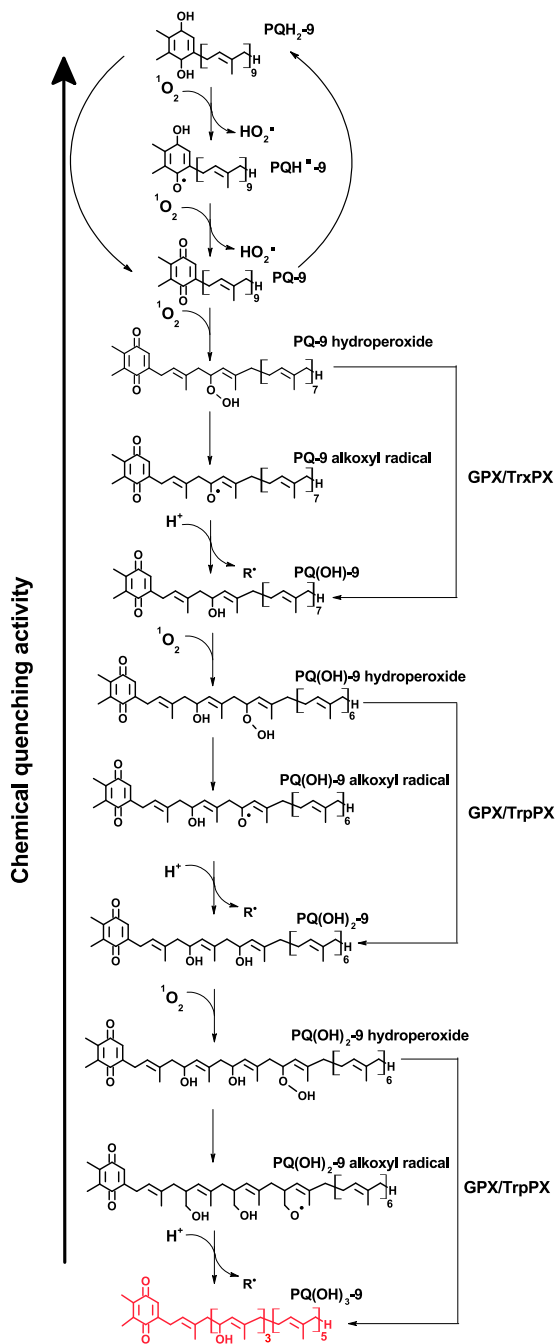
Figure 8. Formation of trihydroxyplastoquinone-9 [PQ(OH)$_3$].
Plastoquinol-9 (PQH$_2$-9) function as an antioxidant of $^1O_2$ is illustrated. After PQH$_2$-9 oxidation with $^1O_2$, a well-known product plastoquinone-9 (PQ-9) via PQH$^•$-9 is formed, producing two molecules of HO$_2^•$ that dismutate into H$_2O_2$. Subsequently, reaction of PQ-9 with another $^1O_2$ leads to hydroxyplastoquinone-9 [PQ(OH)-9] through decomposition of PQ-9 hydroperoxide by: (1) radical reaction pathway comprising of PQ-9 alkoxyl radical as intermediate; or (2) non-radical reaction pathway caused by enzymes of the glutathione peroxidase (GPX) or thioredoxin peroxidase (TrxPX) families. Following oxidation of PQ(OH)-9 probably proceeds similarly through PQ (OH)-9 hydroperoxide decomposition by a radical or non-radical reaction to dihydroxyplastoquinone-9 [PQ(OH)$_2$-9] from which trihydroxyplastoquinone-9 [PQ(OH)$_3$-9] is produced via PQ(OH)$_2$-9 hydroperoxide in the same way. [Colour figure can be viewed at wileyonlinelibrary.com].

Oxidation of PQ-9 by singlet oxygen forms PQ(OH)-9. As we observed, the content of PQ-9 decreased (Figure 5a), and simultaneously the content of PQ(OH)-9 enhanced (Figure 5b) after exposure of Arabidopsis to high light. It is proposed here that the oxidation of PQ-9 to PQ(OH)-9 by $^1O_2$ produces PQ-9 hydroperoxides (Figure 8). In the first reaction, the addition of $^1O_2$ by ene reaction to the carbon with the lowest electronegativity linked to two prenyl units of the PQ-9 polyprenyl side-chain produces PQ-9 hydroperoxides. In agreement with this proposal, our results show that the oxidation of PQ-*n* by $^1O_2$ formed by illumination of Rose Bengal produces PQ-*n* hydroperoxides (Figure S5). In the second reaction, PQ-9 hydroperoxides decompose to PQ(OH)-9. It is proposed that PQ-9 hydroperoxides decompose to PQ-9 hydroxides via either radical or non-radical reaction pathway. In the radical reaction pathway, the reduction of PQ-9 hydroperoxides by trace amounts of catalytic transition metal as ferrous iron or copper results in the formation of PQ-9 alkoxyl radical (Figure 8). The observation that ferrous iron decreased the content of PQ-9 hydroperoxides confirms the decomposition of PQ-9 hydroperoxides (Figure S5). Subsequently, hydrogen abstraction from nearby biomolecules by PQ-9 alkoxyl radical may lead to the formation of R• and PQ(OH)-9 (Figure 8). When R• is not properly quenched, it might oxidize another lipid leading to propagation of lipid peroxidation. In the non-radical reaction pathway, the decomposition of PQ-9 hydroperoxides to PQ-9 hydroxides possibly occurs by enzymes such as glutathione peroxidase (GPX) or thioredoxin peroxidase (TrxPX). In this reaction, GPX or TrxPX catalyses two electron reduction of PQ-9 hydroperoxides to PQ(OH)-9 (Figure 8).

Oxidation of PQ(OH)-9 by singlet oxygen forms PQ(OH)$_3$-9. Evidence for the formation of PQ(OH)$_3$-9 in leaves provided in this study shows that the content of PQ(OH)$_3$-9 is enhanced after exposure of Arabidopsis to high light (Figures 4 and 5c). It is hypothesized here that the interaction of PQ(OH)-9 with $^1O_2$ might produce dihydroxyplastoquinone-9 [PQ(OH)$_2$-9] as a plausible oxidation product. Unfortunately, PQ(OH)$_2$-9 has not been identified yet. It is proposed here that the oxidation of PQ(OH)-9 to PQ(OH)$_2$-9 occurs in a similar manner as the oxidation of PQ-9 to PQ(OH)-9, including intermediates such as PQ(OH)$_2$-9 hydroperoxides and PQ(OH)$_2$-9 alkoxyl radical (Figure 8). The hypothesized non-enzymatic reaction pathway of PQ(OH)$_3$-9 formation comprises of the oxidation of PQ(OH)$_2$-9 by $^1O_2$ to PQ(OH)$_2$-9 hydroperoxides. This reaction is followed by decomposition of PQ(OH)$_2$-9 hydroperoxides to PQ(OH)$_2$-9 alkoxyl radical and as a result hydrogen abstraction from a nearby biomolecule by PQ(OH)$_2$-9 alkoxyl radical, and PQ(OH)$_3$-9 is formed (Figure 8). The enzymatic reaction pathway might plausibly occur by reduction of PQ(OH)$_2$-9 hydroperoxides to PQ(OH)$_3$-9 by GPX or TrxPX enzymes (Figure 8). Obviously, the following oxidation reactions that generate the formation of other multiple PQ-9 hydroxides on polyprenyl side-chain cannot be excluded. It is proposed that other multiple PQ-9 hydroxides might be formed by the interaction of multiple PQ(OH)-9 with $^1O_2$ in a reaction pathway that occurs in a similar manner as it is described here for PQ(OH)$_2$-9 and PQ(OH)$_3$-9.

It was previously demonstrated by EPR spectroscopy that the chemical quenching of $^1O_2$ by PQ-*n* exogenously added to spinach PSII membranes decreased with the length of side-chain (Yadav *et al.*, 2010). It was proposed that the short-chain PQ-*n* are effective in the chemical quenching of $^1O_2$ due to their better penetration in the membranes caused by their different polarity. The comparison of $^1O_2$ chemical quenching activities of PQ-*n* (Figure S3) indicates that chemical quenching activity increases with the length of side-chain. It is proposed here that the long-chain PQ-*n* are more efficient $^1O_2$ chemical quenchers due to the high number of carbons prone to $^1O_2$ addition. As a result of decreased number of carbons available for $^1O_2$ addition, the chemical quenching activity of the side-chain of plastoquinols and their oxidation products decreases with the number of oxidation reactions (Figure 8). As $^1O_2$ modifies the structure of the side-chain, one molecule of PQ-*n* can eliminate solely a few $^1O_2$.

Further, two more alternative pathways for consumption of PQ(OH)-9 involve: (1) the reduction of PQ(OH)-9 to hydroxy plastoquinol either by PSII electron transport in chloroplasts (Kruk and Strzalka, 1998) or catalysed by NAD(P)H-dependent quinone oxidoreductase (NDC1) enzyme in plastoglobuli (Eugeni Piller *et al.*, 2011); and (2) the esterification of PQ(OH)-9 to esterified product of PQ(OH)-9 called plastoquinone-B (PQ-B) (Henninger *et al.*, 1966; Barr *et al.*, 1967; Szymanska *et al.*, 2014; Dluzewska *et al.*, 2015). Obviously, such alternative pathways of consumption of PQ-9 hydroxides that generate the formation of other alternative forms of the multiple PQ-9 hydroxides for example from PQ(OH)$_3$-9 cannot be excluded.

CONCLUSION

In conclusion, chemical quenching of $^1O_2$ by plastoquinols and their oxidation products during high light stress was demonstrated in WT and SPS1oex Arabidopsis. Direct evidence for the chemical quenching of $^1O_2$ by plastoquinols and their oxidation products has been obtained using microscopic techniques *in vivo* and spectroscopic techniques. A natural product PQ(OH)$_3$-9 formed by the interaction of plastoquinols and their oxidation products with $^1O_2$ was identified in Arabidopsis under high light. The oxidation of PQ-9 isolated from plants by $^1O_2$ produced by Rose Bengal involves the formation of PQ-9 hydroperoxides. Even if these observations were obtained in chemical systems, they provide valuable information on the potential mechanism of interactions between $^1O_2$ and

plastoquinols and their oxidation products. Based on the data observed in this study, we have proposed a model on the formation of oxidation products of plastoquinols by interaction of $^1O_2$ with PQ-9. Finally, our results indicate that plastoquinols and their oxidized products are important players in the management of $^1O_2$ and photooxidative stress in plants. The understanding of the interaction pathway of plastoquinols and their oxidation products with $^1O_2$ (Figure 8) might be very helpful for future research, in particular the identification, localization and characterization of other oxidation products of plastoquinols in the plant antioxidant system. It is also worth mentioning that plastoquinols and their oxidation products might be involved in the retrograde chloroplast-to-nucleus signalling network interconnected with other signalling molecules leading to acclimation responses and programmed cell death.

EXPERIMENTAL PROCEDURES

Plant material

In the present work, *Arabidopsis thaliana*, WT (Columbia-0) and SPS1oex (lines #12 and #3) lines (Ksas *et al.*, 2015) were used. Plants were grown on a commercial substrate (Potgrond H, Klasmann-Deilmann Substrate, Germany) in a growing chamber (Photon Systems Instruments, Drásov, Czech Republic) under controlled conditions: photoperiod of 8 h light/16 h dark (120 μmol photons m^{-2} sec^{-1}), temperature of 22°C and humidity 60%.

Chloroplasts preparation

Broken chloroplasts from Arabidopsis were prepared according to Casazza *et al.* (2001) with some modifications. Leaves were homogenized in 10–20 ml of grinding buffer consisting of 400 mM sorbitol, 5 mM Na-EDTA, 5 mM EGTA, 10 mM NaHCO$_3$, 5 mM MgCl$_2$·6H$_2$O, 20 mM Tricine/NaOH and 0.5% (w/v) bovine serum albumin. The homogenate was rapidly filtered through a double layer of cheesecloth and centrifuged at 2600 *g* for 3 min at 4°C. The supernatant was discarded and the pellet was resuspended in 1–2 ml of the grinding buffer. Isolated broken chloroplasts were immediately used for measurements. During the isolation procedure, all the steps were carried out in dim light at 4°C.

Plastoquinones with different side-chain length

Plastoquinone-9 was isolated by extraction of pigment from old leaves and direct HPLC separation of the total pigment extract (Kruk and Strzalka, 1998). Short-chain plastoquinones (PQ-1 to PQ-4) were a gift from Professor H. Koike (Department of Life Sciences, Himeji Institute of Technology, Hyogo, Japan), while PQ-5 was prepared from dimethylhydroquinone and all-E-pentaprenol (kindly provided by Dr Thomas Netscher, Research and Development, DSMNutritional Products, Basel, Switzerland).

High light exposure

Four- to six-week-old plants were harvested at the light period for experiments (control) or exposed to white light (1000 μmol photons m^{-2} sec^{-1}) in Algaetron AG 230 (Photon Systems Instruments, Drásov, Czech Republic) for 13 h at a temperature of 8°C

(high light). Formation of $^1O_2$ by illumination with red light (1000 μmol photons m^{-2} sec^{-1}) in plants or broken chloroplasts was performed using a light-emitting diode (LED) panel source with a light guide (ZETT Optics 177 GmbH 38116, Braunschweig, Germany) for a period mentioned in the text. To avoid the auto-photosensitization of fluorescent probes, a long-pass edge interference filter (>600 nm; Andover, Salem, NH, USA) was used to eliminate the blue-green region of the spectrum. Formation of $^1O_2$ by illumination with white light (1000 μmol photons m^{-2} sec^{-1}) in plants, broken chloroplasts or chemical system was performed using a LED panel (LED Light Source SL 3500, PSI, Drásov, Czech Republic). In the chemical system, $^1O_2$ formation was induced by illumination of 5 μM Rose Bengal in 40 mM MES-NaOH buffer (pH 6.5) with white light as described previously (Yadav *et al.*, 2010).

Confocal laser scanning microscopy

Imaging of $^1O_2$ and ROOH in leaves was performed using fluorescent probes SOSG (Molecular Probes, Eugene, OR, USA) and SPY-LHP (Dojindo Molecular Technologies, Rockville, MD, USA), respectively. SOSG and SPY-LHP probe is commonly used for its high selectivity to $^1O_2$ and ROOH, respectively, without any side-reactions with other reactive oxygen species ($O_2^{•-}$, H_2O_2, $HO^•$). As SOSG-EP fluorescence is in the visible range of the spectrum, the detection is convenient compared with other fluorescent probes (indocyanine green) known to absorb in the near-infrared range. As excitation of SPY-LHPox is in the visible range of the spectrum, live cells are minimally damaged compared with other fluorescent probes (diphenyl-1-pyrenylphosphine) known to absorb in the ultraviolet range. Arabidopsis leaf blade cuts (2 × 2 mm) were incubated in the presence of either 50 μM SOSG or 50 μM SPY-LHP and 40 mM HEPES buffer (pH 7.6) in the dark or under red light for 30 min. Afterwards, the samples were visualized by confocal microscope (FV1000, Olympus Czech Group, Prague, Czech Republic). The excitation of both fluorochromes was performed using a 488 nm line of argon laser, and signal was detected by 505–525 nm emission filter set for $^1O_2$ or by 505–550 nm emission filter set for ROOH. The proper intensity of the laser was set according to unstained samples at the beginning of each experiment (Sedlářová *et al.*, 2011). Post-processing of original images for more clear presentation of results included a threefold increase of contrast in fluorescence channels and setting of signal intensities from initial 0–4095 grades of brightness to 400–1200 for SOSG and 120–800 for SPY-LHP, respectively.

Electron paramagnetic resonance spectroscopy

Singlet oxygen formation was determined by EPR spectroscopy employing TMPD probe. Broken chloroplasts at a concentration of 200 μg Chl ml^{-1} were kept in the dark or illuminated with white light for 30 min in the presence of 50 mM TMPD and 40 mM MES-NaOH buffer (pH 6.5). The chemical systems containing PQ-*n* with different side-chain lengths and Rose Bengal were kept in the dark or illuminated with white light for 5 min in the presence of 50 mM TMPD and 40 mM MES-NaOH buffer (pH 6.5). After illumination, samples were centrifuged at 1000 *g* for 2 min to separate broken chloroplasts or PQ-*n* samples from TEMPONE, and measured by EPR spectrometer. Formation of R$^•$ was measured by EPR spin-trapping spectroscopy using POBN spin-trap. Broken chloroplasts at a concentration of 200 μg Chl ml^{-1} were kept in the dark or illuminated with white light (1000 μmol photons m^{-2} sec^{-1}) for 30 min in the presence of 50 mM POBN and 40 mM MES-NaOH buffer (pH 6.5). After illumination, POBN-R adduct EPR spectra were obtained. EPR spectra were recorded using an EPR spectrometer MiniScope MS400 (Magnettech GmbH, Berlin, Germany).

EPR measurement conditions were as follows: microwave power, 10 mW; modulation amplitude, 1 G; modulation frequency, 100 kHz; sweep width, 89 G; scan rate, 1.62 G sec^{-1}; gain, 500.

Fluorescence spectroscopy

Organic hydroperoxides formation produced in broken chloroplasts from Arabidopsis was determined by fluorescence spectroscopy using SPY-LHP fluorescence probe as described in Khorobrykh *et al.* (2011) with some modifications. Broken chloroplasts suspended in 40 mM MES-NaOH buffer (pH 6.5) at a concentration of 200 μg Chl ml^{-1} were either kept in the dark or illuminated with red light for 30 min in the presence of 2.7 μM SPY-LHP dissolved in absolute ethanol. After incubation, centrifugation of samples at 12 000 ***g*** for 3 min at 4°C was performed and supernatant was taken for fluorescence measurement. Plastoquinone-hydroperoxides production was formed by PQ-*n* with different side-chain length reaction with $^1O_2$ generated by Rose Bengal photosensitization, fluorescence spectroscopy was performed using a fluorescent probe SPY-LHP. A solution of 100 μM PQ-*n* with 5 μM Rose Bengal and 40 mM MES-NaOH buffer (pH 6.5) was illuminated with white light (1000 μmol photons m^{-2} sec^{-1}) for 5 min. After illumination, 2.7 μM SPY-LHP dissolved in absolute ethanol was added and incubated in the dark for 30 min. Samples were centrifuged at 700 ***g*** for 3 min and supernatant was used for fluorescence measurement. Fluorescence spectrum (λ_{ex} = 488 nm, λ_{em} = 500–600 nm) was obtained by fluorescence spectrophotometer Hitachi F4500 (Hitachi, Tokyo, Japan). The intensity of SPY-LHPox fluorescence signal was determined by measuring the relative height of the peak at λ = 535 nm.

Determination of prenylquinols using HPLC

Prenylquinols were measured using the method described in Ksas *et al.* (2015). Leaf discs were ground for 1 min in 2 ml ethyl acetate with an Ultra-Turrax at 24 000 rpm. After centrifugation at 16 900 ***g*** for 3 min, 600 μl of extract was filtered with 0.2 μm PTFE filter. The extract was evaporated under a stream of nitrogen, resuspended in 1 ml of a solution of methanol and hexane in a ratio of 17/1 (v/v) prior to analysis by HPLC-UV/fluorescence. The samples were subjected to reverse phase HPLC using a Phenomenex Kinetex 2.6 μm C18 column (100 × 4.6 mm) operating in the isocratic mode, with mobile phase containing methanol and hexane (17/1, v/v) at a flow rate of 0.8 ml min^{-1}. For determination of PQH$_2$-9 and PC-8 fluorescence detection was used (λ_{ex} = 290 nm, λ_{em} = 330 nm). Plastoquinone-9 was measured using absorbance at 255 nm. Plastoquinones and plastochromanol standards were obtained as described previously (Gruszka *et al.*, 2008).

Determination of plastoquinone-9, hydroxyplastoquinone-9 and trihydroxy-plastoquinone-9 using HPLC

Arabidopsis leaves were ground with 2 ml ethyl acetate, the extract evaporated in a stream of nitrogen, dissolved in 400 μl absolute ethanol, and 50 μl of 5 mM ferricyanide was added to oxidize the prenylquinols. After 10 min of incubation, the solution was evaporated to dryness and dissolved in the HPLC solvent. Total (oxidized and reduced) PQ-9 and PQ(OH)-9 were determined using C18 reverse-phase column (Nucleosil 100, 5 μm, 25 × 0.4 cm, Teknokroma, Barcelona, Spain), using mobile phase containing methanol and hexane in a ratio of 17/1 (v/v) at a flow rate of 1 ml min^{-1}, absorption detection at 255 nm and Pt post-column reduction and fluorescence detection (λ_{ex} = 290 nm, λ_{em} = 330 nm). Total PQ(OH)$_3$-9 was determined using C18 reverse-phase column (Nucleosil 100, 5 μm, 25 × 0.4 cm, Teknokroma, Barcelona, Spain),

N$_2$-flushed methanol containing 25 mM NaClO$_4$ as an eluent, flow rate of 1 ml min^{-1}, decade electrochemical amperometric detector and VT-03 flowcell (ANTEC Leyden, The Netherlands), −0.3 to −0.4 V reducing potential, and temperature of 25°C. The standard of PQ(OH)$_3$-9 was prepared as described in Gruszka *et al.* (2008).

Statistical analysis

Origin software (version 8.5.1) was used for statistical analysis. Data represent average and standard deviation values based on the number of total samples (*n*) taken from at least three independent sample replicates. To calculate significant differences Student's *t*-test and ANOVA were used (P < 0.05).

CONFLICT OF INTERESTS

The authors declare no conflict of interests.

SUPPORTING INFORMATION

Additional Supporting Information may be found in the online version of this article.
Figure S1. Effect of the oxidized form of PQ-*n* with different side-chain lengths on singlet oxygen formed by Rose Bengal photosensitization.
Figure S2. Plastoquinone content in leaves and broken chloroplasts from control and high light-exposed WT and SPS1oex Arabidopsis determined by HPLC.
Figure S3. Plastochromanol-8 content in leaves and broken chloroplasts from control and high light-exposed WT and SPS1oex Arabidopsis determined by HPLC.
Figure S4. Organic hydroperoxides formation in broken chloroplasts from control and high light-exposed WT and SPS1oex Arabidopsis detected by EPR spin-trapping spectroscopy.
Figure S5. Plastoquinone-hydroperoxides formation in PQ-*n* chemical system by Rose Bengal photosensitization.

REFERENCES

Aro, E.M., Suorsa, M., Rokka, A., Allahverdiyeva, Y., Paakkarinen, V., Saleem, A., Battchikova, N. and Rintamäki, E. (2005) Dynamics of photosystem II: a proteomic approach to thylakoid protein complexes. *J. Exp. Bot.* **56**, 347–356.

Barr, R., Henninger, M.D. and Crane, F.L. (1967) Comparative studies on plastoquinone.2. Analysis for plastoquinones A B C and D. *Plant Physiol.* **42**, 1246.

Buettner, G.R. (1987) Spin trapping – electron-spin-resonance parameters of spin adducts. *Free Radic. Biol. Med.* **3**, 259–303.

Casazza, A.P., Tarantino, D. and Soave, C. (2001) Preparation and functional characterization of thylakoids from Arabidopsis thaliana. *Photosynth. Res.* **68**, 175–180.

Dietz, K.J., Turkan, I. and Krieger-Liszkay, A. (2016) Redox- and reactive oxygen species-dependent signaling into and out of the photosynthesizing chloroplast. *Plant Physiol.* **171**, 1541–1550.

Dluzewska, J., Zielinski, K., Nowicka, B., Szymanska, R. and Kruk, J. (2015) New prenyllipid metabolites identified in Arabidopsis during photo-oxidative stress. *Plant, Cell Environ.* **38**, 2698–2706.

Dormann, P. (2007) Functional diversity of tocochromanols in plants. *Planta*, **225**, 269–276.

Eugeni Piller, L., Besagni, C., Ksas, B., Rumeau, D., Brehelin, C., Glauser, G., Kessler, F. and Havaux, M. (2011) Chloroplast lipid droplet type II NAD(P)H quinone oxidoreductase is essential for prenylquinone metabolism and vitamin K-1 accumulation. *Proc. Natl Acad. Sci. USA*, **108**, 14354–14359.

Eugeni Piller, L., Abraham, M., Dormann, P., Kessler, F. and Besagni, C. (2012) Plastid lipid droplets at the crossroads of prenylquinone metabolism. *J. Exp. Bot.* **63**, 1609–1618.

Farmer, E.E. and Mueller, M.J. (2013) ROS-mediated lipid peroxidation and RES-activated signaling. *Annu. Rev. Plant Biol.* **64**, 429–450.

Fischer, B.B., Hideg, E. and Krieger-Liszkay, A. (2013) Production, detection, and signaling of singlet oxygen in photosynthetic organisms. *Antioxid. Redox Signal.* **18**, 2145–2162.

Flors, C., Fryer, M.J., Waring, J., Reeder, B., Bechtold, U., Mullineaux, P.M., Nonell, S., Wilson, M.T. and Baker, N.R. (2006) Imaging the production of singlet oxygen *in vivo* using a new fluorescent sensor, Singlet Oxygen Sensor Green. *J. Exp. Bot.* **57**, 1725–1734.

Foote, C.S., Chang, Y.C. and Denny, R.W. (1970) Chemistry of singlet oxygen. X. Carotenoid quenching parallels biological protection. *J. Am. Chem. Soc.* **92**, 5216–5218.

Foyer, C.H. and Noctor, G. (2009) Redox regulation in photosynthetic organisms: signaling, acclimation, and practical implications. *Antioxid. Redox Signal.* **11**, 861–905.

Gorman, A.A., Hamblett, I., Lambert, C., Spencer, B. and Standen, M.C. (1988) Identification of both preequilibrium and diffusion limits for reaction of singlet oxygen, O-2(1-delta-G), with both physical and chemical quenchers – variable-temperature, time-resolved infrared luminescence studies. *J. Am. Chem. Soc.* **110**, 8053–8059.

Gruszka, J., Pawlak, A. and Kruk, J. (2008) Tocochromanols, plastoquinol, and other biological prenyllipids as singlet oxygen quenchers-determination of singlet oxygen quenching rate constants and oxidation products. *Free Radic. Biol. Med.* **45**, 920–928.

Henninger, M.D., Barr, R. and Crane, F.L. (1966) Plastoquinone B. *Plant Physiol.* **41**, 696.

Jemiola-Rzeminska, M., Kruk, J. and Strzalka, K. (2003) Fluorescence anisotropy of plant membrane prenyllipids as a tool in studies of their localization and mobility in model membranes. *Advanced Research on Plant Lipids*, Chapter 9, 369–372.

Kargul, J. and Barber, J. (2008) Photosynthetic acclimation: structural reorganisation of light harvesting antenna – role of redox-dependent phosphorylation of major and minor chlorophyll a/b binding proteins. *FEBS J.* **275**, 1056–1068.

Khorobrykh, S.A., Khorobrykh, A.A., Yanykin, D.V., Ivanov, B.N., Klimov, V.V. and Mano, J. (2011) Photoproduction of catalase-insensitive peroxides on the donor side of manganese-depleted photosystem II: evidence with a specific fluorescent probe. *Biochemistry*, **50**, 10658–10665.

Khorobrykh, S.A., Karonen, M. and Tyystjarvi, E. (2015) Experimental evidence suggesting that H_2O_2 is produced within the thylakoid membrane in a reaction between plastoquinol and singlet oxygen. *FEBS Lett.* **589**, 779–786.

Kirchhoff, H., Horstmann, S. and Weis, E. (2000) Control of the photosynthetic electron transport by PQ diffusion microdomains in thylakoids of higher plants. *Biochimica et Biophysica Acta-Bioenergetics*, **1459**, 148–168.

Krieger-Liszkay, A. and Trebst, A. (2006) Tocopherol is the scavenger of singlet oxygen produced by the triplet states of chlorophyll in the PSII reaction centre. *J. Exp. Bot.* **57**, 1677–1684.

Krieger-Liszkay, A., Fufezan, C. and Trebst, A. (2008) Singlet oxygen production in photosystem II and related protection mechanism. *Photosynth. Res.* **98**, 551–564.

Kruk, J. and Karpinski, S. (2006) An HPLC-based method of estimation of the total redox state of plastoquinone in chloroplasts, the size of the photochemically active plastoquinone-pool and its redox state in thylakoids of Arabidopsis. *Biochimica et Biophysica Acta-Bioenergetics*, **1757**, 1669–1675.

Kruk, J. and Strzalka, H. (1998) Identification of plastoquinone-C in spinach and maple leaves by reverse-phase high-performance liquid chromatography. *Phytochemistry*, **49**, 2267–2271.

Kruk, J. and Strzalka, K. (1999) Dark reoxidation of the plastoquinone-pool is mediated by the low-potential form of cytochrome b-559 in spinach thylakoids. *Photosynth. Res.* **62**, 273–279.

Kruk, J. and Trebst, A. (2008) Plastoquinol as a singlet oxygen scavenger in photosystem II. *Biochimica et Biophysica Acta-Bioenergetics*, **1777**, 154–162.

Kruk, J., Hollander-Czytko, H., Oettmeier, W. and Trebst, A. (2005) Tocopherol as singlet oxygen scavenger in photosystem II. *J. Plant Physiol.* **162**, 749–757.

Kruk, J., Szymanska, R., Cela, J. and Munne-Bosch, S. (2014) Plastochromanol-8: fifty years of research. *Phytochemistry*, **108**, 9–16.

Kruk, J., Szymanska, R., Nowicka, B. and Dluzewska, J. (2016) Function of isoprenoid quinones and chromanols during oxidative stress in plants. *New Biotechnol.* **33**, 636–643.

Ksas, B., Becuwe, N., Chevalier, A. and Havaux, M. (2015) Plant tolerance to excess light energy and photooxidative damage relies on plastoquinone biosynthesis. *Sci. Rep.* **5**, 10919.

Laloi, C. and Havaux, M. (2015) Key players of singlet oxygen-induced cell death in plants. *Front Plant Sci.* **6**, 39.

Lambreva, M.D., Russo, D., Polticelli, F., Scognamiglio, V., Antonacci, A., Zobnina, V., Campi, G. and Rea, G. (2014) Structure/function/dynamics of photosystem II plastoquinone binding sites. *Curr. Protein Pept. Sci.* **15**, 285–295.

Ledford, H.K. and Niyogi, K.K. (2005) Singlet oxygen and photo-oxidative stress management in plants and algae. *Plant, Cell Environ.* **28**, 1037–1045.

McDonald, A.E., Ivanov, A.G., Bode, R., Maxwell, D.P., Rodermel, S.R. and Hunter, N.P.A. (2011) Flexibility in photosynthetic electron transport: the physiological role of plastoquinol terminal oxidase (PTOX). *Biochim. Biophys. Acta*, **1807**, 954–967.

Mene-Saffrane, L. and Dellapenna, D. (2010) Biosynthesis, regulation and functions of tocochromanols in plants. *Plant Physiol. Biochem.* **48**, 301–309.

Moan, J. and Wold, E. (1979) Detection of singlet oxygen production by ESR. *Nature*, **279**, 450–451.

Mukai, K., Itoh, S., Daifuku, K., Morimoto, H. and Inoue, K. (1993) Kinetic-study of the quenching reaction of singlet oxygen by biological hydro-quinones and related-compounds. *Biochem. Biophys. Acta.* **1183**, 323–326.

Mullineaux, P.M. and Baker, N.R. (2010) Oxidative stress: antagonistic signaling for acclimation or cell death? *Plant Physiol.* **154**, 521–525.

Munné-Bosch, S. (2005) The role of alpha-tocopherol in plant stress tolerance. *J. Plant Physiol.* **162**, 743–748.

Nowicka, B. and Kruk, J. (2012) Plastoquinol is more active than alpha-tocopherol in singlet oxygen scavenging during high light stress of Chlamydomonas reinhardtii. *Biochimica et Biophysica Acta-Bioenergetics*, **1817**, 389–394.

Pospíšil, P. (2012) Molecular mechanisms of production and scavenging of reactive oxygen species by photosystem II. *Biochem. Biophys. Acta.* **1817**, 218–231.

Pospíšil, P. (2016) Production of reactive oxygen species by photosystem II as a response to light and temperature stress. *Front Plant Sci.* **7**, 1950.

Pospíšil, P. and Prasad, A. (2014) Formation of singlet oxygen and protection against its oxidative damage in Photosystem II under abiotic stress. *J. Photochem. Photobiol., B*, **137**, 39–48.

Pospíšil, P. and Yamamoto, Y. (2017) Damage to photosystem II by lipid peroxidation products. *Biochimica et Biophysica Acta-General Subjects*, **1861**, 457–466.

Pospíšil, P., Snyrychova, I., Kruk, J., Strzalka, K. and Naus, J. (2006) Evidence that cytochrome b(559) is involved in superoxide production in photosystem II: effect of synthetic short-chain plastoquinones in a cytochrome b(559) tobacco mutant. *Biochemical J.* **397**, 321–327.

Rumeau, D., Peltier, G. and Cournac, I. (2007) Chlororespiration and cyclic electron flow around PSI during photosynthesis and plant stress response. *Plant Cell Environ.* **30**, 1041–1051.

Sedlářová, M., Petřivalský, M., Piterková, J., Luhová, L., Kocirová, J. and Lebeda, A. (2011) Influence of nitric oxide and reactive oxygen species on development of lettuce downy mildew in Lactuca spp. *Eur. J. Plant Pathol.* **129**, 267–280.

Sies, H. and Menck, C.F.M. (1992) Singlet oxygen induced DNA damage. *Mutat. Res.* **275**, 367–375.

Skovsen, E., Snyder, J.W., Lambert, J.D.C. and Ogilby, P.R. (2005) Lifetime and diffusion of singlet oxygen in a cell. *J. Phys. Chem. B* **109**, 8570–8573.

Soh, N., Ariyoshi, T., Fukaminato, T., Nakajima, H., Nakano, K. and Imato, T. (2007) Swallow-tailed perylene derivative: a new tool for fluorescent imaging of lipid hydroperoxides. *Org. Biomol. Chem.* **5**, 3762–3768.

Stratton, S.P. and Liebler, D.C. (1997) Determination of singlet oxygen-specific versus radical-mediated lipid peroxidation in photosensitized oxidation of lipid bilayers: effect of beta-carotene and alpha-tocopherol. *Biochemistry*, **36**, 12911–12920.

Szymanska, R. and Kruk, J. (2010) Identification of hydroxy-plastochromanol in Arabidopsis leaves. *Acta Biochim. Pol.* **57**, 105–108.

Szymanska, R., Nowicka, B. and Kruk, J. (2014) Hydroxy-plastochromanol and plastoquinone-C as singlet oxygen products during photo-oxidative stress in Arabidopsis. *Plant, Cell Environ.* **37**, 1464–1473.

Telfer, A. (2014) Singlet oxygen production by PSII under light stress: mechanism, detection and the protective role of beta-carotene. *Plant Cell Physiol.* **55**, 1216–1223.

Trebst, A. (2003) Function of beta-carotene and tocopherol in photosystem II. *Z Naturforsch C* **58**, 609–620.

Triantaphylides, C. and Havaux, M. (2009) Singlet oxygen in plants: production, detoxification and signaling. *Trends Plant Sci.* **14**, 219–228.

Van Amerongen, H. and Croce, R. (2013) Light harvesting in photosystem II. *Photosynth. Res.* **116**, 251–263.

Van Breusegem, F. and Dat, J.F. (2006) Reactive oxygen species in plant cell death. *Plant Physiol.* **141**, 384–390.

Vass, I. (2012) Molecular mechanisms of photodamage in the Photosystem II complex. *Biochim. Biophys. Acta*, **1817**, 209–217.

Wang, Y.N. and Eriksson, L.A. (2001) Theoretical studies of electron and hydrogen transfer reactions between semiquinone radicals and oxygen. *Theoret. Chem. Acc.* **106**, 158–162.

Wei, X.P., Su, X.D., Cao, P., Liu, X.Y., Chang, W.R., Li, M., Zhang, X.Z. and Liu, Z.F. (2016) Structure of spinach photosystem II-LHCII supercomplex at 3.2 angstrom resolution. *Nature*, **534**, 69.

Yadav, D.K., Kruk, J., Sinha, R.K. and Pospíšil, P. (2010) Singlet oxygen scavenging activity of plastoquinol in photosystem II of higher plants: electron paramagnetic resonance spin-trapping study. *Biochimica et Biophysica Acta-Bioenergetics*, **1797**, 1807–1811.

Zhang, S.R., Apel, K. and Kim, C.H. (2014) Singlet oxygen-mediated and EXECUTER-dependent signalling and acclimation of Arabidopsis thaliana exposed to light stress. *Philos. Trans. R. Soc. Lond. B Biol. Sci.* **369**, 7.

ORIGINAL ARTICLE

WILEY Plant, Cell & Environment

The plastoquinone pool outside the thylakoid membrane serves in plant photoprotection as a reservoir of singlet oxygen scavengers

Brigitte Ksas[1] | Bertrand Légeret[2] | Ursula Ferretti[3] | Anne Chevalier[1] | Pavel Pospíšil[3] | Jean Alric[1] | Michel Havaux[1] (ID)

[1] CEA Cadarache, CNRS UMR 7265 Biologie Végétale et Microbiologie Environnementales, Aix Marseille Université, Laboratoire d'Ecophysiologie Moléculaire des Plantes, 13108 Saint-Paul-lez-Durance, France

[2] CEA Cadarache, CNRS UMR 7265 Biologie Végétale et Microbiologie Environnementales, Aix Marseille Université, Laboratoire de Bioénergétique et Biotechnologie des Bactéries et Microalgues, 13108 Saint-Paul-lez-Durance, France

[3] Department of Biophysics, Centre of the Region Haná for Biotechnological and Agricultural Research, Faculty of Science, Palacký University, Šlechtitelů 27, 783 71 Olomouc, Czech Republic

Correspondence
Michel Havaux. CEA Cadarache, CNRS UMR 7265 Biologie Végétale et Microbiologie Environnementales, Aix Marseille Université, Laboratoire d'Ecophysiologie Moléculaire des Plantes, 13108 Saint-Paul-lez-Durance, France.
Email: michel.havaux@cea.fr

Funding information
Ministry of Education, Youth and Sports of the Czech Republic, Grant/Award Number: LO1204; French National Research Agency, Grant/Award Number: SLOSAM, 14-CE02-0010-02

Abstract

The Arabidopsis *vte1* mutant is devoid of tocopherol and plastochromanol (PC-8). When exposed to excess light energy, *vte1* produced more singlet oxygen ($^1O_2$) and suffered from extensive oxidative damage compared with the wild type. Here, we show that overexpressing the *solanesyl diphosphate synthase 1* (*SPS1*) gene in *vte1* induced a marked accumulation of total plastoquinone (PQ-9) and rendered the *vte1 SPS1*oex plants tolerant to photooxidative stress, indicating that PQ-9 can replace tocopherol and PC-8 in photoprotection. High total PQ-9 levels were associated with a noticeable decrease in $^1O_2$ production and higher levels of Hydroxyplastoquinone (PQ-C), a $^1O_2$-specific PQ-9 oxidation product. The extra PQ-9 molecules in the *vte1 SPS1*oex plants were stored in the plastoglobules and the chloroplast envelopes, rather than in the thylakoid membranes, whereas PQ-C was found almost exclusively in the thylakoid membranes. Upon exposure of wild-type plants to high light, the thylakoid PQ-9 pool decreased, whereas the extrathylakoid pool remained unchanged. In *vte1* and *vte1 SPS1*oex plants, the PQ-9 losses in high light were strongly amplified, affecting also the extrathylakoid pool, and PQ-C was found in high amounts in the thylakoids. We conclude that the thylakoid PQ-9 pool acts as a $^1O_2$ scavenger and is replenished from the extrathylakoid stock.

KEYWORDS

antioxidant, reactive oxygen species, tocopherol

1 | INTRODUCTION

Plastoquinone-9 (PQ-9) is essentially viewed as a component of the photosynthetic electron transport chain in chloroplasts, carrying electrons from photosystem II (PSII) to cytochrome *b6/f* (Amesz, 1973). It is thus essential for the photosynthetic activity of plants, and mutations inhibiting PQ-9 accumulation led to a lethal phenotype in Arabidopsis and maize (Cook & Miles, 1992; Norris, Barrette, & DellaPenna, 1995). Through its redox state, the PQ-9 pool can also play a role in the regulation of gene expressions and enzyme activities (Pfannschmidt et al., 2009; Rochaix, 2014). However, several observations obtained in recent *in vitro* and *in vivo* studies have raised the idea

that the physiological role of PQ-9 can be more diverse than just electron shuttling from PSII to PSI. *In vitro* studies have revealed that PQ-9, especially in the reduced state (plastoquinol), has antioxidant properties, being able to quench singlet oxygen ($^1O_2$) and to inhibit oxidation of lipid membranes (Gruszka, Pawlak, & Kruk, 2008; Nowicka, Gruszka, & Kruk, 2013; Yadav, Kruk, Sinha, & Pospisil, 2010). In isolated thylakoids, maintenance of the PQ-9 pool in the reduced state with an electron transport inhibitor was associated with a lowering of high light-induced lipid peroxidation, suggesting an antioxidant role for reduced PQ-9 (Hundal, Forsmark-Andrée, Ernster, & Andersson, 1995). Tocopherol and plastoquinone are synthesized through a common pathway until homogentisate where solanesyl diphosphate synthase 1

(SPS1) introduces the bifurcation towards PQ-9 and PC-8. Accumulation of PQ-9 in leaves by overexpression of the *SPS1* gene in *SPS1*oex Arabidopsis plants reduced lipid peroxidation and increased the tolerance to photooxidative stress (Ksas, Becuwe, Chevalier, & Havaux, 2015). However, because the *SPS1*oex plants also accumulated plastochromanol-8 (PC-8), a PQ-9 metabolite with known antioxidative activities (Kruk, Szymanska, Cela, & Munne-Bosch, 2014), photoprotection could not be unambiguously and exclusively attributed to PQ-9. Nevertheless, sudden exposure of Arabidopsis plants to high light stress resulted in a marked loss of total PQ-9 (Ksas et al., 2015) and to an accumulation of oxidized derivatives formed by the interaction between PQ-9 and $^1O_2$ (Szymanska & Kruk, 2010), supporting the idea that PQ-9 (most likely its reduced form) can act as a chemical $^1O_2$ scavenger *in vivo*. Similarly, in the green microalga *Chlamydomonas*, PQ-9 was observed to decrease in high light when its resynthesis was blocked by an inhibitor of hydroxylphenylpyruvate dioxygenase (Kruk & Trebst, 2008).

In this context, an interesting observation was the various localizations of PQ-9 in thylakoid membranes, plastoglobules (PGs; Lichtenthaler & Weinert, 1970; Zbierzak et al., 2009), and chloroplast envelopes (Soll, Schultz, Joyard, Douce, & Block, 1985), suggesting that PQ-9 could play diverse roles in the chloroplasts. To investigate these roles, we have crossed the *vte1* Arabidopsis mutant, deficient in both tocopherols and PC-8 (Porfirova, Bergmuller, Tropf, Lemke, & Dörmann, 2002), with *SPS1*oex lines previously described (Ksas et al., 2015) to generate *vte1 SPS1*oex plants that selectively accumulate PQ-9 in the absence of PC-8. The responses of *vte1 SPS1*oex plants to high light together with the analyses of PQ-9 localization and concentration demonstrate that the total PQ-9 pool has a $^1O_2$-scavenging antioxidant activity *in planta* and show the participation of the extrathylakoid PQ-9 pool in this process through delivery of PQ-9 to the thylakoids in order to replace oxidized PQ-9 molecules.

2 | MATERIAL AND METHODS

2.1 | Plant material and growth conditions

Arabidopsis plants (*Arabidopsis thaliana*, Columbia-0 ecotype) were grown in a phytotron under controlled conditions of light (150 μmol photons m^{-2} s^{-1}, photoperiod of 8 hr), temperature (20 °C/18 °C, day/night), and relative air humidity (60%). Several mutant/transformed plants were examined in this work: the tocopherol cyclase mutant *vte1* deficient in tocopherols (Porfirova et al., 2002), *SPS1*-overexpressing lines described in a previous work (Lines #12 and #14 in Ksas et al., 2015), and a crossing between them (*vte1 SPS1*oex). Selection of homozygous *vte1 SPS1*oex plants was achieved first by screening the progeny for resistance to the herbicide BASTA and then by screening for total absence of tocopherol and PC-8 by HPLC analyses (see below for HPLC method). Photooxidative stress was induced by transferring plants to a growth chamber at 7 °C/15 °C (day/night, air temperature) under a PFD of 1,500 μmol photons m^{-2} s^{-1} and a photoperiod of 8 hr, as previously explained (Ksas et al., 2015). Depending on the experiment, the duration of the treatment was 48

(photooxidative stress experiments) or 2.5 hr (dynamics of the PQ-9 pools), as indicated in the legend of the figures.

2.2 | Prenyl lipid determinations

Leaf discs (three discs, diameter of 1 cm) were grinded in ethyl acetate. After centrifugation, the surpernatant was filtered and evaporated on ice under a stream of N$_2$. The residue was recovered in methanol/hexane (17/1) and analysed by HPLC, as described elsewhere (Ksas et al., 2015; Szymańska, Nowicka, & Kruk, 2014; Kruk & Karpinski, 2006). The column was a Phenomenex Kinetex 2.6 μm, 100 × 4.6 mm, 100 A. Separation of tocopherols, PQ-9 and PC-8, was done in the isocratic mode with methanol/hexane (17/1) as solvent system and a flow rate of 0.8 ml min^{-1}. All prenyl lipids, except oxidized PQ-9, were detected by their fluorescence at 330 nm with an excitation at 290 nm. PQ-9 in the oxidized state was measured by its absorbance at 255 nm. Typical chromatograms are shown in Figure S1. PC-8 and PQ-9 standards were a kind gift from Dr. J. Kruk. Tocopherol standards were purchased from Sigma. Unless specified otherwise, the PQ-9 data given in this article correspond to the total content (oxidized PQ-9 + reduced PQH$_2$-9).

Determination of the photoactive and nonactive fractions of PQ-9 was done following the protocol described in Kruk and Karpinski (2006) modified by Ksas et al. (2015). Leaf samples were frozen in liquid nitrogen as quickly as possible to avoid changes in the plastoquinone redox state during sample preparation. Two discs (diameter of 0.8 cm) were punched out from each leaf. To determine the pool of photoactive PQ-9, we first measured the amount of reduced PQ-9 (plastoquinol-9) in one disc after a dark-adaptation period of 2 hr. The dark-adapted samples were frozen in liquid nitrogen after 3-s illumination with far-red light to ensure full oxidation of the photoactive pool of plastoquinone. Then, plastoquinol-9 was requantified in the disc that had been exposed to a high PFD of white light (2,000 μmol photons m^{-2} s^{-1}) for 15 s. Illumination was done in a mortar that was filled with liquid nitrogen after the 15-s illumination in order to freeze the samples in the light. The size of the photoactive pool was calculated as the difference between the plastoquinol-9 content in the light and the plastoquinol-9 content in the dark. The size of the nonphotoactive pool of PQ-9 was the sum of the amount of plastoquinol-9 in the dark (not reoxidable in the dark) and the amount of oxidized PQ-9 in the light (not reducible by high light). This pool corresponds mainly to the plastoquinone molecules present in the PGs and the chloroplast envelope (Lichtenthaler, 2007), which are not involved in photosynthetic electron transport.

2.3 | PQ-C determination by UPLC-MS/MS

Hydroxyplastoquinone (PQ-C) was analysed using an UPLC-MS/MS system (UPLC ultimate RS 3000; Thermo Fisher with QTOF 5600; AB Sciex) connected to a Kinetex C18 2.1 × 150 mm column (Phenomenex). The APCI source was operated in negative mode. A binary solvent system was used, in which mobile Phase A consisted of acetonitrile:water (60:40, *v/v*) and 10 mm ammonium formate and mobile Phase B consisted of isopropanol:acetonitrile (90:10, *v/v*), 10 mm ammonium formate, and 0.1% formic acid (*v/v*). The gradient

started with 27% of solution B and was increase to 97% of solution B within 20 min at a speed of 0.3 ml min^{-1}, and then maintained at 97% for 5 min. Solution B was then decreased to a 27% enrichment during 7 min for column re-equilibration. Column temperature was set at 45 °C. Oxidized and reduced PQ-9 and PQ-C identification was achieved based on the comparison of retention times and accurate masses with standards. Reduced PQ-9 and PQ-C were obtained by reducing the oxidized PQ-9 and PQ-C standards with sodium borohydride. In samples, PQ-C and PQ-9 contents were measured in selected reaction monitoring mode using the following transition: m/z 764.6 → m/z 202.095 +/− 0.025 (CE = −70 eV) and m/z 748.6 → m/z 149.058 +/− 0.025 (CE = −70 eV), respectively. Examples of extracted-ion chromatograms for PQ-C are shown in Figure S2.

2.4 | Chloroplast fractionation

Chloroplasts, isolated from leaves of 6-week-old plants, were hypotonically ruptured and subplastidial compartments were isolated by centrifugation using sucrose-density gradient following the protocol described in Besagni, Eugeni Piller, and Bréhélin (2011), except that plants were not preadapted to darkness. Thirty-two fractions of 1 ml were collected from the centrifuged tubes (from top to bottom), and 400 µl of each fraction were diluted to obtain a final sucrose concentration of 5%. The diluted fractions were then grinded in mortar glass tube with 5 ml of cold ethyl acetate and sonicated (Digital Sonifer, Brandon, USA) for 1 min with a 50% "duty cycle" at 40% of power in an ice bath. The extracts were centrifuged for 13 min at 9,600 g at 4 °C. Five hundred microliter of supernatant was evaporated in a stream of nitrogen and dissolved in 300 µl of methanol/hexane (17/1, v/v). One hundred microliter were immediately analysed by HPLC, as described above.

2.5 | Chlorophyll fluorescence

The maximal quantum yield of PSII photochemistry was measured on attached leaves with a PAM-2000 fluorometer (Walz) as Fv/Fm = (Fm − Fo)/Fm, where Fm is the maximal fluorescence level obtained with an 800-ms pulse of intense white light and Fo is the initial level obtained after a 2-s pulse of far-red light. Measurements were done in the dark in leaves dark adapted for 30 min.

Chlorophyll fluorescence induction curves were measured with a JTS-10 spectrophotometer/ fluorimeter (BIoLogic, France), and the number of PSII two-electron acceptors was estimated as described in Joliot and Joliot (2002) as the area over the fluorescence rise measured in dark-adapted leaves divided by the area over the curve for leaves infiltrated with DCMU (one electron transferred to Q_A in the light). Chlorophyll fluorescence imaging was done with a laboratory-built instrument described in Johnson et al. (2009).

2.6 | Lipid peroxidation

Lipids were extracted from approximately 0.5 g of leaves frozen in liquid nitrogen. The leaves were grinded in an equivolume methanol/chloroform solution containing 5 mM Triphenyl Phosphine, 1 mM 2,6-tert-butyl-p-cresol (5 ml g^{-1} fresh weight), and citric acid (2.5 ml g^{-1} fresh weight), using an Ultraturax blender. Internal standard 15-HEDE was added to a final concentration of 100 nmol g^{-1} fresh

weight, and mixed properly. After centrifugation at 700 rpm and 4 °C for 5 min, the lower organic phase was carefully taken out with the help of a glass syringe into a 15 ml glass tube. The syringe was rinsed with approximately 2.5 ml chloroform and transferred back into the tube. The process was repeated and the lower layer was again collected and pooled to the first collection. The solvent was evaporated under N$_2$ gas at 40 °C. The residues were recovered in 1.25 ml absolute ethanol and 1.25 ml of 3.5 N NaOH and hydrolysed at 80 °C for 30 min. The ethanol was evaporated under N$_2$-gas at 40 °C for ~10 min. After cooling to room temperature, pH was adjusted to 4–5 with 2.1 ml citric acid. Hydroxy fatty acids were extracted with hexane/ether 50/50 (v/v). The organic phase was analysed by straight phase HPLC-UV, as previously described (Montillet et al., 2004). The hydroxyoctadecatrienoic acid isomers (9-, 12-, 13-, and 16-hydroxyoctadecatrienoic acid derived from the oxidation of the main fatty acid in Arabidopsis leaves, linolenic acid) were quantified based on the 15-HEDE internal standard.

Lipid peroxidation was also visualized in whole plants by autoluminescence imaging. Stressed plants were dark adapted for 2 hr, and the luminescence emitted from the spontaneous decomposition of lipid peroxides was captured by a highly sensitive liquid N$_2$-cooled charge-coupled device camera, as previously described (Birtic et al., 2011). The images were treated using Image J software (NIH, USA).

2.7 | SOSG-EP fluorescence

Production of $^1O_2$ was measured in attached leaves from the fluorescence of the $^1O_2$-specific singlet oxygen sensor green (SOSG) fluorescent probe (Invitrogen), as described previously (Ramel et al., 2012). With the help of a 1-ml syringe (without the needle), 100 µM SOSG was pressure-infiltrated into the leaves through the lower surface. Plants with SOSG-infiltrated leaves were exposed to a PFD of 1,500 µmol photons m^{-2} s^{-1} at 7 °C for 20 min. As a control treatment, plants with SOSG-infiltrated leaves were placed in the dark at room temperature for 20 min. SOSG-endoperoxide (EP) fluorescence was then measured from leaf discs punched from the SOSG-infiltrated leaves using a fiberoptics-equipped Perkin-Elmer spectrofluorometer (LS 50B) with a 475 nm excitation light. SOSG-EP fluorescence at 524 nm (F524) was normalized to chlorophyll fluorescence at 680 nm (F680) for each leaf disc. SOSG-EP fluorescence was calculated as ([F524 in the light − F524 in the dark]/F680) × 10.

2.8 | EPR spectroscopy

For the preparation of thylakoid membranes, 7 g of leaves (fresh weight) were grinded for 2 s in 50 ml of extraction buffer (330 mM sorbitol, 50 mM Tricine, 2 mM EDTA(Na2), 1 mM MgCl$_2$, 2 mM Ascorbate, pH 7.7) with 5 mM dithiothreitol in a Warring blendor at low speed. The liquid phase was removed and set aside, and 50 ml of extraction buffer was added for a second extraction. The extracts were filtered onto four Miracloth layers, and the filtrate was centrifuged for 4 min at 1,500 g at 4 °C. The pellet was washed twice with the extraction buffer and centrifuged for 4 min at 1,500 g at 4 °C. The washed pellet was resuspended in 21 ml of lysis buffer pH 7.8 (10 mM

Tricine, 10 mM NaCl, 10 mM $MgCl_2$) with 1 mM phenylmethylsulfonyl with occasional stirring for 15 min. The sample was centrifuged at 48,400 g for 15 min. The pellet was resuspended in 1.75 ml of storage buffer (100 mM Tricine, 10 mM NaCl, 10 mM $MgCl_2$, 400 mM sucrose, pH 7.8) and stored at −80 °C before analyses.

Singlet oxygen formation was monitored by electron paramagnetic resonance (EPR) spectroscopy using the spin probe 2,2,6,6-tetramethyl-4-piperidone (TEMPD) purified by vacuum distillation. The oxidation of TEMPD by $^1O_2$ forms 2,2,6,6-tetramethyl-4-piperidone-1-oxyl detectable by EPR spectroscopy. Thylakoid membranes (25 µg Chl ml^{-1}) were illuminated in the presence of 50 mM TEMPD and 40 mM MES-NaOH buffer (pH = 6.5) for 30 min under 1,000 µmol photons m^{-2} s^{-1}. After illumination, thylakoid membranes were centrifuged at 1,000 g for 2 min to separate sample from spin probe. The EPR spectra were recorded using an EPR spectrometer Mini Scope MS400 (Magnettech GmbH, Berlin, Germany). EPR measurement conditions were as follows: microwave power, 10 mW; modulation amplitude, 1 G; modulation frequency, 100 G; scan rate, 1.62 G s^{-1}.

3 | RESULTS

3.1 | Overexpression of the *SPS1* gene in the *vte1* mutant leads to a marked accumulation of total PQ-9, mainly in the PGs and the chloroplastic envelopes

Ksas et al. (2015) previously showed that overexpressing the *SPS1* gene in Arabidopsis brings about a noticeable increase in the leaf content in both PQ-9 and PC-8. This was confirmed here with one of the *SPS1*oex lines previously described, with a 50%-increase in the total PQ-9 content and a threefold increase in PC-8 compared with WT (Figure 1a). Please note that throughout the text, the term PQ-9 is used as a generic term for total PQ-9, that is, oxidized PQ-9 + reduced PQH_2-9 (plastoquinol). In all genotypes, PQ-9 was highly reduced, with PQH_2-9 representing around 75% of the total pool (Figure S3). The tocopherol cyclase mutant *vte1* is devoid of both tocopherols and PC-8 (Zbierzak et al., 2009). The loss of those two lipid-soluble antioxidants in *vte1* leaves was accompanied by a significant decrease in the total PQ-9 levels, as previously reported (Ksas et al., 2015). When the *vte1* mutant was crossed with the *SPS1*-overexpressing line (Line #12 in Ksas et al., 2015) to generate a double mutant *vte1 SPS1*oex, the total PQ-9 content of the leaves was strongly increased, reaching values above the WT levels. Compared with *vte1*, *vte1 SPS1*oex contained approximately three times more PQ-9. The changes in tocochromanols observed in *vte1*, *SPS1*oex, and *vte1 SPS1*oex had no significant effect on the growth phenotype of the plants in low light (Figure 1b) and did not affect significantly the efficiency of photosynthetic electron transport in young and mature leaves as measured by the chlorophyll fluorescence parameter Φ_{PSII} (Figure 1c). Compared with the *SPS1* overexpressors, a decrease in Φ_{PSII} was nevertheless observed in the older leaves of *vte1* and, to a lesser extent, of WT. Thus, high total PQ-9 levels appear to be helpful to maintain the efficiency of PSII-mediated electron flow in old, presenescing leaves.

To determine the localization of the extra PQ-9 that accumulated in *SPS1*-overexpressing plants, chloroplast membranes were
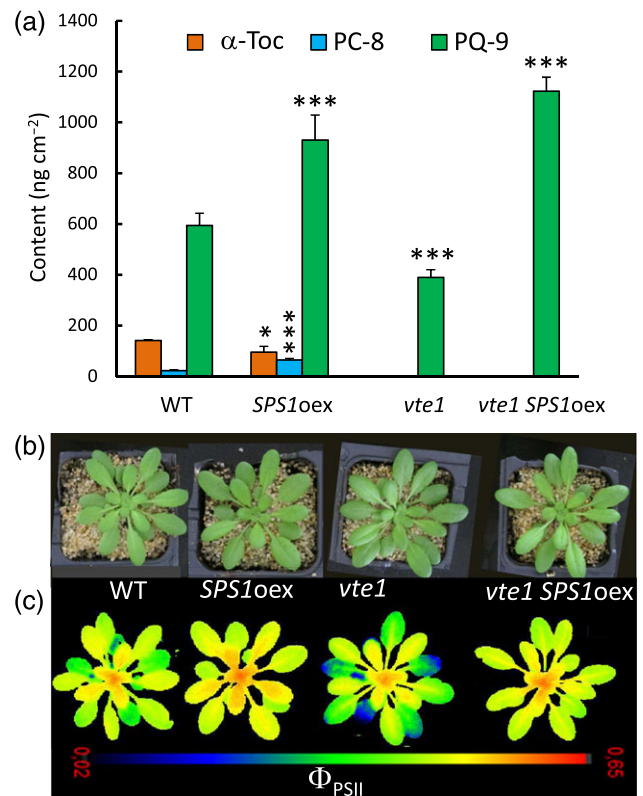
FIGURE 1 Accumulation of PQ-9 in the Arabidopsis *vte1 SPS1*oex plants. (a) α-Toc, PC-8, and PQ-9 concentrations in leaves of WT Arabidopsis, the single mutant *vte1*, the *SPS1* overexpressor *SPS1*oex, and the double mutant *vte1 SPS1*oex (obtained by crossing *vte1* with the *SPS1*oex Line #12 previously described in Ksas et al., 2015). Data are mean values of four separate measurements ± *SD*. (b) Picture of the different genotypes at the age of 4 weeks. (c) Images of the efficiency of PSII-mediated electron transport Φ_{PSII} in plants illuminated with red light of PFD 230 µmol photons m^{-2} s^{-1}. * and ***, different from WT at *p* < .01 and .001 (Student's *t* test). PC-8 = plastochromanol-8; PQ-9 = plastoquinone-9; α-Toc = α-tocopherol; PSII = photosystem II

fractionated by ultracentrifugation on sucrose gradient (Besagni et al., 2011). As expected (Besagni et al., 2011; Vidi et al., 2006), three pigmented fractions were obtained (Figure 2a): PGs were found floating at the top of the tubes and forming a whitish layer, whereas an intermediate yellowish zone corresponding to the outer and inner chloroplast envelope membranes separated from the green zone at the bottom containing chlorophyll-binding thylakoid membranes. Thirty-two fractions were collected from top (Fraction 1) to bottom (Fraction 32) and analysed for their PQ-9 content (Figure 2b; Figure S4). PQ-9 was found in all fractions, with an almost equivalent partitioning between the thylakoids and the two other fractions (envelopes + PGs) in WT leaves (Figure S4). We checked the abundance of the PG marker protein Plastoglobulin 35 in the different fractions by Western blotting. Compared with the PG fraction, the abundance of Plastoglobulin 35 in the envelope fraction was very low (Figure S5). Consequently, the almost similar amounts of PQ-9 found in the PGs and the envelopes (Figure S4) are not attributable to a contamination of the envelopes by PGs. Surprisingly, Fractions 24–28 contain very little PQ-9 although they are green. It is possible that those fractions

FIGURE 2   Localization of PQ-9 in the chloroplasts. (a) Fractionation of chloroplast membranes by ultracentrifugation on sucrose gradient showing zones corresponding to the PG, the envelopes, and the thylakoids. The scale on the right shows the position of the different fractions collected for the PQ-9 analyses. (b) Quantification of PQ-9 in 1-ml fractions from top (Fraction 1) to bottom (Fraction 32) for WT, *vte1*, *SPS1*oex, and *vte1 SPS1*oex leaves. The same amounts of chlorophyll were loaded on the sucrose gradient. (c) Estimation of the photochemically active and nonactive pools of PQ-9 in Arabidopsis leaves. Data are mean values of four separate measurements ± *SD*. (d) Induction of chlorophyll fluorescence in intact leaves. Insert: pool sizes of PSII two-electron acceptors estimated from the fluorescence induction curves in the presence and absence of DCMU. ** and ***; different from WT at $p < .005$ and .001 (Student's *t* test). PG = plastoglobules; PQ-9 = plastoquinone-9; PSII = photosystem II
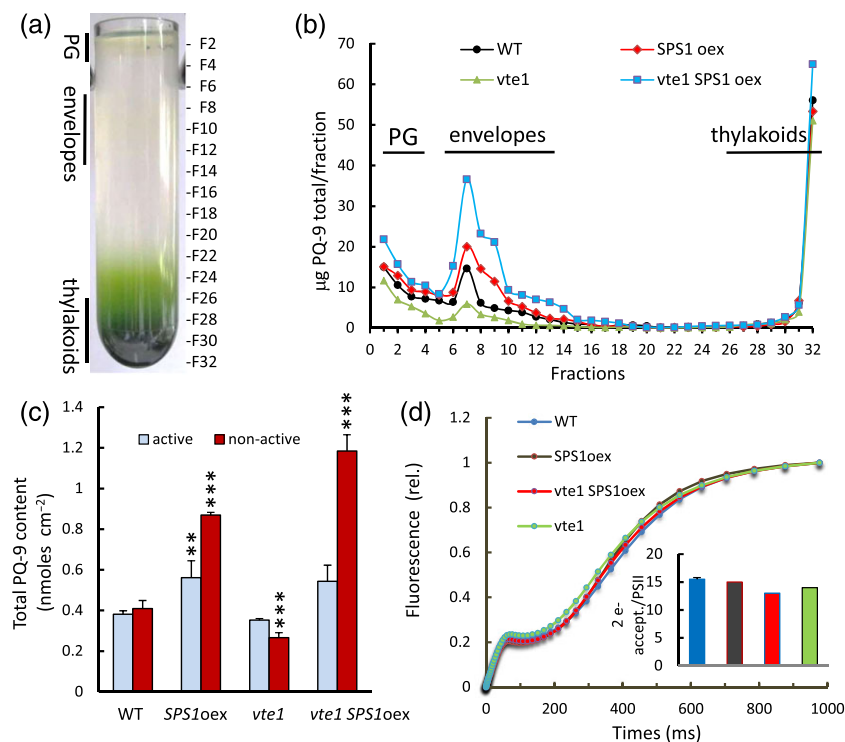

contain photosynthetic pigmented complexes released from the thylakoids during preparation. In *vte1*, the loss of PQ-9 concerned exclusively the PG and envelope fractions (Fractions 1–4 and 5–14, respectively), with the levels in the thylakoids (Fractions 26–32) being virtually unchanged relative to WT. Similarly, the accumulation of total PQ-9 in *SPS1*oex and *vte1 SPS1*oex leaves impacted mainly the PG and envelope fractions. Thus, thylakoid membranes appear to accommodate a relatively constant amount of PQ-9 (presumably ensuring optimum electron transport), whereas the PG and envelope fractions function as PQ-9 storage sites that can absorb large variations in total PQ-9 in the chloroplasts. This was confirmed by the estimation of the photochemically active and nonactive pools of PQ-9 using a previously described procedure based on HPLC analysis of reduced and oxidized PQ-9 in the dark and upon intense illumination (Ksas et al., 2015). For each genotype, we found that the pool sizes of the active plus nonactive pools (Figure 2c) were matching, within experimental accuracy, the total pool size (Figure 1a; in nmol cm^{-2}, 0.91 ± 0.07 in WT, 1.43 ± 0.15 in *SPS1*oex, 0.60 ± 0.04 in *vte1*, and 1.73 ± 0.08 in *vte1 SPS1*oex). Figure 2c shows that the photoactive pool (reflecting the thylakoid PQ-9 pool involved in photosynthetic electron transport) showed relatively little variations in the different genotypes, whereas the nonphotoactive pool (reflecting the pool, located outside the thylakoid membranes, not involved in electron transport) exhibited strong variations, with *SPS1*oex and *vte1 SPS1*oex having by far the largest pools of extrathylakoid PQ-9 (Figure 2c), in agreement with the analyses of Figures 2b and S4.

It is also possible to estimate the size of the functional pool of PSII electron acceptors by *in vivo* chlorophyll fluorescence measurements (Forbush & Kok, 1968; Malkin & Kok, 1966). The chlorophyll fluorescence induction curves of Figure 2d showed little differences between the different genotypes, confirming that the functional pool in the thylakoids was not much affected by the total PQ-9 levels. From the

fluorescence induction curves of Figure 2d and the corresponding curves obtained in the presence of DCMU, we estimated that the number of PSII two-electron acceptors is in the range 13–16 molecules (insert of Figure 2d), which is consistent with the previous estimations in various photosynthetic organisms (Forbush & Kok, 1968; Kolber & Falkowski, 1993).

3.2 | Accumulation of total PQ-9 in the *vte1 SPS1*oex mutant compensated for the lack of tocopherols and PC-8 and increased tolerance to photooxidative stress

Plants grown in low light (150 μmol photons m^{-2} s^{-1}) were transferred to photooxidative stress conditions (1,500 μmol photons m^{-2} s^{-1}, 7°C). After 2 days, this treatment led to leaf bleaching (Figure 3a), low Fv/Fm ratio indicative of PSII photoinhibition (Figure 3d), and enhanced lipid peroxidation (Figure 3b,c) in WT leaves. These symptoms of photodamage were markedly attenuated in *SPS1*oex plants, as previously shown (Ksas et al., 2015). In striking contrast, *vte1* exhibited a very high sensitivity to photooxidative stress, showing dramatic effects on leaves (severe bleaching and loss of turgescence), intense lipid peroxidation, and drastic inhibition of PSII activity relative to WT. This confirms the photoprotective role of tocopherol and/or PC-8 that are absent in *vte1* (Havaux, Eymery, Porfirova, Rey, & Dörmann, 2005). Interestingly, overexpression of *SPS1* suppressed the photobleaching phenotype of *vte1*. Furthermore, *vte1 SPS1*oex was more tolerant to lipid peroxidation than *vte1*. The data of Figure 3 thus demonstrate that total PQ-9 can compensate for the lack of tocopherol and PC-8 in *vte1* leaves, leading to a markedly increased tolerance to photooxidative stress. This effect was confirmed in another *SPS1*-overexpressing *vte1* mutant and under longer stress exposure (4 days; Figure S6).
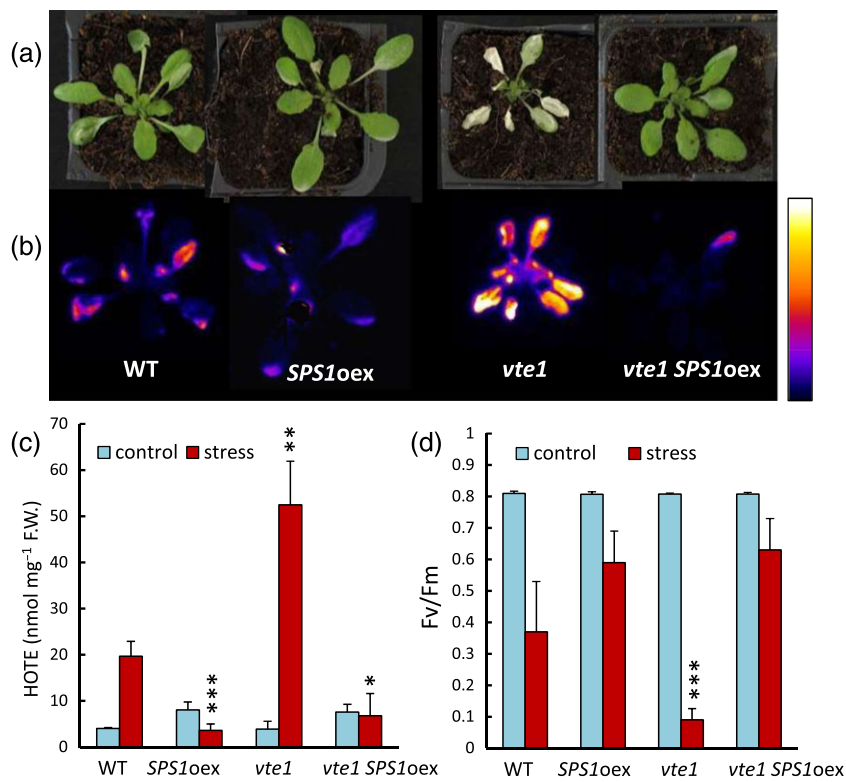
FIGURE 3 Plastoquinone-9 accumulation increases plant tolerance to photooxidative stress. Plants were exposed for 2 days to high light stress (1,500 μmol photons m^{-2} s^{-1}) and low temperature (7 °C). (a) Picture of the plants after the high light treatment. (b) Autoluminescence imaging of lipid peroxidation after high light treatment. The colour palette shows the luminescence signal intensity from low (black) to high values (white). (c) HOTE levels in leaves (in nmoles per mg F.W.) before and after the high light stress. Data are mean values of three or four separate measurements ± SD. (d) Maximal photosystem II photochemical efficiency, as measured by the Fv/Fm chlorophyll fluorescence ratio, before and after the high light stress. Data are mean values of 8 to 12 separate measurements ± SD. *, **, and ***, different from WT and $p < .01$, .005, and .001 (Student's t test).
HOTE = hydroxyoctadecatrienoic acid; F. W. = fresh weight

3.3 | Plastoquinone as a singlet oxygen scavenger in planta

The $^1O_2$ production by illuminated leaves was monitored by measuring the intensity of SOSG-EP fluorescence at 525 nm (Flors et al., 2006; Kim, Fujitsuka, & Majima, 2013). As shown in Figure 4a, the photosensitivity of *vte1* leaves correlated with an increased production of $^1O_2$ compared with WT, in line with the known function of tocopherols as $^1O_2$ quenchers (Choe, 2017; Di Mascio, Devasagayam, Kaiser, & Sies, 1990; Fahrenholtz, Doleiden, Trozzolo, & Lamola, 1974; Krieger-Liszkay, Fufezan, & Trebst, 2008). It was decreased in *vte1 SPS1*oex, showing that replacement of tocopherols by total PQ-9 restores the $^1O_2$ quenching capacities. This finding was confirmed by the analysis of $^1O_2$ production by illuminated
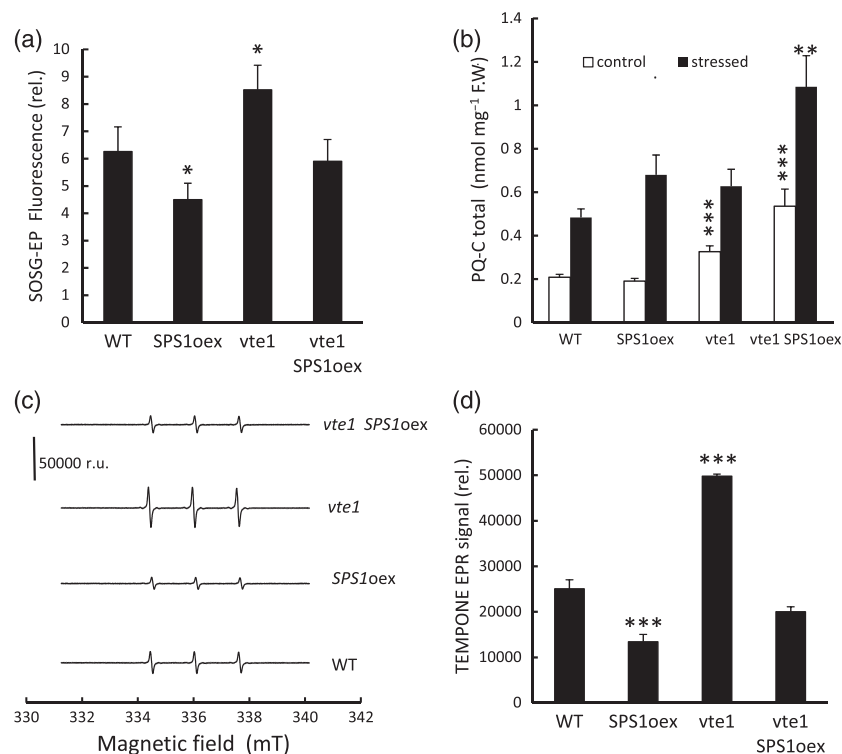
FIGURE 4 $^1O_2$ scavenging by plastoquinone-9. (a) $^1O_2$ production by leaves in the light as measured by SOSG-EP fluorescence. Attached leaves infiltrated with SOSG were exposed for 20 min to light (1,500 μmol photons m^{-2} s^{-1}) at 7 °C. Data are mean values of minimum four measurements. (b) Total PQ-C levels in leaves before and after high light stress (1,500 μmol photons m^{-2} s^{-1} for 2 days at 7 °C). Data are mean values (in nmoles per mg leaf fresh weight) of three separate measurements ± SD. (c–d) $^1O_2$ production by thylakoids as measured by the spin probe TEMPONE and EPR spectroscopy. No signal was detected in the dark. (c) TEMPONE EPR traces and (d) quantification of the TEMPONE EPR signal. Data are mean values of three separate measurements ± SD. *, **, and ***, different from WT at $p < .01$, .005, and .001 (Student's t test). $^1O_2$ = singlet oxygen; SOSG = singlet oxygen sensor green; EP = endoperoxide; PQ-C = Hydroxyplastoquinone; F.W. = fresh weight; TEMPONE = 2,2,6,6-tetramethyl-4-piperidone-1-oxyl; EPR = electron paramagnetic resonance

thylakoid membranes using EPR spectroscopy and the $^1O_2$-specific spin probe 2,2,6,6-tetramethyl-4-piperidone-1-oxyl (Figure 4c,d). The production rate of $^1O_2$ was the highest in *vte1* thylakoid membranes, whereas accumulation of PQ-9 by *SPS1* overexpression in both WT and *vte1* backgrounds resulted in the lowest $^1O_2$ production levels in the light, emphasizing the role of total PQ-9 in the quenching of $^1O_2$ *in vivo*.

Oxidation of PQ-9 by $^1O_2$ has been shown to produce some specific derivatives, such as the hydroxy derivative PQ-C (Szymańska et al., 2014). The latter compound was shown to be a stable product of $^1O_2$ action in plants, particularly when $^1O_2$ production is elevated during short-term exposure to high light stress. Quantification of PQ-C in control Arabidopsis leaves showed the presence of this compound in all genotypes (Figure 4b). Similarly to PQ-9, PQ-C was predominantly in the reduced state (PQH_2-OH; Figure S3). PQ-C accumulation is consistent with the attribution of a $^1O_2$ scavenging function to PQ-9: the amount of this PQ-9 hydroxy derivative, formed by $^1O_2$, is the highest in *vte1 SPS1*oex where total PQ-9 is the most abundant and is the major lipid-soluble antioxidant in the absence of tocopherol and PC-8.

3.4 | High light stress preferentially consumes the thylakoid PQ-9 pools

Arabidopsis plants were exposed for 2.5 hr to high PFD (1,500 μmol photons m^{-2} s^{-1}) and low temperature (7 °C). The total PQ-9 concentration was decreased by around 30% in WT leaves after this treatment (Figure 5a). Figure 5b shows that the PQ-9 losses were particularly marked for the thylakoid-located photochemically active PQ-9 pool (−60%), whereas the extrathylakoid, photochemically nonactive pool was not significantly affected. Because the photosystems in the thylakoids are the main source of ROS in the light, a preferential oxidation of this photochemically active pool is expected. This is actually confirmed by the analysis of $^1O_2$-specific PQ-C compound in the different membrane fractions of the chloroplasts: PQ-C was predominantly found in the thylakoids, with the concentration in the PGs and the envelopes being very low (Figure 5c). In *vte1*, the photoinduced decrease in total PQ-9 content was very marked (>50%; Figure 5a), and the photochemically active pool was almost completely depleted after the high light treatment (Figure 5b). However, contrary to WT, the size of the extrathylakoid, photochemically nonactive PQ-9 pool was also decreased in the mutant, although to a lesser extent (−40%) than the active pool (Figure 5b). Figure 5c shows that, similarly to WT, PQ-C in *vte1* chloroplasts was present mainly in the thylakoids, confirming that PQ-9 oxidation occurred at this level. As shown at the leaf level (Figure 3), the PQ-C concentration was noticeably higher in *vte1* thylakoids compared with WT thylakoids, indicating enhanced oxidation of PQ-9 in this mutant. In *vte1 SPS1*oex leaves that rely on high levels of total PQ-9 for their phototolerance, a considerable loss of total PQ-9 was observed during high light stress (Figure 5a,b), with a very strong accumulation of PQ-C in the thylakoids (Figure 5c). Thus, our data suggest that, under conditions of massive oxidative
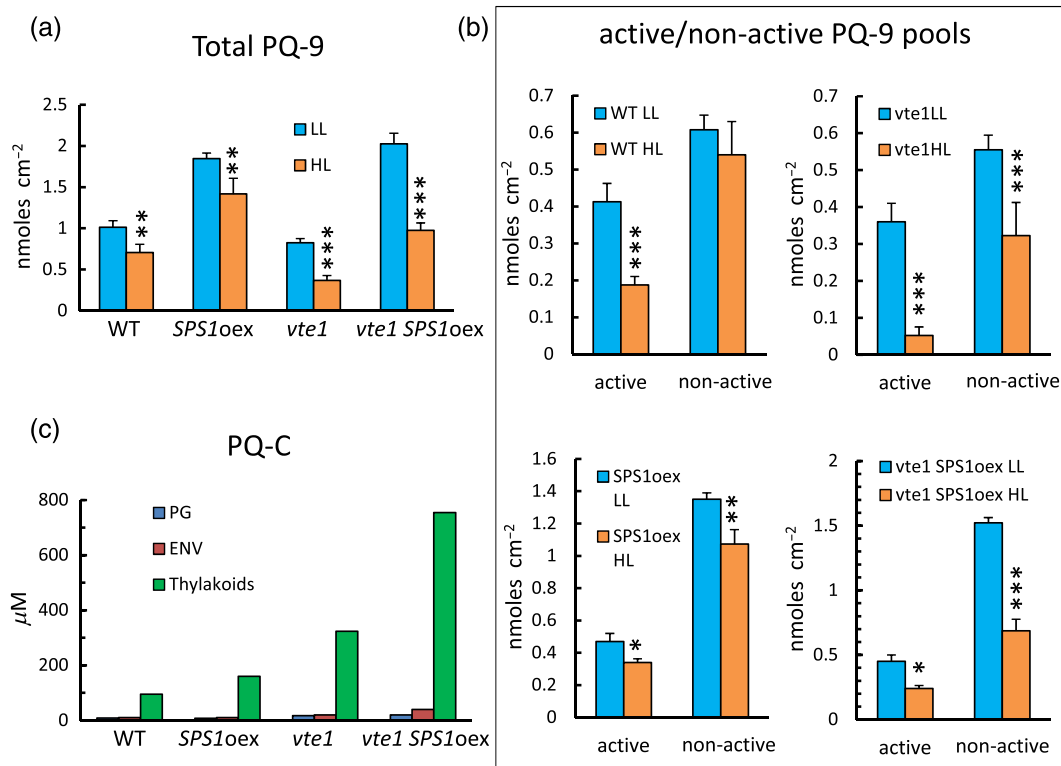
FIGURE 5 Dynamics of the PQ-9 pools. Effects of high light stress (HL = 2.5 hr at 1,500 μmol photons m^{-2} s^{-1}) on (a) the PQ-9 levels in Arabidopsis leaves and (b) on the repartition of PQ-9 between the photochemically active pool (in the thylakoids) and the nonactive pool (in the plastoglobules and the envelopes). Data are mean values of minimum three separate measurements ± *SD*. (c) PQ-C concentration in different chloroplast fractions, PG, ENV, and thylakoids separated by ultracentrifugation on sucrose gradient (Fractions 1–4, 5–10, and 30–32, respectively, see Figure 2b). LL corresponds to the growth light conditions (150 μmol photons m^{-2} s^{-1}). Data are mean values of three experiments ± *SD*. *, **, and ***, different from LL at $p < .01$, .005, and .001 (Student's *t* test)

degradation of PQ-9 in the thylakoids of vte1 and vte1 SPS1oex chloroplasts, there is a transfer of PQ-9 molecules from the PGs and/or the envelope to the thylakoid membranes in order to compensate for PQ-9 photooxidation, hence lowering the PQ-9 levels in the storage sites outside the thylakoid membranes. Owing to their high accumulation levels of total PQ-9, vte1 SPS1oex leaves were able to maintain the total PQ-9 content close to the WT levels after the high light treatment (Figure 5a), and this was associated with a high resistance to photooxidative stress (Figure 3).

4 | DISCUSSION

The essential role of PQ-9 in photosynthesis as an electron carrier has long been recognized (Amesz, 1973; Crane, 2010). However, it is clear from this study that PQ-9 also fulfils an important photoprotective function that is not directly related to photosynthetic electron transport. Actually, only a fraction of the total PQ-9 pool is located in the thylakoid membranes where it can participate in linear and cyclic electron fluxes. We estimated that, in WT Arabidopsis leaves under normal growth conditions, the photochemically active PQ-9 corresponds to around 15 molecules per PSII and 50% of the total PQ-9 content. The latter value is higher than the previous reports (ca. 30%; Kruk & Karpinski, 2006; Szymanska & Kruk, 2010), possibly due to different growth conditions. The size of the total thylakoid-associated PQ-9 pool was found to be stable in control conditions, showing relatively little variation among the different genotypes studied here or in response to changes in the total PQ-9 content of the leaves. This stability contrasts with the nonphotochemically active pool, the size of which exhibited large variations. As confirmed in this study, the latter PQ-9 pool partitions between the PGs (Zbierzak et al., 2009) and the envelope membranes (Soll et al., 1985). The size of the extrathylakoid PQ-9 pool drastically decreased in the photosensitive vte1 mutant, whereas it was selectively increased when PQ-9 biosynthesis was stimulated. The highest PQ-9 levels were found in vte1 SPS1oex leaves in which approximately two-thirds of the total PQ-9 pool was not in the thylakoids. In contrast, only 40% of the total pool was outside the thylakoid membrane in the vte1 single mutant that contains the lowest levels of total PQ-9. Somehow, the PQ-9 reservoir stored in the PGs and the chloroplast envelopes functions as a buffer that can manage large variations in the total PQ-9 levels in the leaves.

The multilocation storage of PQ-9 suggests a multifunctionality for this compound. Previously, PQ-9 was reported to be involved in biosynthesis pathways, as a component of phytoene desaturase in the carotenoid biosynthesis pathway (Norris et al., 1995) and of NDC1, a type-II NAD(P)H quinone oxidoreductase involved in vitamin K1 synthesis (Eugeni Piller et al., 2011). This work shows that total PQ-9 also has a ROS scavenging activity protecting the chloroplasts against photodamage by a mechanism that could possibly be similar to the antioxidant activity of tocopherol. Indeed, overexpression of SPS1 in the tocopherol-deficient vte1 mutant concomitantly enhanced leaf PQ-9 levels and decreased plant photosensitivity, indicating that a large total PQ-9 pool can replace tocopherols in photoprotection. Tocopherol has been shown to act as a $^1O_2$ quencher (Choe, 2017; Di Mascio et al., 1990; Fahrenholtz et al., 1974; Falk & Munné-Bosch,

2010; Krieger-Liszkay et al., 2008) and a terminator of lipid peroxidation (Burton & Ingold, 1986; Ham & Liebler, 1995). PQ-9, particularly in its reduced form (plastoquinol), can also do both. Indeed, Nowicka et al. (2013) showed that reduced or oxidized PQ-9 incorporated into liposomes precludes lipid oxidation, and the present work demonstrates that high total PQ-9 levels lowered $^1O_2$ accumulation levels. Moreover, high light stress leads to a loss of PQ-9 and a concomitant formation of PQ-C indicating $^1O_2$ oxidation of PQ-9. As expected, the accumulation of PQ-C was the highest in vte1 SPS1oex leaves, which rely the most on total PQ-9 for their resistance to photooxidative stress. PQ-C was found almost exclusively in the thylakoids where ROS are produced in the light, either by excitation energy transfer ($^1O_2$) or by electron transfers (superoxide anion radical, hydrogen peroxide, or hydroxyl radical; Asada, 2006; Krieger-Liszkay et al., 2008; Li, Wakao, Fischer, & Niyogi, 2009; Pospíšil, 2014).

PQ-9, especially when it is in the reduced state, possesses a number of features that are likely to make this compound an excellent antioxidant. First, it is present in high amounts as a diffusible molecule in thylakoids. As shown in Figure 1, the concentration of total PQ-9 in Arabidopsis leaves is higher than tocopherol + plastochromanol levels. Leaf enrichment in total PQ-9 relative to tocopherols can be even amplified during long-term acclimation of plants to high light intensities (Ksas et al., 2015; Lichtenthaler, 2007). Second, the PQ-9 side chain bears several double bonds contrary to tocopherols. Double bonds are known to be preferential targets of $^1O_2$ for oxidation (Triantaphylides & Havaux, 2009), and therefore the unsaturated side-chain of PQ-9 could provide a possibility for PQ-9 to quench $^1O_2$ by a chemical mechanism. Nevertheless, the antioxidant activity is mainly bearded by the phenolic group of reduced PQ-9 (Kim & Min, 2008), so that reduced PQ-9 is a better $^1O_2$ quencher than oxidized PQ-9. Third, in thylakoid membranes, photosynthetic electron transport relies on the interaction between PQ-9 and the PSII reaction centres that are the main $^1O_2$ generators during photosynthesis (Krieger-Liszkay et al., 2008). It was initially hypothesized that, in the thylakoid membranes, PQ-9 is located in the fluid bilayer-midplane region allowing rapid lateral movements between cytochrome b6/f and PSII complexes (Millner & Barber, 1984). However, more recent data favour a close compartmentization of PSII, PQ-9, and cytochrome b6/f complex in membrane microdomains (Johnson, Vasilev, Olsen, & Hunter, 2014; Lavergne & Joliot, 1991). Moreover, PQ-9 diffusion towards/from PSII was recently proposed to occur via several entries/exits in the PSII reaction centre with an exchange cavity where PQ-9 can diffuse around (Van Eerden, Melo, Frederix, Periole, & Marrink, 2017). These characteristics of the interactions between PSII and PQ-9 are likely to augment the opportunities for reduced PQ-9 to scavenge $^1O_2$ produced in the reaction centres. Consequently, reduced PQ-9 could constitute a first line of defence against photosynthesis-produced ROS, supplementing the action of the β-carotene molecules bound to the PSII centres.

Chemical quenching involves oxidation of the quencher, and therefore total PQ-9 is expected to be consumed during its antioxidant activity, as indeed observed in plants exposed to photooxidative stress conditions (Ksas et al., 2015; Figure 5). In the vte1 mutant, the total PQ-9 levels are constitutively lower than in WT, and this can be attributed to the chronic oxidation of PQ-9 in the absence of

tocopherol. The increased levels of PQ-C in the *vte1* mutants compared with WT corroborate this interpretation. This phenomenon concerns mainly the extrathylakoid PQ-9 pool, with the total thylakoid-located PQ-9 levels being virtually unchanged relative to WT levels under control conditions. Because ROS are produced in the light in the thylakoids, a dynamic exchange of PQ-9 molecules must exist between the thylakoids and their storage sites in the PGs and the envelopes to replace photooxidized PQ-9 molecules in the thylakoid membranes with new PQ-9 molecules and to maintain a constant pool in the thylakoid membranes. Accordingly, PGs have been shown to be physically coupled to thylakoids in a way allowing bidirectional channelling of lipid metabolites (Austin 2nd, Frost, Vidi, Kessler, & Staehelin, 2006; Bréhélin & Kessler, 2008). However, experimental data measuring the nature and the rate of this metabolite exchange are not available. When Arabidopsis plants were suddenly exposed to high light stress, total PQ-9 levels drastically decreased in the thylakoids, as expected when excess light energy leads to high $^1O_2$ production levels by the photosystems. Moreover, PQ-C was detected predominantly in the thylakoid fractions, indicating that $^1O_2$ oxidation of PQ-9 occurs at this level. This is in agreement with a previous study by Szymanska and Kruk (2010) who showed a selective decrease in the photochemically active PQ-9 in Arabidopsis leaves exposed to high light stress. However, we also observed a significant reduction of the total PQ-9 concentration, though less pronounced, in the photochemically nonactive pool when the photostress was severe and PQ-9 degradation was very pronounced such as in the *vte1* background. This effect of high light stress is consistent with a transfer of PQ-9 molecules from the PGs and/or envelopes to the thylakoids to compensate the oxidative modification of PQ-9 during its scavenging activity. In this context, it is worth mentioning that reduced PQ-9 showed a high mobility in lipid membranes compared with α-tocopherol (Jemiola-Rzeminska, Kruk, & Strzalka, 2003). Nevertheless, the rate of this transfer appeared to be slow compared with the rate of PQ-9 oxidation in high light because it could not maintain the pool size of photochemically active PQs to the control levels measured in low light.

Because PQ-9 somehow functions as a sacrificial antioxidant consumed during oxidative stress, it must be resynthesized for the pool being refilled. Accordingly, most genes of the PQ-9 biosynthesis pathway are strongly upregulated during acclimation of Arabidopsis to high light intensities (Block et al., 2013; Ksas et al., 2015). This induction of PQ-9 biosynthesis genes was accompanied by a concomitant rise in the size of the total PQ-9 pool, whereas there was less effect on the tocopherol content (Ksas et al., 2015; Szymanska & Kruk, 2010). The selective accumulation of total PQ-9 during growth in high light environments was reported in other species such as beech or fig trees (Lichtenthaler, 2007), consistently with the photoprotective role described for this compound in the present work.

ACKNOWLEDGEMENTS

CONFLICT OF INTEREST

The authors claim no conflict of interest.

ORCID

Michel Havaux http://orcid.org/0000-0002-6434-393X

REFERENCES

Amesz, J. (1973). The function of plastoquinone in photosynthetic electron transport. *Biochimica et Biophysica Acta*, 301, 35–51.

Asada, K. (2006). Production and scavenging of reactive oxygen species in chloroplasts and their functions. *Plant Physiology*, 141, 391–396.

Austin, J. R. 2nd, Frost, E., Vidi, P. A., Kessler, F., & Staehelin, L. A. (2006). Plastoglobules are lipoprotein subcompartments of the chloroplast that are permanently coupled to thylakoid membranes and contain biosynthetic enzymes. *Plant Cell*, 18, 1693–1703.

Besagni, C., Eugeni Piller, L., & Bréhélin, C. (2011). Preparation of plastoglobules from Arabidopsis plastids for proteomic analysis and other studies. *Methods in Molecular Biology*, 775, 223–239.

Birtic, S., Ksas, B., Genty, B., Mueller, M. J., Triantaphylides, C., & Havaux, M. (2011). Using spontaneous photon emission to image lipid oxidation patterns in plant tissues. *Plant Journal*, 67, 1103–1115.

Block, A., Fristedt, R., Rogers, S., Kumar, J., Barnes, B., Barnes, J., ... Basset, G. J. (2013). Functional modeling identifies paralogous solanesyl-diphosphate synthases that assemble the side chain of plastoquinone-9 in plastids. *Journal of Biological Chemistry*, 200, 27594–27606.

Bréhélin, C., & Kessler, F. (2008). The plastoglobule: A bag full of lipid biochemistry tricks. *Photochemistry and Photobiology*, 84, 1388–1394.

Burton, G. W., & Ingold, K. U. (1986). Vitamin E: Application of the principles of physical organic chemistry to the exploration of its structure and function. *Accounts of Chemical Research*, 19, 194–201.

Choe, E. (2017). Effects and mechanism of minor compounds in oil on lipid oxidation. In C. A. Koh (Ed.), *Food lipids: Chemistry, nutrition, and biotechnology* (pp. 567–590). Boca Raton: CRC Press.

Cook, W. B., & Miles, D. (1992). Nuclear mutations affecting plastoquinone accumulation in maize. *Photosynthesis Research*, 31, 99–111.

Crane, F. L. (2010). Discovery of plastoquinone: A personal perspective. *Photosynthesis Research*, 103, 195–209.

Di Mascio, P., Devasagayam, T. P., Kaiser, S., & Sies, H. (1990). Carotenoids, tocopherols and thiols as biological singlet molecular oxygen quenchers. *Biochemical Society Transactions*, 18, 1054–1056.

Eugeni Piller, L., Besagni, C., Ksas, B., Rumeau, D., Bréhélin, C., Glauser, G., ... Havaux, M. (2011). Chloroplast lipid droplet type II NAD(P)H quinone oxidoreductase is essential for prenylquinone metabolism and vitamin K1 accumulation. *Proceedings National Academy of Sciences USA*, 108, 14354–14359.

Fahrenholtz, S. R., Doleiden, F. H., Trozzolo, A. M., & Lamola, A. A. (1974). On the quenching of singlet oxygen by alpha-tocopherol. *Photochemistry and Photobiology*, 20, 505–509.

Falk, J., & Munné-Bosch, S. (2010). Tocochromanol functions in plants: Antioxidant and beyond. *Journal of Experimental Botany*, 61, 1549–1566.

Flors, C., Fryer, M. J., Waring, J., Reeder, B., Bechtold, U., Mullineaux, P. M., ... Baker, N. R. (2006). Imaging the production of singlet oxygen in vivo

using a new fluorescent sensor, singlet oxygen sensor green. *Journal of Experimental Botany*, 57, 1725–1734.

Forbush, B., & Kok, K. (1968). Reaction between primary and secondary electron acceptors of photosystem II of photosynthesis. *Biochimica et Biophysica Acta*, 162, 243–253.

Gruszka, J., Pawlak, A., & Kruk, J. (2008). Tocochromanols, plastoquinol, and other biological prenyllipids as singlet oxygen quenchers— Determination of singlet oxygen rate constants and oxidation products. *Free Radicals in Biology and Medecine*, 45, 920–928.

Ham, A.-J. L., & Liebler, D. C. (1995). Vitamin E oxidation in rat liver mitochondria. *Biochemistry*, 34, 5754–5761.

Havaux, M., Eymery, F., Porfirova, S., Rey, P., & Dörmann, P. (2005). Vitamin E protects against photoinhibition and photooxidative stress in Arabidopsis thaliana. *Plant Cell*, 17, 3451–3469.

Hundal, T., Forsmark-Andrée, P., Ernster, L., & Andersson, B. (1995). Antioxidant activity of reduced plastoquinone in chloroplast thylakoid membranes. *Archives of Biochemistry and Biophysics*, 324, 117–122.

Jemiola-Rzeminska, M., Kruk, J., & Strzalka, K. (2003). Anisotropy measurements of intrinsic fluorescence of prenyllipids reveal much higher mobility of plastoquinol than alpha-tocopherol in model membranes. *Chemistry and Physics of Lipids*, 123, 233–243.

Johnson, M. P., Vasilev, C., Olsen, J. D., & Hunter, C. N. (2014). Nanodomains of cytochrome b6f and photosystem II complexes in spinach grana thylakoid membranes. *Plant Cell*, 26, 3051–3061.

Johnson, X., Vandystadt, G., Bujaldon, S., Wollman, F.-A., Dubois, R., Roussel, P., … Béal, D. (2009). A new setup for in vivo fluorescence imaging of photosynthetic activity. *Photosynthesis Research*, 102, 85–93.

Joliot, P., & Joliot, A. (2002). Cyclic electron transfer in plant leaf. *Proceedings National Academy of Sciences USA*, 99, 10209–10214.

Kim, H. J., & Min, D. B. (2008). Tocoperol stability and prooxidant mechanisms of oxidized tocopherols in lipids. In C. A. Koh, & D. B. Min (Eds.), *Food lipids: Chemistry, nutrition, and biotechnology* (pp. 435–447). Boca Raton: CRC Press.

Kim, S., Fujitsuka, M., & Majima, T. (2013). Photochemistry of singlet oxygen sensor green. *Journal of Physical Chemistry B*, 117, 13986–13992.

Kolber, Z., & Falkowski, P. G. (1993). Use of active fluorescence to estimate phytoplankton photosynthesis in situ. *Limnology and Oceanography*, 38, 1646–1665.

Krieger-Liszkay, A., Fufezan, C., & Trebst, A. (2008). Singlet oxygen production in photosystem II and related protection mechanism. *Photosynthesis Research*, 98, 551–561.

Kruk, J., & Karpinski, S. (2006). An HPLC-based method of estimation of the total redox state of plastoquinone in chloroplasts, the size of the photochemically active plastoquinone-pool and its redox state in thylakoids of Arabidopsis. *Biochimica et Biophysica Acta*, 1757, 1669–1675.

Kruk, J., Szymanska, R., Cela, J., & Munne-Bosch, S. (2014). Plastochromanol-8: Fifty years of research. *Photochemistry*, 108, 9–16.

Kruk, J., & Trebst, A. (2008). Plastoquinol as a singlet oxygen scavenger in photosystem II. *Biochimica et Biophysica Acta*, 1777, 154–162.

Ksas, B., Becuwe, N., Chevalier, A., & Havaux, M. (2015). Plant tolerance to excess light energy and photooxidative damage relies on plastoquinone biosynthesis. *Scientific Reports*, 5, 10919.

Lavergne, J., & Joliot, P. (1991). Restricted diffusion in photosynthetic membranes. *Trends in Biochemical Sciences*, 16, 129–134.

Li, Z., Wakao, S., Fischer, B. B., & Niyogi, K. K. (2009). Sensing and responding to excess light. *Annual Review of Plant Biology*, 60, 239–260.

Lichtenthaler, H. K. (2007). Biosynthesis, accumulation and emission of carotenoids, alpha-tocopherol, plastoquinone, and isoprene in leaves under high photosynthetic irradiance. *Photosynthesis Research*, 92, 163–179.

Lichtenthaler, H. K., & Weinert, H. (1970). The correlation between lipoquinone accumulation and plastoglobuli formation in the chloroplasts of *Ficus elastica* Roxb. *Zeitschrift für Naturforschung*, 25b, 619–623. 266

Malkin, S., & Kok, B. (1966). Fluorescence induction studies in isolated chloroplasts I. Number of components involved in the reaction and quantum yields. *Biochimica et Biophysica Acta*, 126, 413–432.

Millner, P. A., & Barber, J. (1984). Plastoquinone as a mobile redox carrier in the photosynthetic membrane. *FEBS Letters*, 169, 1–6.

Montillet, J.-L., Cacas, J.-L., Garnier, L., Montane, M. H., Douki, T., Bessoule, J. J., … Triantaphylides, C. (2004). The upstream oxylipin profile of *Arabidopsis thaliana*: A tool to scan for oxidative stresses. *Plant Journal*, 40, 439–451.

Norris, S. R., Barrette, T. R., & DellaPenna, D. (1995). Genetic dissection of carotenoid synthesis in arabidopsis defines plastoquinone as an essential component of phytoene desaturation. *Plant Cell*, 7, 2139–2149.

Nowicka, B., Gruszka, J., & Kruk, J. (2013). Function of plastochromanol and other biological prenyllipids in the inhibition of lipid peroxidation —A comparative study in model systems. *Biochimica et Biophysica Acta*, 1828, 233–240.

Pfannschmidt, T., Bräutigam, K., Wagner, R., Dietzel, L., Schröter, Y., Steiner, S., & Nykytenko, A. (2009). Potential regulation of gene expression in photosynthetic cells by redox and energy state: Approaches towards better understanding. *Annals of Botany*, 103, 599–607.

Porfirova, S., Bergmuller, E., Tropf, S., Lemke, R., & Dörmann, P. (2002). Isolation of an Arabidopsis mutant lacking vitamin E and identification of a cyclase essential for all tocopherol biosynthesis. *Proceedings National Academy Sciences USA*, 99, 12495–12500.

Pospíšil, P. (2014). The role of metals in production and scavenging of reactive oxygen species in photosystem II. *Plant Cell Physiology*, 55, 1224–1232.

Ramel, F., Birtic, S., Cuiné, S., Triantaphylidès, C., Ravanat, J. L., & Havaux, M. (2012). Chemical quenching of singlet oxygen by carotenoids in plants. *Plant Physiology*, 158, 1267–1278.

Rochaix, J. D. (2014). Redox regulation of thylakoid protein kinases and photosynthetic gene expression. *Antioxidants and Redox Signaling*, 18, 2184–2201.

Soll, J., Schultz, G., Joyard, J., Douce, R., & Block, M. A. (1985). Localization and synthesis of prenylquinones in isolated outer and inner envelope membranes from spinach chloroplasts. *Archives of Biochemistry and Biophysics*, 238, 290–299.

Szymanska, R., & Kruk, J. (2010). Plastoquinol is the main prenyllipid synthesized during acclimation to high light conditions in Arabidopsis and is converted to plastochromanol by tocopherol cyclase. *Plant and Cell Physiology*, 51, 537–546.

Szymańska, R., Nowicka, B., & Kruk, J. (2014). Hydroxy-plastochromanol and plastoquinone-C as singlet oxygen products during photooxidative stress in Arabidopsis. *Plant, Cell & Environment*, 37, 1464–1473.

Triantaphylides, C., & Havaux, M. (2009). Singlet oxygen in plants: Production, detoxification and signaling. *Trends in Plant Science*, 14, 219–228.

Van Eerden, F. J., Melo, M. N., Frederix, P. W. J. M., Periole, X., & Marrink, S. J. (2017). Exchange pathways of plastoquinone and plastoquinol in the photosystem II complex. *Nature Communications*, 8, 15214.

Vidi, P. A., Kanwischer, M., Baginsky, S., Austin, J. R., Csucs, G., Dörmann, P., … Bréhélin, C. (2006). Tocopherol cyclase (VTE1) localization and vitamin E accumulation in chloroplast plastoglobule lipoprotein particles. *Journal of Biological Chemistry*, 281, 11225–11234.

Yadav, D. K., Kruk, J., Sinha, R. K., & Pospisil, P. (2010). Singlet oxygen scavenging activity of plastoquinol in photosystem II of high plants: Electron paramagnetic resonance spin-trapping study. *Biochimica et Biophysica Acta*, 1797, 1807–1811.

Zbierzak, A. M., Kanwischer, M., Wille, C., Vidi, P. A., Giavalisco, P., Lohmann, A., ... Dörmann, P. (2009). Intersection of the tocopherol and plastoquinone metabolic pathways at the plastoglobule. *Biochemical Journal*, *425*, 389–399.

SUPPORTING INFORMATION

Additional Supporting Information may be found online in the supporting information tab for this article.

SCIENTIFIC REP😊RTS

Singlet oxygen production in *Chlamydomonas reinhardtii* under heat stress

Ankush Prasad[1], Ursula Ferretti[1], Michaela Sedlářová[2] & Pavel Pospíšil[1]

In the current study, singlet oxygen formation by lipid peroxidation induced by heat stress (40 °C) was studied *in vivo* in unicellular green alga *Chlamydomonas reinhardtii.* Primary and secondary oxidation products of lipid peroxidation, hydroperoxide and malondialdehyde, were generated under heat stress as detected using swallow-tailed perylene derivative fluorescence monitored by confocal laser scanning microscopy and high performance liquid chromatography, respectively. Lipid peroxidation was initiated by enzymatic reaction as inhibition of lipoxygenase by catechol and caffeic acid prevented hydroperoxide formation. Ultra-weak photon emission showed formation of electronically excited species such as triplet excited carbonyl, which, upon transfer of excitation energy, leads to the formation of either singlet excited chlorophyll or singlet oxygen. Alternatively, singlet oxygen is formed by direct decomposition of hydroperoxide via Russell mechanisms. Formation of singlet oxygen was evidenced by the nitroxyl radical 2,2,6,6-tetramethylpiperidine-1-oxyl detected by electron paramagnetic resonance spin-trapping spectroscopy and the imaging of green fluorescence of singlet oxygen sensor green detected by confocal laser scanning microscopy. Suppression of singlet oxygen formation by lipoxygenase inhibitors indicates that singlet oxygen may be formed via enzymatic lipid peroxidation initiated by lipoxygenase.

Reactive oxygen species (ROS) are formed by activation of non-reactive molecular oxygen during photosynthetic light reaction in chloroplasts, cellular respiration in mitochondria and defence against microorganisms in phagocyte plasma membrane[1]. The activation of molecular oxygen occurs either by an electron transport reaction known to form superoxide anion radical ($O_2^{\bullet-}$), hydrogen peroxide (H_2O_2), hydroxyl radical ($HO^\bullet$) or by energy transfer reaction known to form singlet oxygen ($^1O_2$). Under circumstances when the formation of ROS exceeds the antioxidant capacity of the system, the equilibrium between production and scavenging is disturbed and the dangerous ROS induces damage to biomolecules, such are lipids, proteins and nucleic acids[1].

Oxidation of lipids, known as lipid peroxidation, is initiated both by the non-enzymatic reactions involving the oxidation of lipids by ROS or by enzymatic reactions comprising oxidation of lipid mediated by enzymes such as lipoxygenase[2]. In the non-enzymatic reaction pathway, the lipid peroxidation is initiated either by radical ROS comprising $HO^\bullet$, generated by the Fenton reaction[1,3], or by non-radical ROS involving $^1O_2$ formed by the Type II photosensitisation reaction[4–6]. The initiation of lipid peroxidation by $HO^\bullet$ involves abstraction of weakly bonded hydrogen from polyunsaturated fatty acids known to form alkyl radical ($L^\bullet$) which in the presence of molecular oxygen, forms peroxyl radical ($LOO^\bullet$)[1]. Hydrogen abstraction from another polyunsaturated fatty acid by $ROO^\bullet$ forms hydroperoxides ($LOOH$)[7]. The initiation of lipid peroxidation by $^1O_2$ involves the cycloaddition of $^1O_2$ to polyunsaturated fatty acids that forms LOOH. In the enzymatic reaction pathway, lipid peroxidation is initiated by lipoxygenase known to exhibit dioxygenase activity. In this reaction, the ferric non-heme iron catalyzes the initial hydrogen abstraction forming ferrous non-heme iron and $R^\bullet$. The insertion of O_2 at the C-atom of the polyunsaturated fatty acid known to form $LOO^\bullet$ is followed by reduction of ferrous non-heme iron and protonation of $LOO^\bullet$ to LOOH. Under reducing conditions such as reduced free and bound metals, LOOH is reduced to alkoxyl radical ($LO^\bullet$) which might further cause hydrogen abstraction from nearby located polyunsaturated fatty acids.

Several lines of evidence have been provided that indicates that lipid peroxidation is associated with formation of electronically excited species[8,9]. Decomposition of LOOH into peroxyl radical was proposed as a potential

[1]Department of Biophysics, Centre of the Region Haná for Biotechnological and Agricultural Research, Faculty of Science, Palacký University, Šlechtitelů 27, 783 71 Olomouc, Czech Republic. [2]Department of Botany, Faculty of Science, Palacký University, Šlechtitelů 27, 783 71 Olomouc, Czech Republic. Correspondence and requests for materials should be addressed to P.P. (email: pavel.pospisil@upol.cz)

source of electronically excited species in biological systems[10–14]. In this reaction, LOOH is oxidized to LOO$^\bullet$ under oxidizing conditions such are oxidized transition metals, ferric heme iron of cytochrome c, peroxynitrite, chloroperoxide, and hypochlorous acid. Peroxyl radical might either undergoes cyclization to dioxetane or recombines to tetroxide[11,15–19]. These high energy intermediates decompose to triplet excited carbonyls ($^3L = O^*$) which might transfer triplet energy either to pigments forming excited pigments or molecular oxygen forming $^1O_2$[10,20–24]. In addition, tetroxide might decompose directly to $^1O_2$ by Russell mechanism[25].

Under the environmental conditions, photosynthetic organisms such as cyanobacteria, algae and plants are exposed to various abiotic and biotic stress factors. Heat stress is a major environmental stress that is known to be involved in lipid peroxidation in photosynthetic organisms[26–28]. Extensive lipid peroxidation under heat stress was shown to be promoted by the enhancement in polyunsaturation of fatty acid in which hydrogen abstraction from the carbon next to double bond is energetically more feasible[29,30]. In agreement with this proposal, experimental data from many models indicate that the exposure of photosynthetic organisms to heat stress leads to the formation of lipid peroxidation secondary product, malondialdehyde (MDA), as detected by TBARS assay[31–34]. *In vitro*, it has been shown that exposure to heat stress results in the formation of the MDA-(TBA)$_2$ adduct both in thylakoid membranes and PSII membranes isolated from higher plants[31–33]. *In vivo*, it has been demonstrated that exposure of leaf and root segments of *Phalaenopsis* to 40 °C enhanced lipoxygenase activity and MDA formation[31–34].

Moreover, experimental evidence supports *in vitro* $^1O_2$ formation in chloroplasts, thylakoid and PSII membranes exposed to heat stress[31,35,36]. Using EPR spin-trapping spectroscopy, Hideg and Vass (1993) demonstrated that exposure of mung bean chloroplasts and etiolated thylakoid membranes to a non-physiological high temperature of 75 °C results in $^1O_2$ formation. The authors tentatively attributed $^1O_2$ formation to lipid peroxidation, although no experimental data were presented in this study. Later, it was shown that exposure of PSII membranes to 47 °C is accompanied by $^1O_2$ formation[35]. The observation that $^1O_2$ formation was unaffected either by catalase (known to decompose hydrogen peroxide to water and molecular oxygen) or mannitol as HO$^\bullet$ scavenger revealed that HO$^\bullet$ formed by incomplete water oxidation on PSII electron donor side unlikely initiated lipid peroxidation. Similarly, $^1O_2$ formation was observed when spinach thylakoid and PSII membranes were exposed to heat stress at the temperature of 40 °C[31]. The authors demonstrated that the amount of MDA estimated spectroscopically by detection of the MDA-(TBA)$_2$ adduct was formed in parallel to $^1O_2$ formation. Based on the observation that the Q_B site on the PSII electron acceptor side was primarily damaged by heat stress, the authors proposed that $^1O_2$ is formed near the Q_B site. In spite of the fact that $^1O_2$ formation was demonstrated in chloroplast, thylakoid and PSII membranes, experimental evidence on $^1O_2$ formation *in-vivo* has not yet been provided.

Our current study provides *in vivo* evidence that $^1O_2$ is formed in the unicellular green alga *Chlamydomonas reinhardtii*. It is demonstrated herein that exposure of *Chlamydomonas* cells to heat stress (40 °C) results in the formation of 1) LOOH, the primary product of lipid peroxidation, as monitored by swallow-tailed perylene derivative (Spy-LHP) fluorescence as detected by confocal laser scanning microscopy, 2) MDA, the secondary product of lipid peroxidation, as monitored by HPLC detection of MDA-DNPH adduct, 3) $^3L = O^*$ as measured by ultra-weak photon emission and 4) $^1O_2$ localized by fluorescence of Singlet Oxygen Sensor Green (SOSG) visualized by confocal laser scanning microscopy and measured by electron paramagnetic resonance (EPR) spin-trapping spectroscopy utilising the oxidation of lipophilic diamagnetic 2,2,6,6-tetramethylpiperidine (TEMP). Attempts have been made to discuss the mechanism of $^1O_2$ formation via lipid peroxidation initiated by enzymatic reaction catalysed by lipoxygenase.

Results

Hydroperoxide imaging using confocal laser scanning microscopy.
The formation of LOOH in *Chlamydomonas* cells exposed to 40 °C was monitored using a fluorescent probe Spy-LHP detected by laser confocal scanning microscopy. Spy-LHP is known to react with LOOH leading to the formation of its oxidized derivative, Spy-LHPOx which provides a strong fluorescence at 535 nm. Figure 1 shows Nomarski DIC, Spy-LHPOx fluorescence, chlorophyll fluorescence and integral distribution of Spy-LHPOx fluorescence intensity measured in *Chlamydomonas* cells. Whereas no Spy-LHPOx fluorescence was detected in non-heated *Chlamydomonas* cells, pronounced Spy-LHPOx fluorescence was observed in heated *Chlamydomonas* cells exposed to 40 °C. The observation that localisation of chlorophyll fluorescence corresponds to localisation of Spy-LHPOx fluorescence indicates that LOOH is formed mainly in chloroplasts. In addition to this, bright spots of Spy-LHPOx fluorescence were observed which can be attributed to small-sized organelles such as vacuoles which usually are found in *Chlamydomonas* cells under various stress conditions. The integral distribution of Spy-LHPOx fluorescence intensity shows that Spy-LHPOx fluorescence in heated *Chlamydomonas* cells is enhanced by about 4 times as compared to non-heated *Chlamydomonas* cells. These results reveal that exposure of *Chlamydomonas* cells to heat stress leads to the formation of LOOH.

To test whether lipid peroxidation is initiated by non-enzymatic (ROS) or enzymatic (lipoxygenase) reactions, the effect of lipoxygenase inhibitors such as catechol and caffeic acid on LOOH formation was measured in heated *Chlamydomonas* cells (Fig. 1). Catechol and caffeic acid are known to inhibit lipoxygenase by binding to non-heme iron of enzyme and enzyme-substrate complex, respectively[37,38]. In non-heated *Chlamydomonas* cells, no effect of catechol on Spy-LHPOx fluorescence was observed. Interestingly, catechol suppressed significantly Spy-LHPOx fluorescence in heated *Chlamydomonas* cells as compared to heated cells measured in the absence of catechol. Similarly, no effect of caffeic acid on Spy-LHPOx fluorescence was observed in non-heated *Chlamydomonas* cell while Spy-LHPOx fluorescence was pronouncedly suppressed by caffeic acid in heated *Chlamydomonas* cells. The integral distribution of Spy-LHPOx fluorescence showed that in the presence of catechol and caffeic acid, Spy-LHPOx fluorescence was suppressed by approximately 40% and 70%, respectively, in heated *Chlamydomonas* cell. These results revealed that the inhibition of lipoxygenase by catechol and caffeic acid partially prevents LOOH formation.
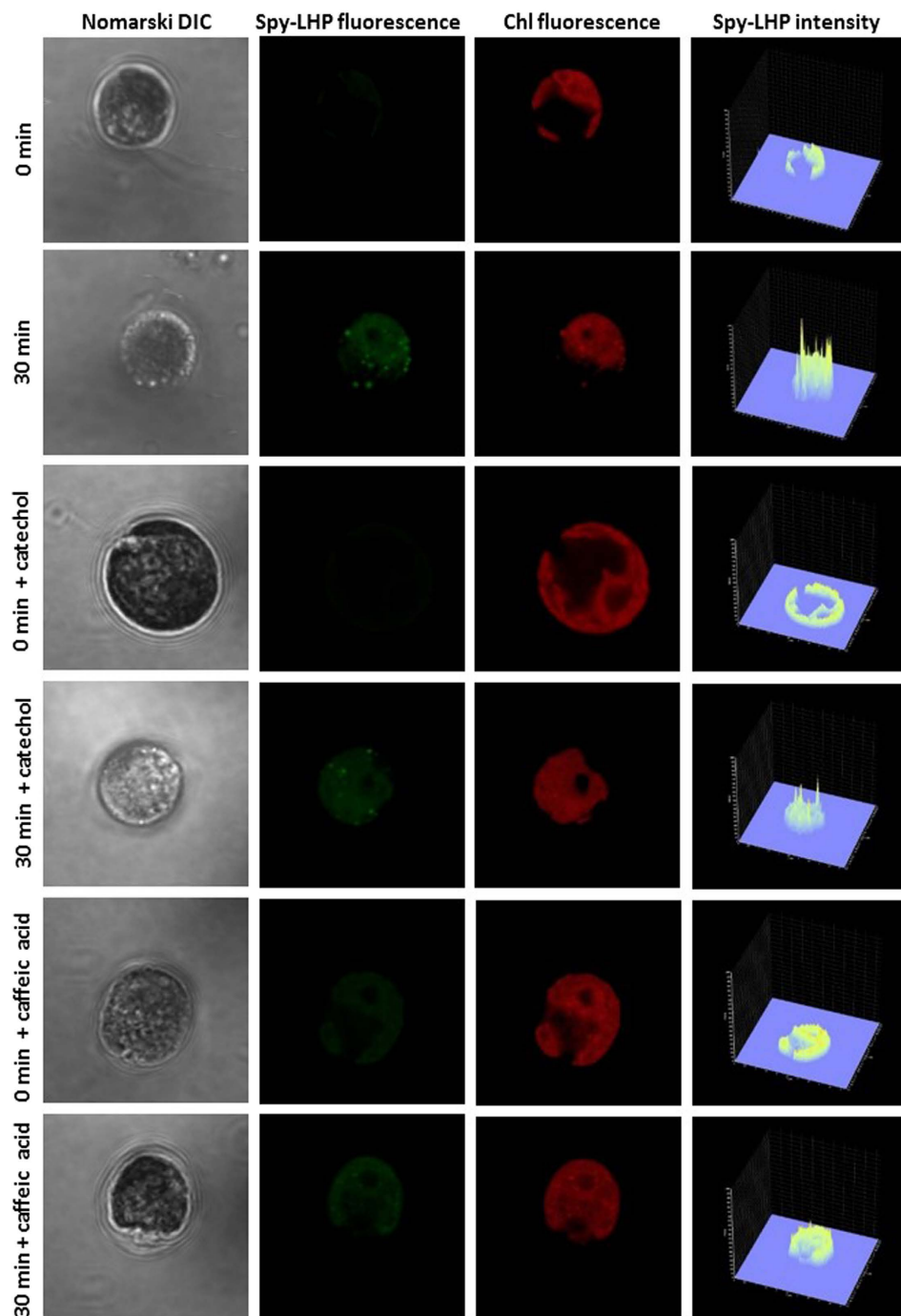
Figure 1. Detection of hydroperoxide in *Chlamydomonas* cells by laser confocal scanning microscopy.
The formation of LOOH was measured in non-heated and heated *Chlamydomonas* cells in the presence and the absence of catechol and caffeic acid using fluorescent probe Spy-LHPOx. Heated cells were treated for 30 min in a water bath at 40 °C under dark. The images represent from left to right: Nomarski DIC, Spy-LHPOx fluorescence, chlorophyll fluorescence and integral distribution of Spy-LHPOx signal intensity (0–4096) in the 12-bit microphotographs.

Quantification of hydroperoxides using ferrous oxidation-xylenol orange assay. To quantify LOOH formation in *Chlamydomonas* cells, ferrous oxidation-xylenol orange (FOX) colorimetric assay was used. In this method, the oxidation of ferrous to ferric irons by LOOH occurs with the subsequent binding of ferric irons to the dye xylenol orange, causing changes in its colour from yellow to red. Figure 2A shows FOX absorption spectra obtained as difference of spectra observed in heated and non-heated *Chlamydomonas* cells. The observation that absorption at 560 nm increased with a period of heat treatment shows gradual LOOH formation. The observation that catalase has no significant effect on absorption at 560 nm (data not shown) reveals that
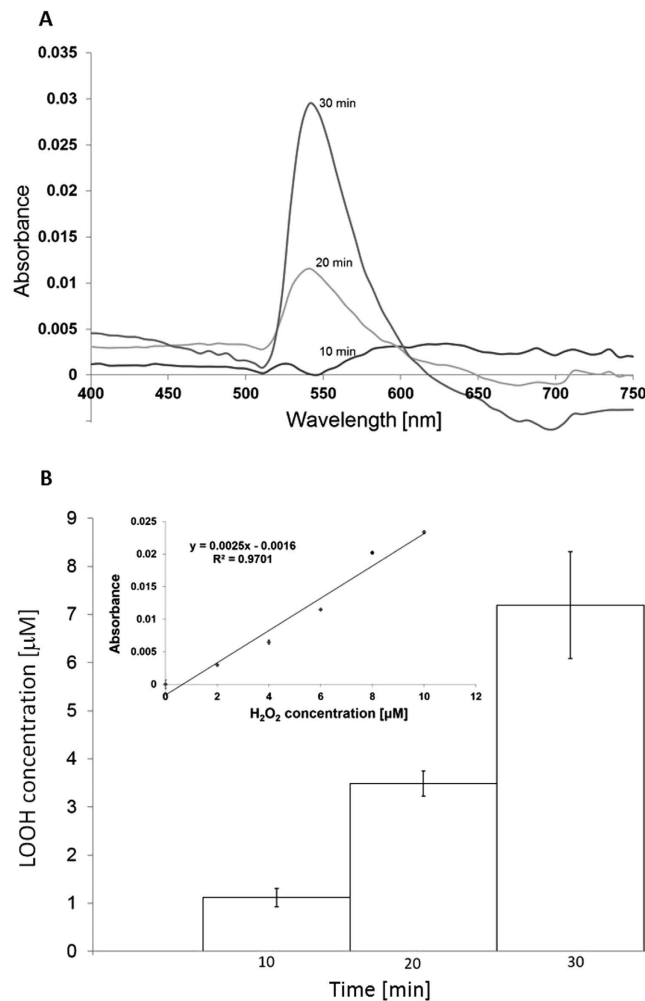
Figure 2. Quantification of hydroperoxide formation in *Chlamydomonas* cells ferrous oxidation-xylenol orange assay. In (**A**) absorption spectra of FOX reagent with *Chlamydomonas* cells heated for 10, 20 and 30 min measured in the spectral ranges of 400–750 nm. In (**B**) the concentrations of LOOH was established from calibration curve (equation y = 0.0025x−0.0016) were as following: $1.12 \pm 0.19\,\mu$mol (10 min), $3.49 \pm 0.26\,\mu$mol (20 min) and $7.19 \pm 1.11\,\mu$mol (30 min). The coefficient of determination R^2 was determined as 0.9701. Insert shows calibration curve of FOX assay obtained using H_2O_2 as substrate.

absorption changes are solely related to the LOOH formation with no contribution of H_2O_2. For determination of LOOH concentration formed in heated cells, the calibration curve was measured by FOX assay with H_2O_2 as the substrate (Fig. 2B, insert). The concentration of LOOH formed in heated *Chlamydomonas* cells is in the concentration range of several units of micromoles (Fig. 2B).

Determination of the MDA-DNPH adduct using HPLC. To examine the level of lipid peroxidation in *Chlamydomonas* cells exposed to heat stress, a secondary product of lipid peroxidation MDA was detected using isocratic reversed-phase HPLC separation of MDA-DNPH adduct. Figure 3A shows a chromatogram of the MDA-DNPH adduct measured in the *Chlamydomonas* cells treated at 40 °C for 0 min and 30 min. The MDA-DNPH adduct peak was observed at the retention time 2.75 min. To confirm the retention time of the MDA-DNPH adduct observed in *Chlamydomonas* cells, chromatogram of MDA standard 1,1,3,3-tetrahydroxypropane (TEP) was measured (Fig. 3B). To determine the concentration of MDA-DNPH adduct observed in heated cells, the calibration curve was established by plotting the peak area at 310 nm for various MDA-DNPH adduct concentrations obtained from MDA standard TEP (Fig. 3B, insert). Figure 3C shows that the concentration of MDA-DNPH adduct formed in heated *Chlamydomonas* cells is in the concentration range of several units of nanomoles.

Detection of triplet excited carbonyl using ultra-weak photon emission. To monitor the formation of $^3L = O^*$ during lipid peroxidation, two-dimensional ultra-weak photon emission was measured in the *Chlamydomonas* cell using a highly sensitive charge coupled device (CCD) camera. Figure 4 shows the effect of heat treatment on the ultra-weak photon emission measured with accumulation time of 10, 20 and 30 min in the *Chlamydomonas* cells treated at 40 °C for 10, 20 and 30 min. When the cells were treated at 40 °C for a
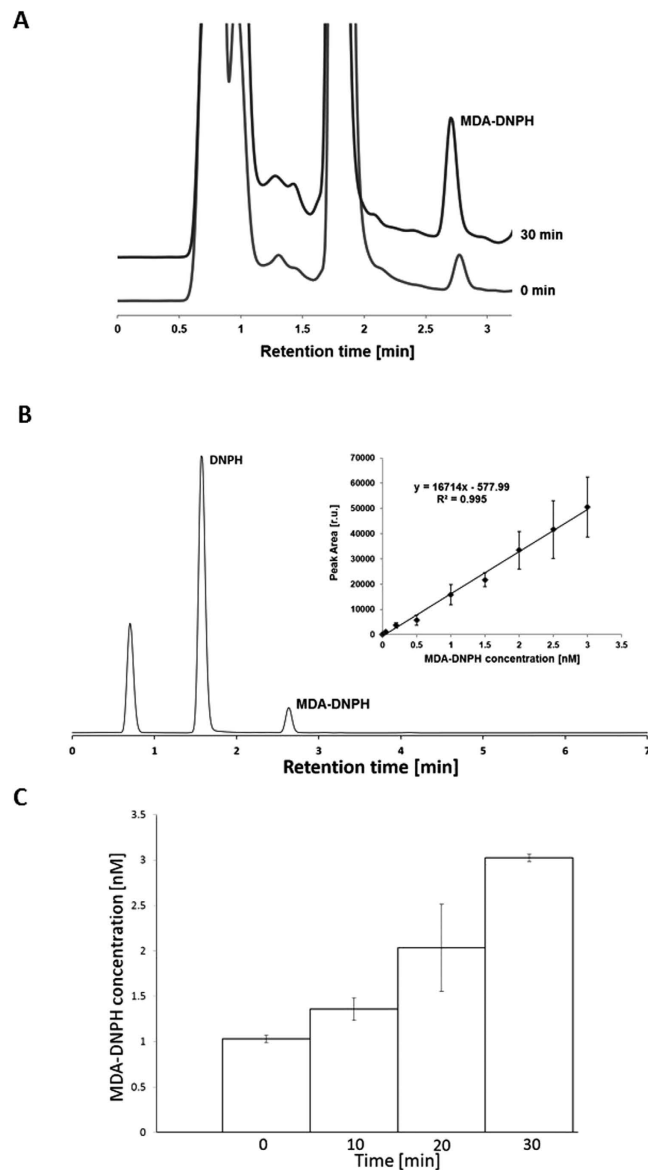
Figure 3. Detection of malondialdehyde by HPLC analysis in *Chlamydomonas* cells. The chromatogram of MDA-DNPH adduct in *Chlamydomonas* cells (**A**); MDA-DNPH adduct from standard TEP (**B**) and determination of MDA-DNPH adduct concentrations under heat stress (**C**). In A, chromatogram of MDA-DNPH adduct is shown in control (0 min) and heated (30 min) *Chlamydomonas* cells. Representative chromatograms were obtained as average of 3 chromatograms. In (**B**) chromatogram of MDA-DNPH adduct from MDA standard with a retention time of 2.75 min. The insert shows the dependence of average peak area (n = 5, ±SD) on the concentration of MDA-DNPH adduct from MDA standard TEP. In (**C**) the concentrations of MDA-DNPH adduct established from calibration curve (y = 16714x–577.99) were as following: 1.03 ± 0.04 nmol (0 min), 1.36 ± 0.12 nmol (10 min), 2.03 ± 0.48 nmol (20 min) and 3.02 ± 0.04 nmol (30 min), (n = 3, ±SD). The coefficient of determination R^2 was determined as 0.995.

different time interval, photon emission was enhanced in proportion to the heat treatment period. To quantify ultra-weak photon emission from the cells, one-dimensional ultra-weak photon emission was measured using a low-noise PMT. Figure 5A shows that the photon emission in heated cells was found to be highest after 30 min, while the lowest photon emission was observed in cells without heat treatment. The photon emission in heated *Chlamydomonas* cells was found to be approximately enhanced by 30%, 40% and 50% in 10, 20 and 30 min of heat treatment, respectively compared to non-heated *Chlamydomonas* cells (Fig. 5B). These results indicates that exposure of *Chlamydomonas* cells to 40 °C results in the formation of $^3L = O^*$.

Singlet oxygen imaging using confocal laser scanning microscopy. To visualise $^1O_2$ formation in the heated *Chlamydomonas* cells, $^1O_2$ imaging was performed using the fluorescent probe SOSG as detected by laser confocal scanning microscopy. Figure 6 shows the Nomarski DIC images, the SOSG fluorescence, the chlorophyll
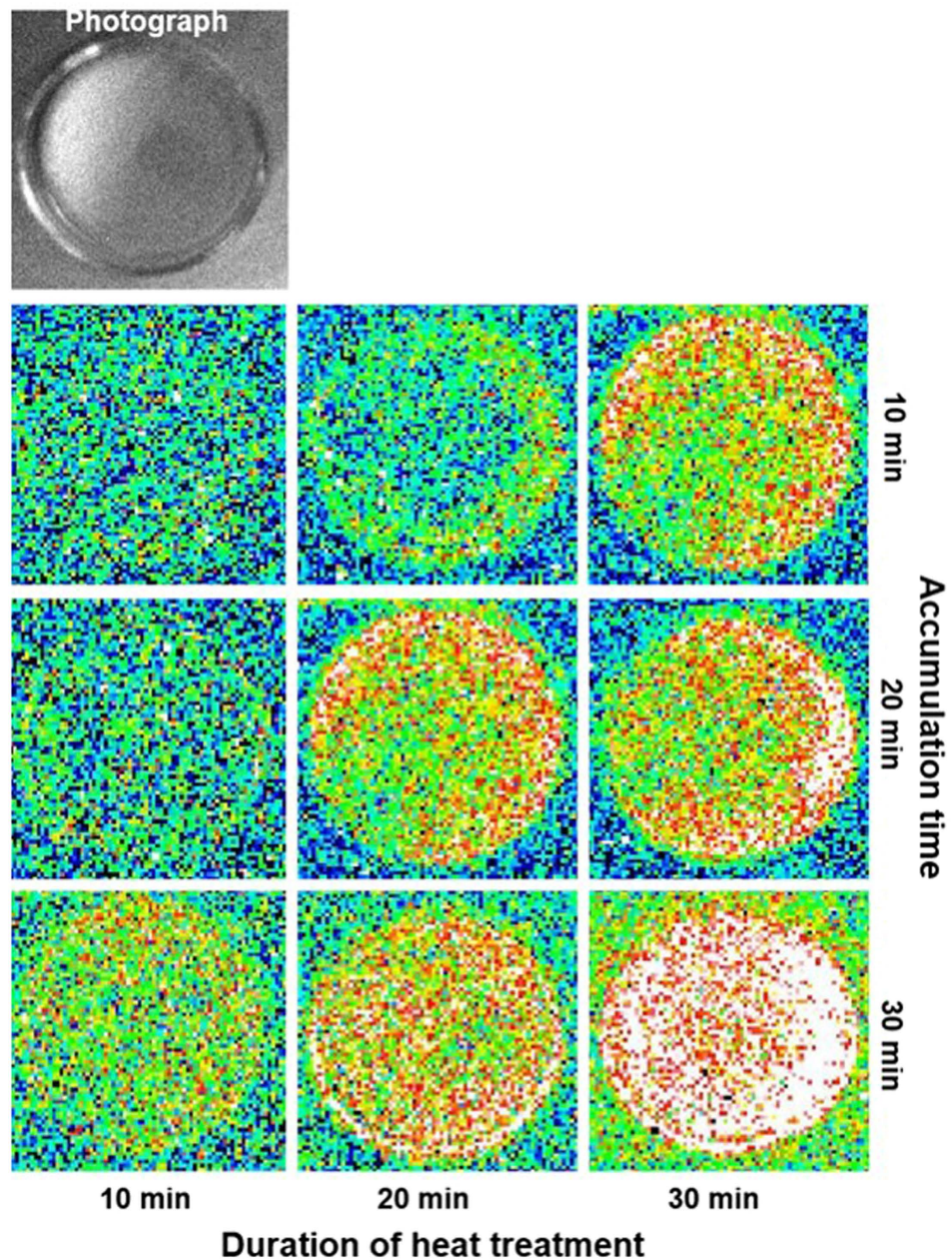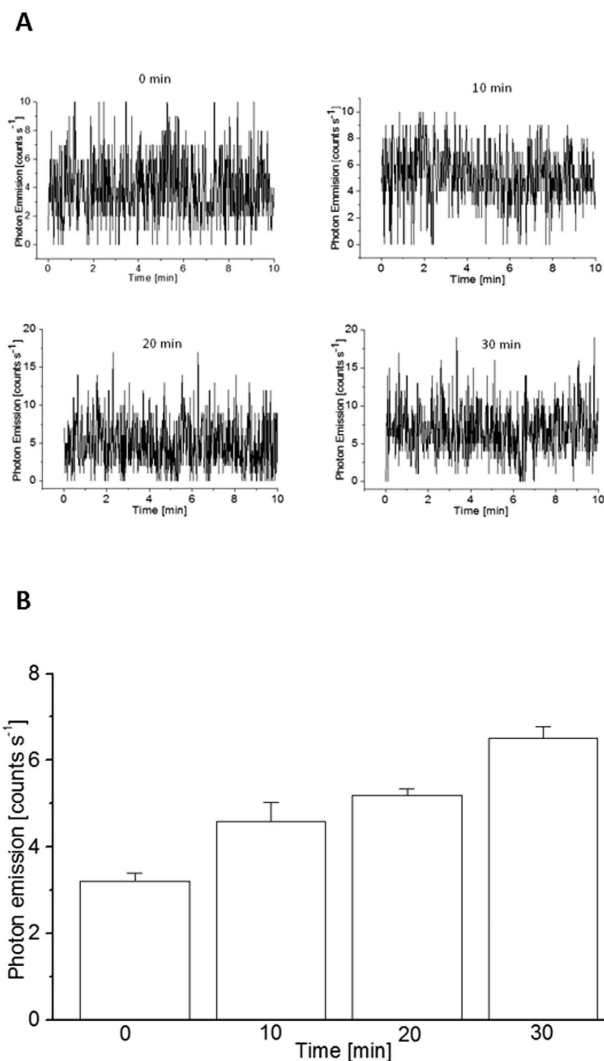
Figure 4. Two-dimensional imaging of ultra-weak photon emission from *Chlamydomonas* cells. Two-dimensional imaging of the spontaneous and induced ultra-weak photon emission from the *Chlamydomonas* cells was measured using highly sensitive CCD camera. The images and photographs of ultra-weak photon emission from the heated *Chlamydomonas* cells at 40 °C for 10, 20 and 30 min (X-axis). Ultra-weak photon emission imaging was measured with an accumulation time of 10, 20 and 30 min (Y-axis).

fluorescence and the integral distribution of SOSG fluorescence intensity measured in *Chlamydomonas* cells. *Chlamydomonas* cells incubated with SOSG at room temperature exhibited very low SOSG fluorescence, whereas cells exposed to 40 °C emitted strong SOSG fluorescence representing $^1O_2$ formation. SOSG fluorescence measured in multiple number of *Chlamydomonas* cells showed that distribution of $^1O_2$ is not uniform among the cells (Supplementary data 1). The integral distribution of SOSG fluorescence intensity shows that SOSG fluorescence in heated *Chlamydomonas* cells is enhanced by about 6 times as compared to non-heated *Chlamydomonas* cells.

To localise $^1O_2$ formation in heated *Chlamydomonas* cells, Nomarski DIC (A), SOSG fluorescence (B) and chlorophyll fluorescence (C) channels were compared for a series of optical sections through samples (Supplementary data 2). The observation that localisation of SOSG fluorescence corresponds to chlorophyll fluorescence reveals that $^1O_2$ is formed predominantly in chloroplasts (Supplementary data 2A). Nomarski DIC images and SOSG fluorescence measured in multiple layers of *Chlamydomonas* cells show that SOSG fluorescence

A

B

Figure 5. One-dimensional ultra-weak photon emission from *Chlamydomonas* cells. One-dimensional spontaneous and heat-induced ultra-weak photon emission were measured from *Chlamydomonas* cells using low-noise PMT. In (**A**) ultra-weak photon emission was measured in spontaneous and in heated *Chlamydomonas* cells at 40 °C for 0, 10, 20 and 30 min. In (**B**) mean photon emission intensity were measured in non-heated and heated *Chlamydomonas* cells. Heat treatment was done at 40 °C for 0, 10, 20 and 30 min. The presented data are expressed as the mean value and the standard deviation of at least three measurements (mean ± SD, n = 3).

from the cytoplasm, pyrenoid and vacuoles also partially contributes to the overall SOSG fluorescence, indicating that $^1O_2$ formation in other part of protoplast cannot be completely ruled out (Supplementary data 2B).

The effect of lipoxygenase inhibitors, catechol and caffeic acid on $^1O_2$ was measured in heated *Chlamydomonas* cells. Figure 6 shows the Nomarski DIC, the SOSG fluorescence and the chlorophyll fluorescence images measured in the presence of catechol and caffeic acid in non-heated and heated *Chlamydomonas* cells. No significant effect on the SOSG fluorescence in the presence of catechol was observed in non-heated *Chlamydomonas* cell whereas the SOSG fluorescence was found to be significantly suppressed in the presence of catechol in the heated *Chlamydomonas* cell. The integral distribution of the SOSG fluorescence intensity measured in heated *Chlamydomonas* cells shows that the SOSG fluorescence intensity in the presence of catechol was lowered by approximately 60% as compared to the SOSG fluorescence intensity in the absence of catechol. Similarly, the effect of caffeic acid was tested on $^1O_2$ imaging in heated *Chlamydomonas* cells. In non-heated *Chlamydomonas* cell, no change in SOSG fluorescence was observed under the effect of caffeic acid while in heated *Chlamydomonas* cells caffeic acid reduced signal to values of unheated samples as shown by the integral distribution of signal intensity (Fig. 6). These results reveal that inhibition of lipoxygenase by catechol and caffeic acid prevents $^1O_2$ formation.

Quantification of singlet oxygen using EPR spin-trapping spectroscopy. To quantify $^1O_2$ formation in *Chlamydomonas* cells exposed to 40 °C, $^1O_2$ was measured by EPR spin-trapping spectroscopy. The detection of $^1O_2$ was accomplished using oxidation of lipophilic diamagnetic 2,2,6,6-tetramethylpiperidine (TEMP)
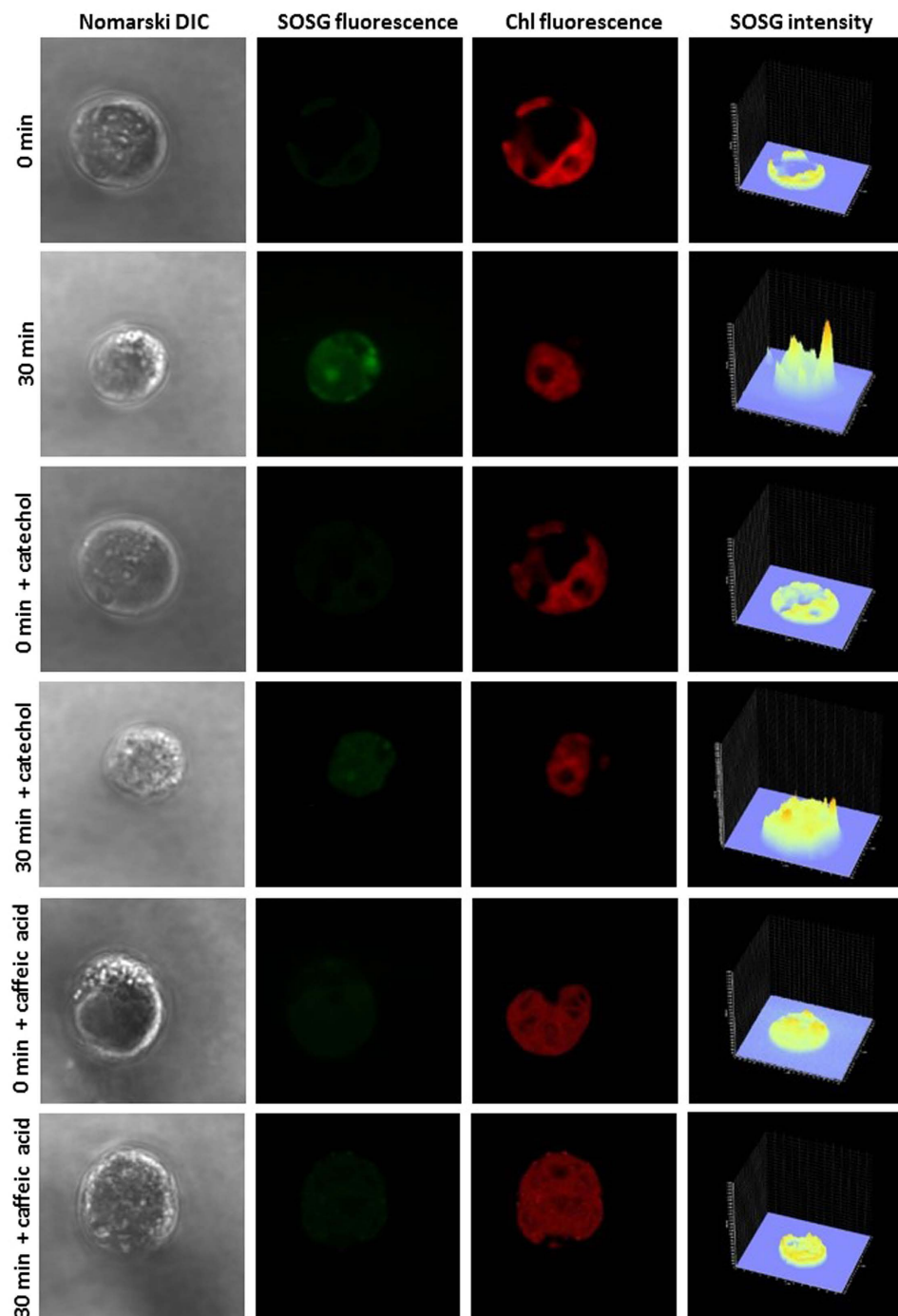
Figure 6. Detection of singlet oxygen in *Chlamydomonas* cells by laser confocal scanning microscopy. The formation of $^1O_2$ was measured in non-heated and heated *Chlamydomonas* cells in the presence and the absence of catechol and caffeic acid using fluorescent probe SOSG. Heated cells were treated for 30 min in a water bath at 40 °C under dark. The images represent from left to right: Nomarski DIC, SOSG fluorescence, chlorophyll fluorescence and integral distribution of SOSG signal intensity (0–4096) in the 12-bit microphotographs.

by $^1O_2$, which yields paramagnetic 2,2,6,6-tetramethylpiperidine-1-oxyl (TEMPO) (Fig. 7). In non-heated *Chlamydomonas* cells, the addition of TEMP shows a negligible TEMPO EPR signal caused by impurity of the spin trap. The treatment of *Chlamydomonas* cells to a temperature of 40 °C in the presence of TEMP resulted in the formation of the TEMPO EPR signal (Fig. 7A). To establish the concentration of $^1O_2$ formed in heated cells, the calibration curve was obtained using TEMPO as a standard (Fig. 7B, insert). Figure 7B shows that the concentration of $^1O_2$ formed in heated *Chlamydomonas* cells is in the concentration range of several tens to hundreds of nanomoles.
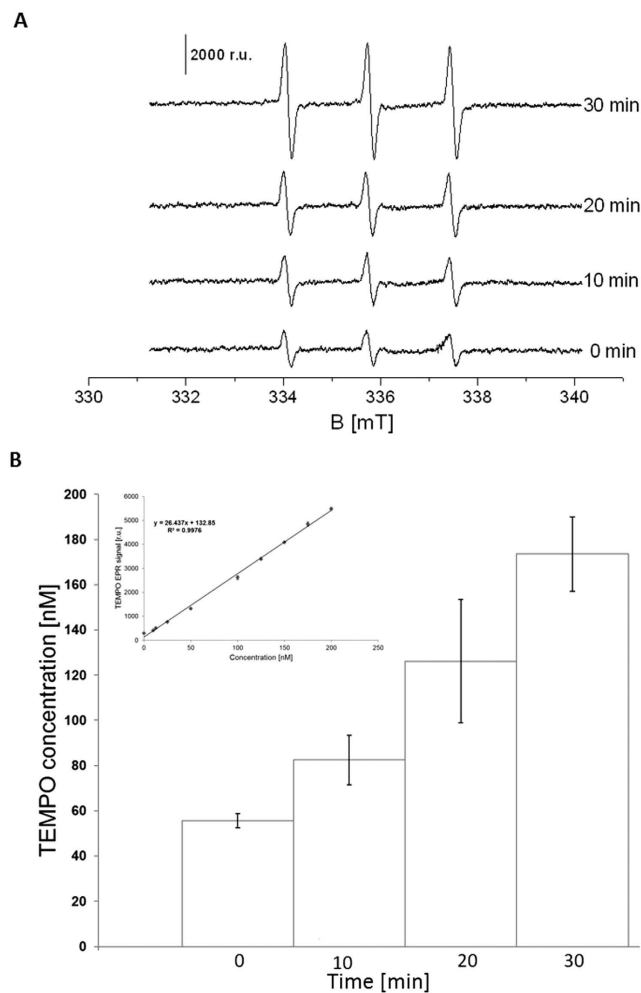
Figure 7. EPR spin-trapping detection of singlet oxygen formation from Chlamydomonas cells. Detection of $^1O_2$ by EPR spin-trapping spectroscopy in *Chlamydomonas* cells. EPR spectra were detected after heat treatment for 0, 10, 20 and 30 min at 40 °C in the presence of 50 mM TEMP. In (**A**) shows time profile of TEMPO EPR spectra. The intensity of EPR signal was determined by measuring the relative height of central peak of the EPR absorption spectrum. Bar represents 2000 r.u. In (**B**) The presented data are expressed as the mean value and the standard deviation of at least three measurements (mean ± SD, n = 3). In (**B**) the concentrations of TEMPO was established from calibration curve (equation y = 26.437x + 132.85) were as following: 55.64 ± 3.04 nmol (0 min), 82.49 ± 10.89 nmol (10 min), 126.09 ± 27.28 nmol (20 min) and 173.55 ± 16.39 nmol (30 min). The coefficient of determination R^2 was determined as 0.9976. Insert shows calibration curve of FOX assay obtained using H_2O_2 as substrate.

Discussion

Several pieces of evidence have been provided that indicate that the increase in temperature is associated with lipid peroxidation[33,34,39,40]. In agreement with this evidence, we showed that the exposure of *Chlamydomonas* cells to 40 °C leads to the formation of LOOH (Fig. 1). The observation that lipoxygenase inhibitors (catechol and caffeic acid) significantly suppressed LOOH formation reveals that lipid peroxidation is initiated by lipoxygenase (Fig. 1). Quantification of LOOH formation using FOX assay showed that LOOH was formed in the concentration range of several units in micromoles (Fig. 2). In the propagation phase, the lipid peroxidation process propagates via the formation of LOOH formed upon reaction of LOO· with another lipid molecule. In termination, the cyclisation of LOO· is known to form cyclic endoperoxide, the decomposition of which leads to the formation of MDA. Our observation that the MDA-DNPH adduct detected by HPLC (Fig. 3) was enhanced in heated *Chlamydomonas* cells compared to non-heated cells reveals a higher degree of lipid peroxidation under heat stress.

Alternatively, the cyclisation of LOO• is known to form cyclic dioxetane or the recombination of LOO• forms linear tetroxide[18,20,21]. The decomposition of dioxetane or tetroxide results in the formation of $^3L=O^*$[16,17]. Our recent results on the spectral analysis of linoleic acid induced ultra-weak photon emission from *Chlamydomonas* cells using band pass filters showed that the photon emission is in red region of the visible spectrum (> 600 nm), with a photon emission maximum at 680 nm indicating that the photon emission is predominantly from singlet excited chlorophylls. The photon emission in the blue-green region of the spectrum from $^3L=O^*$ is quite

negligible because the energy transfer from $^3L = O^*$ to chlorophyll is more efficient than the photon emission. As singlet excited chlorophylls are formed solely by excitation energy transfer from $^3L = O^*$ to chlorophylls[21], ultra-weak photon emission might serve as an indirect indicator of $^3L = O^*$ formation. In agreement with our observations, it has been previously demonstrated that exposure of spinach leaves and isolated chloroplasts to heat stress is accompanied by the photon emission from singlet excited chlorophyll[41]. The authors showed that photon emission is dominant in the wavelength range from 700–800 nm under heat treatment. The photon emission from both the samples was found to increase with the increase in temperature from 0 to 40 °C. The slow increase in photon emission in the temperature range of 0–25 °C can be because of initiation of metabolic processes; however, a steep rise in the temperature range of 25–45 °C can be related to the high activity of lipoxygenase present in leaves and isolated chloroplasts. Based on these considerations, the enhancement in ultra-weak photon emission observed in *Chlamydomonas* cells exposed to heat stress (Figs 4 and 5) indicates that $^3L = O^*$ are formed in the heated *Chlamydomonas* cells during lipid peroxidation likely initiated by lipoxygenase.

The triplet-singlet excitation energy transfer from $^3L = O^*$ to molecular oxygen leads to the formation of $^1O_2$. Alternatively, $^1O_2$ is formed directly by decomposition of tetroxide to $^1O_2$ via the Russell reaction[10,18,21]. Due to elimination of $LOO^•$ by the antioxidant system in *Chlamydomonas* cells, the probability of recombination of two $LOO^•$ is significantly low. Under these circumstances, $^1O_2$ formation via decomposition of LOOOOL via the Russell reaction is less expected[11,42,43]. Based on these considerations, it seems to be likely that cyclisation of $LOO^•$ to LOOL and its subsequent decomposition to $^3L = O^*$ is the probable reaction pathway for $^1O_2$ formation. EPR spin-trapping spectroscopy showed that exposure of *Chlamydomonas* cells to 40 °C results in the formation of $^1O_2$ (Fig. 7A). The observation that $^1O_2$ formation linearly increases up to 30 min of heat treatment indicates continuous $^1O_2$ formation with increase in duration of heat treatment (Fig. 7B). The imaging of $^1O_2$ using the green fluorescence of SOSG detected by confocal laser scanning microscopy confirmed that exposure of *Chlamydomonas* cells to 40 °C results in the formation of $^1O_2$ (Fig. 6). Based on the results obtained using green fluorescence of SOSG and chlorophyll fluorescence, it is evident that $^1O_2$ formation occurs predominantly within chloroplast (Supplementary data 1); however, the contribution of other parts of a cell protoplast are very probable to contribute to the $^1O_2$ pool in the heated *Chlamydomonas* cells (Supplementary data 2). The observation that inhibition of lipoxygenase by catechol partially prevented $^1O_2$ formation indicates that the lipid peroxidation that leads to $^1O_2$ formation is initiated by lipoxygenase (Fig. 6).

Differences in the localisation of LOOH (Fig. 1) and the $^1O_2$ (Fig. 6 and Supplementary data 2) suggest that formation of both LOOH and $^1O_2$ is localised predominantly in chloroplasts. Contrary to LOOH, $^1O_2$ formation was also observed in pyrenoid, cytoplasm and vacuoles likely due to the short-distance diffusion of $^1O_2$ from the site of its formation. These results provide experimental support for the correlation of lipid peroxidation and $^1O_2$ formation.

Methods

Chlamydomonas reinhardtii growth conditions. Algae strain, *Chlamydomonas reinhardtii* (wild type: CC-002) was obtained from the Chlamydomonas Genetic Center (Duke University, Durham, NC, USA). The cells were cultivated in Tris-Acetate-Phosphate (TAP) medium in a continuous white light (100 μmol photons m^{-2} s^{-1}) in Algaetron AG 230 (Photon Systems Instruments, Drásov, Czech Republic). The growth was achieved under permanently stirred condition using shaker (Orbital Shaker PSU-10i, Biosan, Riga, Latvia) to obtain constant CO_2 concentration in the growing medium. The cells were studied at a density of approximately 7×10^7 cells ml^{-1} during the stationary growth phase. The cell density was determined by an automated cell counter (TC20 Automated Cell Counter, BioRad, Hercules, CA, U.S.A.).

Heat treatment. The lipid peroxidation in *Chlamydomonas* cells were induced using heat stress. The cell were exposed solely to heat stress and any effect of light was prevented. Samples were treated for 10, 20 and 30 min at temperature of 40 °C using in a water bath (Julabo GmbH, Germany) in Eppendorf tubes.

Confocal laser scanning microscopy. *In-vivo* imaging of LOOH and $^1O_2$ was based on their reaction with a swallow-tailed perylene derivative (Spy-LHP) (Dojindo Molecular Technologies Inc. Rockville, MD, USA) and SOSG (Molecular Probes Inc., Eugene, OR, USA), respectively. *Chlamydomonas* cells were incubated either in the presence of 20 μM Spy-LHP or 50 μM SOSG in darkness for 30 min. To study an influence of temperature stress, samples were kept at room temperature or subjected to 40 °C. Immediately after staining, the cells were transferred to a fresh TAP medium and visualized by confocal laser scanning microscopy (Fluorview 1000 unit attached to IX80 microscope; Olympus Czech Group, Prague, Czech Republic). The excitation of both fluorochromes were achieved by a 488 nm line of an argon laser and signal was detected either by a 505–550 nm emission filter for LOOH or by a 505–525 nm emission filter for $^1O_2$. Chlorophyll fluorescence from chloroplasts of *Chlamydomonas* cells was achieved by excitation with 543 nm helium-neon laser, and emission recorded with a 655–755 nm band filter. Cell morphology was visualized by transmitted light detection module with 405 nm excitation using a near ultraviolet (405 nm) diode laser and Nomarski DIC filters. The proper intensity of all lasers was set according to unstained samples at the beginning of each experiment (Sedlářová *et al.* 2011)[44]. Integral distribution of signal intensity (0–4096) in 12-bit microphotographs was evaluated by image analysis software FV10-ASW Viewer (Olympus).

High performance liquid chromatography (HPLC). Malondialdehyde, a product of lipid or protein oxidation was measured using HPLC. The isolation and derivatization of MDA using 2,4-dinitrophenylhydrazine (DNPH) was performed as described in Pilz *et al.* (2000) with some modifications[45]. After heat treatment, cells were centrifuged at 2000 x g for 10 min and the supernatant was removed. The pellet was resuspended in 200 μl of phosphate buffer saline (PBS, pH = 7.5) and 100 μl 0.06% butylhydroxytoluene (BHT) dissolved in methanol.

Using a sonicator for 90 s (Sonicator, Ultrasonic homogenizer Model 3000, Biologics Inc., Manassas, VA, U.S.A.), the *Chlamydomonas* cells were disrupted. This step was followed by centrifugation at 2000 x g for 10 min and 125 μl of supernatant was taken for following step. To achieve alkaline hydrolysis of protein bound MDA, 25 μl of 6 M aqueous sodium hydroxide was added to the samples and sample were treated in a 60 °C dry bath for 30 min (Thermo-Shaker TS100, Biosan, Riga, Latvia). To reach the precipitation of proteins in samples, 62.5 μl of 35% (v/v) perchloric acid was added to the sample, vortexed and centrifuged at 16000 x g for 10 min. 125 μl of supernatant was taken into a vial and resuspended in 1 μl of 50 mM DNPH dissolved in 50% sulphuric acid and treated in dark at room temperature for 30 min. DNPH bound to MDA to create a MDA-DNPH adduct. An amount of 25 μl was injected into the HPLC system (Alliance e 2695 HPLC System, Waters, Milford, MA, U.S.A.) and detected at 310 nm using UV/VIS detector. A Symmetry C18 (3.5 μm; 4.6 × 75 mm) Column (Waters, Milford, MA, U.S.A.) was used. The analysis was performed isocratically (1 ml/min at 35 °C) using mobile phase comprised of mixture of 25 mM trimethylamine (pH 3.5) and acetonitrile in the ratio 50:50 (v:v). To remove impurities from the column after every measurement, the column was rinsed by 100% methanol.

Ferrous oxidation-xylenol orange assay. For the quantification of LOOH in *Chlamydomonas* cells, FOX assay (John M. DeLong *et al.* 2002) was used with minor modifications. FOX reagent was prepared by mixing 50 mM xylenol orange and 5 mM iron(II) sulfate heptahydrate in proportion 1:1. For the measurement 100 μl of sample (reference) and 2000 μl FOX reagent was used. FOX reagent was added to *Chlamydomonas* cells prior to heat treatment and absorption changes were measured 30 min after start of heat treatment to keep the total period constant. Hydroperoxide formation was monitored by following the absorbance changes at 560 nm using Olis RSM 1000 spectrometer (Olis Inc., Bogart, Georgia, USA).

Ultra-weak photon emission measurement. *Chlamydomonas* cells in TAP medium (total volume of 2 ml) in a glass Petri dish (3 cm diameter) were used for ultra-weak photon emission measurements. For two-dimensional photon emission imaging, the photons were reflected by a mirror to the CCD camera positioned horizontally. For one-dimensional photon counting, the Petri dish was placed below the vertically positioned photomultiplier tube (PMT) at a distance of 3 cm. The cells were dark-adapted for 30 min to eliminate any interference by delayed luminescence.

Highly sensitive CCD camera VersArray 1300B (Princeton instruments, Trenton, NJ, USA) with spectral sensitivity in the range of 200–1000 nm restricted to 350–1000 nm due to the objective lens mounted and almost 30% quantum efficiency in the visible range of the spectrum was used for two-dimensional photon imaging. For reduction of dark current, CCD camera was cooled down to −104 °C using a liquid-nitrogen cooling system. The data correction was made by subtracting the background noise before every measurement. The measurement was done in the image format of 1340 × 1300 pixels with following CCD camera parameters: scan rate, 100 kHz; gain, 3; accumulation time, 30 min.

One-dimensional photon counting was done using low-noise photon counting unit C9744 (Hamamatsu Photonics K.K., Iwata city, Japan) with a spectral sensitivity in the range of 160–710 nm. For reduction of thermal electrons, PMT was cooled down to −30 °C using thermoelectric cooler C9143 (Hamamatsu Photonics, K.K., Iwata city, Japan). The PMT was kept vertically to minimize the dark counts to ~2 counts s^{-1} at −1150 mV. The photon emission measurements were done in the experimental darkroom (3 m × 1.5 m × 2.5 m) painted with black colour. The door in the experimental darkroom was protected completely with a black curtain to restrict any diffusion of light from external source.

Electron paramagnetic resonance (EPR) spectroscopy. EPR spin-trapping spectroscopy was used to measure the $^1O_2$ production. *Chlamydomonas* cells suspended in TAP media with 50 mM TEMP spin trap were heated at 40 °C and EPR spectra were recorded using an EPR spectrometer MiniScope MS400 (Magnettech GmbH, Berlin, Germany). To eliminate impurity TEMPO EPR signal, TEMP was purified twice by vacuum distillation. EPR conditions are as follows: microwave power, 10 mW; modulation amplitude, 1 G; modulation frequency, 100 kHz; sweep width, 100 G; scan rate, 1.62 G s^{-1}.

References

1. Halliwell, B. & Gutteridge, J. In *Free radicals in biology and medicine* (2nd Eds.) (Oxford University Press, 2007).
2. Farmer, E. & Mueller, M. ROS-Mediated Lipid Peroxidation and RES-Activated Signaling. *Annu. Rev. Plant Biol.* **64,** 429–450 (2013).
3. Gutteridge, J. Lipid peroxidation initiated by superoxide-dependent hydroxyl radicals using complexed iron and hydrogen peroxide. *FEBS Lett.* **172,** 245–249 (1984).
4. Garry, B.R. Molecular targets of photosensitization–some biological chemistry of singlet oxygen, *In: Free radical and Radiation Biology & ESR Facility, Med labs B180*, The University of Iowa, Iowa City (2008) http://www.photobiology.info/Buettner.html. (Accessed: 1st November 2015).
5. Kruft, B. & Greer, A. Photosensitization Reactions *In Vitro* and *In Vivo*. *Photochem. Photobiol.* **87,** 1204–1213 (2011).
6. Kanofsky, J. Measurement of Singlet-Oxygen *In Vivo*: Progress and Pitfalls. *Photochem. Photobiol.* **87,** 14–17 (2011).
7. Girotti, A. W. Lipid hydroperoxide generation, turnover, and effector action in biological System. *J. Lipid Res.* **39,** 1529–42 (1998).
8. Cilento, G. & Waldemar, A. From Free Radicals to Electronically Excited Species. *Free Rad. Biol. Med.* **19,** 103–14 (1995).
9. Cilento, G. & Waldemar, A. Photochemistry and photobiology without light. *Photochem. Photobiol.* **48,** 361–68 (1988).
10. Miyamoto, S. *et al.* Biological hydroperoxides and singlet molecular oxygen generation. *TBMB IUBMB Life* **59,** 322–331 (2007).
11. Miyamoto, S., Martinez, G. R., Medeiros, M. H. G. & Di Mascio, P. Singlet molecular oxygen generated from lipid hydroperoxide by the Russell mechanism: studies using 18O-labeled linoleic acid hydroperoxide and monomol light emission measurements. *J Am. Chem. Soc.* **125,** 6172–6179 (2003).
12. Miyamoto, S., Martinez, G. R., Martins, A. P. B., Medeiros, M. G. G. & Di Mascio, D. Direct Evidence of Singlet Molecular Oxygen [O2(1ΔG)] Production in the Reaction of Linoleic Acid Hydroperoxide with Peroxynitrite. *J. Am. Chem. Soc.* **125,** 4510–517 (2003).
13. Mano, N., Mao, F. & Heller, A. Characteristics of a Miniature Compartment-less Glucose−O 2 Biofuel Cell and Its Operation in a Living Plant. *J. Am. Chem. Soc.* **125,** 6588–594 (2003).
14. Miyamoto, S. *et al.* Linoleic Acid Hydroperoxide Reacts with Hypochlorous Acid, Generating Peroxyl Radical Intermediates and Singlet Molecular Oxygen. *PNAS* **103.** 2, 293–98 (2006).

15. Adam, W., Kazakov, D. V. & Kazakov, V. P. Singlet-Oxygen Chemiluminescence in Peroxide Reactions. *Chem. Rev.* **105,** 3371–387 (2005).
16. Cilento, G. & Adam, W. From free radicals to electronically excited species. *Free Radical Bio. Med* **19,** 103–114 (1995).
17. Cilento, G. & Nascimento, A. Generation of electronically excited triplet species at the cellular level: A potential source of genotoxicity. *Toxicology Lett.* **67,** 17–28 (1993).
18. Miyamoto, S., Martinez, G., Medeiros, M. & Mascio, P. Singlet molecular oxygen generated by biological hydroperoxides. *J Photochem. Photobiol. B: Biology* **139,** 24–33 (2014).
19. Brivida, K., Saha-Moller, C. R., Adam, W. & Sies, H. Formation of singlet oxygen in the thermal decomposition of 3-hydroxymethyl-3,4,4-trimethyl-1-,2-dioxetane, a chemical source of triplet excited ketones. *Biochem. Mol. Biol. Int.* **38,** 647–651 (1996).
20. Havaux, M., Triantaphylides, C. & Genty, B. Autoluminescence Imaging: A Non-invasive Tool for Mapping Oxidative Stress. *Trends Plant Sci.* **11,** 480–84 (2006).
21. Pospíšil, P. The role of metals in production and scavenging of reactive oxygen species in Photosystem II. *Plant and Cell Physiol.* **55,** 1224–1232 (2014).
22. Cilento, G., De Baptista, R. C. & Brunetti, I. L. Triplet Carbonyls: From Photophysics to Biochemistry. *J. Mol. Struct.* **324,** 45–48 (1994).
23. Cilento, G. "*Electronic Excitation in Dark Biological Processes*" in *Chemical and Biological Generation of Excited States* Ch. 9, 277–307 (Academic press, 1982).
24. Mano, C. M. *et al.* Excited Singlet Molecular O2 (1△g) Is Generated Enzymatically from Excited Carbonyls in the Dark. *Sci. Rep.* **4** (2014).
25. Frankel, E. N. *Photooxidation in unsaturated fats in Lipid oxidation* 2nd edn Ch. 3, 51–66 (Oily Press, 2005).
26. Liu, X. & Huang, B. Heat Stress Injury in Relation to Membrane Lipid Peroxidation in Creeping Bentgrass. *Crop Sci.* **40,** 503–510 (2000).
27. Larkindale, J. & Knight, M. R. Protection against Heat Stress-Induced Oxidative Damage in Arabidopsis Involves Calcium, Abscisic Acid, Ethylene, and Salicylic Acid. *Plant Physiol.* **128,** 682–95 (2002).
28. Kipp, E. & Boyle, M. The Effects of Heat Stress on Reactive Oxygen Species Production and Chlorophyll Concentration in Arabidopsis Thaliana. *Research in Plant Sciences* **2,** 20–23 (2013).
29. Allakhverdiev, S. *et al.* Heat stress: An overview of molecular responses in photosynthesis. *Photosynth. Res.* **98,** 541–550 (2008).
30. Murata, N. & Los, D. A. Membrane fluidity and temperature perception. *Plant Physiol.* **115,** 875–879 (1997).
31. Yamashita, A. *et al.* Quality Control of Photosystem II: Reactive oxygen species are responsible for the damage to photosystem ii under moderate heat stress. *J Biol. Chem.* **283,** 28380–28391 (2008).
32. Mishra, R. & Singhal, G. Function of Photosynthetic Apparatus of Intact Wheat Leaves under High Light and Heat Stress and Its Relationship with Peroxidation of Thylakoid Lipids. *Plant Physiol.* **98,** 1–6 (1992).
33. El-Shitinawy, F., Ebrahim, M. K. H., Sewelam, N. & El-Shourbagy, M. N. Activity of photosystem 2, lipid peroxidation, and the enzymatic antioxidant protective system in heat shocked barley seedlings. *Photosynthetica* **42,** 15–21 (2004).
34. Hasanuzzaman, M., Nahar, K., Alam, M., Roychowdhury, R. & Fujita, M. Physiological, Biochemical, and Molecular Mechanisms of Heat Stress Tolerance in Plants. *IJMS International Journal of Molecular Sciences* **14,** 9643–9684 (2013).
35. Pospíšil, P., Šnyrychová, I. & Nauš, J. Dark production of reactive oxygen species in photosystem II membrane particles at elevated temperature–EPR spin-trapping study. *Biochim. Biophys. Acta* **1767,** 854–859 (2007).
36. Hideg, É. & Vass, I. The 75 °C Thermoluminescence Band of Green Tissues: Chemiluminescence From Membrane-Chlorophyll Interaction. *Photochem. Photobiol.* **58,** 280–283 (1993).
37. Koshihara, Y. *et al.* Caffeic acid is a selective inhibitor for leukotriene biosynthesis. *Biochim. Biophys. Acta* **792,** 92–97 (1984).
38. Sud'ina, G. F. *et al.* Caffeic acid phenethyl ester as a lipoxygenase inhibitor with antioxidant properties. *Feder. Eur. Biochem. Soc.* **329,** 21–24 (1993).
39. Ali, M., Hahn, E. & Paek, K. Effects of temperature on oxidative stress defense systems, lipid peroxidation and lipoxygenase activity in Phalaenopsis. *Plant Physiol. Bioch.* **43,** 213–223 (2005).
40. Chan, T. *et al.* Quality Control of Photosystem II: Lipid Peroxidation Accelerates Photoinhibition under Excessive Illumination. *PLoS One* **7,** 12 (2012).
41. Hideg, È. & Inaba, H. Biophoton Emission (Ultraweak Photoemission) From Dark Adapted Spinach Chloroplasts. *Photochem. Photobiol.* **53,** 137–142 (1991).
42. Russell, G. A. Deuterium-isotope effects in the autoxidation of aralkyl hydrocarbons – mechanism of the interaction of peroxy radicals. *J. Am. Chem. Soc.* **79,** 3871–3877 (1957).
43. Howard, J. A. & Ingold, K. U. Self reaction of sec-butylperoxy radicals. Confirmation of Russell mechanism. *J Am. Chem. Soc.* **90,** 1056–1058 (1968).
44. Sedlářová, M. *et al.* Influence of Nitric Oxide and Reactive Oxygen Species on Development of Lettuce Downy Mildew in Lactuca Spp. *Eur. J Plant Pathol.* **129,** 267–280 (2011).
45. Pilz, J. Meineke, I. & Gleiter, C. H. Measurement of free and bound malondialdehyde in plasma by high-performance liquid chromatography as the 2,4-dinitrophenylhydrazine derivative. *J Chromatogr. B* **742,** 315–325 (2000).

Acknowledgements

Author Contributions

A.P. and P.P. contributed to the conception and design of the work, interpretation of data, analysis, and drafted the manuscript. A.P., U.F. and M.S. performed the measurements. All authors approved the final version of the manuscript.

Additional Information

Supplementary information accompanies this paper at http://www.nature.com/srep

Competing financial interests: The authors declare no competing financial interests.

How to cite this article: Prasad, A. *et al.* Singlet oxygen production in *Chlamydomonas reinhardtii* under heat stress. *Sci. Rep.* **6,** 20094; doi: 10.1038/srep20094 (2016).